

UNIVERSIDADE DE SÃO PAULO
INSTITUTO DE QUÍMICA
Programa de Pós-Graduação em Ciências Biológicas (Bioquímica)

ISABELLA FERNANDA DANTAS PINTO

**Exploring the Role of Lipids in Protein Modification and
Amyotrophic Lateral Sclerosis**

Versão corrigida da Tese conforme Resolução CoPGr 5890

O original se encontra disponível na Secretaria de Pós-Graduação do IQ-USP

São Paulo

Data do Depósito na SPG:

25/06/2019

ISABELLA FERNANDA DANTAS PINTO

**Explorando o Papel dos Lipídeos na Modificação de
Proteínas e Esclerose Lateral Amiotrófica**

*Tese apresentada ao Instituto de Química da
Universidade de São Paulo para obtenção do
Título de Doutora em Ciências (Bioquímica)*

Orientadora: Profa. Dra. Sayuri Miyamoto

São Paulo

2019

Autorizo a reprodução e divulgação total ou parcial deste trabalho, por qualquer meio convencional ou eletrônico, para fins de estudo e pesquisa, desde que citada a fonte.

Ficha Catalográfica elaborada eletronicamente pelo autor, utilizando o programa desenvolvido pela Seção Técnica de Informática do ICMC/USP e adaptado para a Divisão de Biblioteca e Documentação do Conjunto das Químicas da USP

Bibliotecária responsável pela orientação de catalogação da publicação:
Marlene Aparecida Vieira - CRB - 8/5562

P659e Pinto, Isabella Fernanda Dantas
Explorando o Papel dos Lipídeos na Modificação de Proteínas e Esclerose Lateral Amiotrófica / Isabella Fernanda Dantas Pinto. - São Paulo, 2019.
177 p.

Tese (doutorado) - Instituto de Química da Universidade de São Paulo. Departamento de Bioquímica.

Orientador: Miyamoto, Sayuri

1. Lipídeos. 2. Estresse oxidativo. 3. Esclerose lateral amiotrófica. 4. Espectrometria de massas. 5. Lipidômica. I. T. II. Miyamoto, Sayuri, orientador.

Dedico este trabalho à minha família.

AGRADECIMENTOS

Acredite nos seus sonhos. É com esta frase que inicio os meus agradecimentos. Acreditar nos sonhos, acreditar em si mesmo e acima de tudo ser grato. Assim, agradeço ao universo que me proporcionou essa intensa experiência de vida.

Agradeço imensamente a minha vó Terezinha (*In memorian*). Aqui as palavras não são suficientes para expressar o tamanho da minha gratidão! Ela deve estar no céu dançando de felicidade. A saudade é eterna, voinha.

Aos meus pais Milton e Naide pelo amor incondicional e por acreditar que a educação é o bem mais precioso que se pode dar a um filho. Agradeço especialmente a minha mãe por me incentivar a terminar o doutorado apesar dos momentos difíceis que surgiram nessa jornada.

Agradeço aos meus irmãos Amanda e Miltinho por sempre se preocuparem comigo e compreenderem a minha ausência durante esses anos.

Agradeço ao meu namorado Igor pela paciência e pelo carinho.

Agradeço aos meus amigos Adriano, Railmara e Lucas pelos anos de convivência na faculdade, iniciação científica e doutorado. É muita história! Ensinarão-me muito sobre o valor da amizade. Não teria conseguido sem vocês! Afinal, quem tem amigos tem tudo! Também agradeço aos amigos que fiz durante o doutorado: Ao Albert pelos inúmeros momentos de descontração e pelas jantas preparadas a partir de caixas surpresas. À Marcela pelas conversas principalmente na reta final do doutorado. Ao Alex e à Larissa pela convivência diária no laboratório e pelos rolês. Ao Marcos por ter me ensinado lipidômica, pela ajuda nas correções dos textos em inglês, pelas discussões dos dados e pelos conselhos que vou levar para vida! Não sei como agradecer.

Agradeço aos meus colegas de laboratório pelos momentos de partilha no dia-a-dia de trabalho.

Agradeço aos técnicos do Instituto de Química, especialmente à Adriana Wendel por cuidar da parte burocrática. À Sirlei por cuidar da limpeza das vidrarias. Ao Fernando Coelho, à Janaína e à Edilaine por serem sempre muito prestativos nos experimentos que precisei de ajuda. E ao Emerson pela ajuda com as análises no espectrômetro de massas no início do doutorado.

Agradeço ao Professor Dr. Humberto Matos pela oportunidade que me deu durante a iniciação científica de conhecer a USP e a me incentivar a seguir a carreira científica.

Agradeço a Professora Dra. Sayuri Miyamoto pela oportunidade de fazer parte do seu grupo de trabalho, pelo incentivo e pelos ensinamentos durante esses anos. Agradeço ainda por me acolher em vários momentos sempre se preocupando com meu bem-estar.

Agradeço ao Instituto de Química e a Universidade de São Paulo que me acolheram e me proporcionaram oportunidades para o meu crescimento profissional.

Agradeço à Fundação de Amparo à Pesquisa do Estado de São Paulo (FAPESP, Processo número 2014/11556-2), à Coordenação de Aperfeiçoamento de Pessoal de Nível Superior (CAPES) e ao Conselho Nacional de Desenvolvimento Científico e Tecnológico (CNPq) pelo apoio financeiro e institucional que viabilizou a execução dessa tese.

Agradeço ao presidente Lula e sua equipe de governo por implementar programas federais de apoio ao ensino e à pesquisa. Através desses programas tive oportunidade de chegar até aqui.

Enfim, agradeço a todos que de forma direta ou indiretamente contribuíram para o êxito desse projeto, que para mim foi um desafio gigantesco, e que agregou valor à minha visão de mundo e de como fazer ciência.

Every stormy night has a sunny morning. NEVER lose hope...

RESUMO

Pinto, I.F.D. **Explorando o Papel dos Lipídeos na Modificação de Proteínas e Esclerose Lateral Amiotrófica** (175p). Tese (Doutorado) – Programa de Pós-Graduação em Ciências Biológicas (Bioquímica). Instituto de Química, Universidade de São Paulo, São Paulo.

Os lipídeos são moléculas que possuem várias funções biológicas importantes, atuando como componente de membranas celulares, servindo com fonte de reserva de energia e participando de vias de sinalização. Os ácidos graxos poli-insaturados esterificados aos fosfolipídeos, por exemplo, são potenciais alvos para o ataque de radicais livres gerando produtos oxidados que são capazes de modificar resíduos de aminoácidos em proteínas levando a modulação das vias de sinalização e balanço redox. Por outro lado, alteração na homeostase do metabolismo dos lipídeos está relacionada ao desenvolvimento e progressão de doenças neurodegenerativas. Tendo em vista a importância dos lipídeos nos processos biológicos, os objetivos desse estudo foram (i) investigar o papel dos lipídeos na agregação proteica (capítulo 1 e 2), (ii) investigar as alterações na composição lipídica do plasma de rato modelo SOD1G93A de esclerose lateral amiotrófica (ELA) (capítulo 3) e (iii) investigar o efeito da suplementação de dietas hiperlipídicas na composição lipídica do plasma de rato modelo SOD1G93A (capítulo 4). No capítulo 1 e 2, a interação do citocromo c (citic) com hidroperóxido de cardiolipina (CLOOH) e hidroperóxido de colesterol (ChOOH) promove a agregação covalente do citc. Análise por nLC-MS/MS dos peptídeos digeridos identificou resíduos de lisina (K72) e histidina (H26) modificado por 4-hidroxininental (4-HNE), enquanto os resíduos K27, K73 e K88 foram modificados por 4-oxinonental (4-ONE). Pela primeira vez, nós caracterizamos ditirosinas (Y48-Y74, Y48-97 e Y74-Y97) na reação do citc com CLOOH. Também foram caracterizadas ditirosinas envolvendo os resíduos Y48-Y48, Y48-Y74 e Y48-Y97 na reação com ChOOH. Esses resultados corroboram com estudos anteriores que sugerem um mecanismo de agregação proteica envolvendo a perda da carga positiva de lisina e formação

de ditirosina pela combinação de radicais de tirosil. No capítulo 3, a análise da composição lipídica do plasma de ratos SOD1G93A utilizando LC-MS/MS revelou alterações significativas na composição de triglicérides, glicerofosfolipídeos e esfingolipídeos em ratos sintomáticos comparado com os assintomáticos. É importante destacar que pela primeira vez acilceramidas foram identificadas em plasma de rato modelo para ALS. Análise da composição lipídica de lipoproteínas isoladas, maior fonte de lipídeos circulantes no plasma, mostraram alterações de triglicérides e glicerofosfolipídeos em VLDL. As acilceramidas e as hexosilceramidas, por sua vez, foram encontradas em maior abundância em HDL. No capítulo 4, a suplementação com dietas hiperlipídicas (rica em banha de porco e óleo de peixe) alterou significativamente o perfil lipídico do plasma em relação a doença. Contudo, não foi observado aumento significativo na sobrevivência dos ratos ALS comparado com dieta controle. Independente da dieta, a concentração plasmática de acilcarnitina, hexosilceramidas e acilceramidas foram significativamente aumentadas em ratos ALS comparado com WT. A análise do perfil lipídico do plasma mostrou que a acilceramida d18:1/24:1+20:4 pode ser um potencial marcador de progressão da ALS. Dessa forma, os resultados mostrados fornecem uma visão enriquecedora sobre o evento a nível molecular que conduz a desregulação lipídica na ELA. Coletivamente, nossos resultados reforçam a importância dos lipídeos na modulação dos processos celulares ligados a agregação de proteínas e na neurodegeneração.

Palavras-chaves: dityrosine, lipidômica, dieta hiperlipídica, esclerose lateral amiotrófica, espectrometria de massas.

ABSTRACT

Pinto, I.F.D. **Exploring the Role of Lipids in Protein Modification and Amyotrophic Lateral Sclerosis.** (175p). PhD Thesis – Graduate Program in Biochemistry. Instituto de Química, Universidade de São Paulo, São Paulo.

Lipids are a diverse and ubiquitous group of compounds, which have several biological functions such as structural components of cell membranes, energy storage, and participation in signaling pathways. Free radicals or reactive oxygen species could attack polyunsaturated fatty acid esterified to phospholipids generating oxidized products. Once oxidized, lipids are able to modify amino acids residues in proteins leading to modulation signaling pathways and cellular redox balance. Furthermore, alteration of lipid homeostasis is also linked to development and progression of neurodegenerative diseases. The purposes of this study were (i) to investigate the role of lipids in protein aggregation, (ii) to investigate the plasma lipidome of an ALS rat model (SOD1G93A rats), and (iii) to investigate the effect of high-fat diet in plasma lipidome of an ALS rat model. In chapters 1 and 2, the interaction between cytochrome c (cytc) and cardiolipin hydroperoxide (CLOOH), as well as cholesterol hydroperoxide (ChOOH) promoted protein aggregation. Mass spectrometry analysis of tryptic peptides from CLOOH-containing reaction revealed K72 and H26 consistently modified by 4-hydroxynonenal (4-HNE). Further, adduction of K27, K73 and K88 were detected with 4-oxynonenal (4-ONE). For the first time, we characterized the dityrosine cross-linked peptides at Y48-Y74, Y48-97 and Y74-Y97 in oligomeric cytc. Similarly, ChOOH-containing reaction showed dityrosine cross-linked peptides at Y48-Y48, Y48-Y74 and Y48-Y97 in dimeric cytc. In accordance to previous studies, the proposed mechanism under covalent protein oligomerization mediated by lipid hydroperoxide could be related to modification of lysine and tyrosine residues. In chapter 3, we characterized the lipid composition of blood plasma in amyotrophic lateral sclerosis (ALS), since dysregulation of lipid metabolism is increasingly

associated with neuropathology. Using untargeted lipidomics approach based on liquid chromatography coupled to mass spectrometry, we found main alterations in triglycerides, phospholipids and sphingolipids in symptomatic ALS rats relative to controls. Additionally, for the first time we reported acylceramides species in the plasma. In order to investigate the source of these lipid alterations, we analyzed the lipid content of fractioned lipoproteins. Triglycerides and phospholipids were found in very low-density lipoprotein (VLDL), while acylceramides and hexosylceramides were found enriched in high-density lipoprotein (HDL). In chapter 4, high-fat diet containing lard or high-fish oil as much as 60% of total lipids has both the largest change on plasma lipid composition. Overall survival was not statistically different when compared to control diet. Increased levels of acylceramides, hexosylceramides and acylcarnitines were observed in ALS rats fed a control diet or high-fat diet in comparison to WT controls. Importantly, untargeted lipidomic analysis of blood plasma highlighted acylceramide d18:1/24:1+20:4 as potential biomarkers of ALS progression. Thus, our lipidomic analysis provides a novel insight into the molecular level event driving molecular dysregulation in ALS. Additional research is needed to determine the effect of plasma lipid alteration on motor neuron process and energetic metabolism. Collectively, our findings reinforce the idea that lipids play a relevant role in modulating cellular processes linked to protein aggregation and neurodegeneration.

Keywords: dityrosine, lipidomics, acylceramides, amyotrophic lateral sclerosis, mass spectrometry

SUMMARY

1. Introduction	14
1.1. Lipids and their structural diversity	14
1.2. Biological function of lipids	17
1.3 Subcellular localization and synthesis of lipids	19
1.4 Lipid damage by reactive oxygen species	21
1.5 Lipid in amyotrophic lateral sclerosis	24
1.6 Mass spectrometry-based lipidomics	26
2. Objective	33
2.1 General objective	33
2.2 Specific objectives	33
CHAPTER 1	34
Highlights.....	35
Abstract.....	36
Abbreviations.....	37
1. Introduction	38
2. Material and Methods	41
2.1. Materials.....	41
2.2. Synthesis and purification of cardiolipin hydroperoxide	41
2.3. Liposome preparation.....	42
2.4. Cytochrome c-liposome binding assay	42
2.5. Kinetics of the reaction of cytochrome c with lipid hydroperoxides	43
2.6. SDS Polyacrylamide gel electrophoresis (SDS-PAGE).....	43
2.7. Size exclusion chromatography (SEC)	44
2.8. nLC MS/MS analysis	44
2.9. Data Analysis	45
2.10 Statistical analysis	45
3. Results	46
3.1. Cytochrome c reacts with cardiolipin hydroperoxide faster than with hydrogen hydroperoxide.....	46
3.2. Cytochrome c release from liposomes depends on cardiolipin hydroperoxide concentration	46
3.3. Oxidized cardiolipin promotes cytochrome c covalent modifications.....	49
4. Discussion.....	51
5. Acknowledgments	55

6. References	56
Supplementary figures	59
Supplementary tables	65
CHAPTER 2	67
Highlights.....	68
Abstract.....	69
Abbreviations.....	70
1. Introduction	71
2. Materials and methods.....	73
2.1 Materials.....	73
2.2 Synthesis and purification of cholesterol hydroperoxide.....	74
2.3 Cytochrome c reaction with SDS micelles.....	74
2.4 Sodium dodecyl sulfate polyacrylamide gel electrophoresis (SDS-PAGE)	74
2.5 Bis-ANS binding.....	75
2.6 In-gel tryptic digestion of cytochrome c	75
2.7 nLC-MS/MS analysis.....	75
3. Results	77
3.1 7 α -ChOOH promotes an increase of cytochrome c hydrophobicity and a rapid conversion into dimer and trimer	77
3.2 7 α -ChOOH induces of dityrosine cross-links leading to cytochrome c dimerization	79
4. Discussion.....	82
5. Acknowledgements	87
6. References	87
Supplementary figures	92
CHAPTER 3	94
Abstract.....	95
Highlights.....	96
Abbreviation	97
1. Introduction	98
2. Materials and Methods	99
2.1 Materials.....	99
2.2 Animals	100
2.3 Blood plasma lipoprotein isolation by FPLC.....	100
2.4 Lipid extraction	101
2.5 Lipidomic analysis	101
2.6 Data processing	102
2.7 Statistical analysis	103

3. Results	103
3.1 Global lipidomic analysis of blood plasma in SOD1G93A rats	103
3.2 Panel of potential lipids markers in the plasma of SOD1G93A rats.....	108
3.3 Lipid profile of lipoproteins fractions	109
4. Discussion.....	111
5. Acknowledgments	113
6. References	114
Supplementary information	118
Supplementary figures	122
Supplementary methods.....	124
Supplementary tables.....	128
CHAPTER 4.....	133
Abstract.....	134
Highlights.....	135
Abbreviation	136
1. Introduction	137
2. Materials and Methods	139
2.1. Materials.....	139
2.2. Animals and Diets	139
2.3. Lipidomic Analysis	140
2.4. Data analysis	141
2.5. Statistical analysis	142
3. Results	142
3.1. Effect of high-fat diet on body weight, food intake and survival	142
3.2 Plasma lipidomic signature of ALS SOD1G93A fed a high-fat diet.....	143
3.3 Effect of high fat diets on plasma triglyceride, acylcarnitine, hexosylceramide and acylceramide in ALS.....	147
4. Discussion.....	149
5. Acknowledgments	154
6. References	154
Supplementary information	159
Supplementary figure.....	163
Supplementary tables.....	164
3. Final remarks.....	167
APPENDIX	171
CURRICULUM VITAE	173

1. Introduction

1.1. Lipids and their structural diversity

Lipids are defined as biological molecules that are generally hydrophobic in nature and in many cases soluble in organic solvents (1). Thus, they represent a diverse group of compounds, and their diversity is pivotal for their cellular functions. In fact, 5% of all human genes are devoted to lipid synthesis (2). Therefore, it is crucial to understand the extent of the structural diversity of lipids and how membranes differ in lipid composition before addressing the biological consequences of lipid diversity (3). Broadly speaking, to facilitate international communication, lipids can be classified into several categories, such as fatty acyls, glycerophospholipids, glycerolipids, sterol lipids, sphingolipids, prenol lipids and saccharolipids, whose structures is depicted in Figure 1 (1).

The huge structural diversity found in lipids arises from the biosynthesis of various combinations of these building blocks. The fatty acyl structure represents the most fundamental monomeric component of all lipid types. The fatty acyl group in the fatty acids and conjugates class is characterized by a repeating series of methylene groups that terminates in the carboxylic acid functional group. Fatty acids are categorized into different subclasses based on the length of the carbon, number of double bond position and hydroxylation (4). According to the number of double bonds fatty acids are classified in saturated (zero double bond), monounsaturated (one double bond) and polyunsaturated (more than two double bond). Among the unsaturated fatty acids, they can be further classified based on the position of the first double bond from the omega end. For instance, in omega-3 fatty acids, the first double bond occurs on the third carbon, but in omega-6 fatty acids, the first double bond is on the six-carbon atom, counting from the methyl end (denoted as omega) (3).

The major structural lipids in eukaryotic membranes are the glycerophospholipids, which have a glycerol backbone with combination of two fatty acids at the sn-1 and sn-2 positions.

The sn-1 fatty acid is usually saturated or monounsaturated, whereas the sn-2 fatty acid is more often monounsaturated or polyunsaturated (5). In addition, the head group consists of phosphate and an alcohol. The types of head groups in glycerophospholipids are choline, ethanolamine, serine, inositol or glycerol groups (2). Ether lipids are unique class of glycerophospholipids that have an alkenyl chain attached to the sn-1 position linked by an ether bond. The alcohol moiety attached to the phosphate group in ether lipids is generally choline or ethanolamine, but occasionally inositol or serine have also been observed (6). Other special glycerophospholipid with dimeric structure containing four acyl chains is named cardiolipin (7).

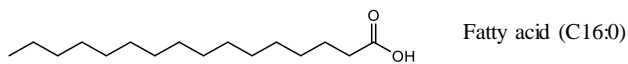
Sphingolipids constitute another class of structural lipids. Their chemical diversity arises from variations in the length and type of the sphingoid base, N-acyl chain and head group (8). Hydroxylation and unsaturation define the sphingoid base type, whereas the head group defines the sphingolipid name. The sphingoid base is composed by hydrocarbon chain (usually 18 carbons), with presence (ceramide) or absence of double bond (dihydroceramide) (9). The N-acyl chain is longer (from 16 to 30 carbons) and less unsaturated (from one to two double bonds) (3). The simplest sphingolipids are the ceramides, which consist of a sphingosine backbone linked to a fatty acid chain (10). They can be converted to more complex sphingolipid species by addition of phosphocholine (sphingomyelin), carbohydrates (glucosylceramide and galactosylceramide), phosphate and fatty acyl (acylceramide) groups (11).

Sterol, of which cholesterol and its derivatives are the most predominant forms in mammalian membranes, constitute an important component of membrane lipids, along with glycerophospholipids and sphingomyelins (2). Cholesterol is defined by its tetracyclic (A-D) ring structure. A double bond in the ring B between carbon atoms 5 and 6 confers rigidity to the molecule. The hydrophobic tetracyclic ring system is complemented by rather flexible iso-

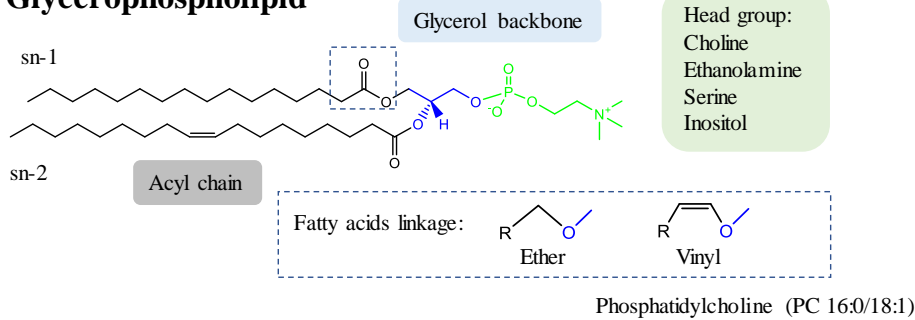
octanoyl chain. Thus, the only hydrophilic feature of cholesterol is a β -hydroxyl group at C3 position (12).

Glycerolipids are mono-, di-, and tri-substituted glycerol, the most well-known being the triglycerides. Variation in glycerolipids structure arises from the fatty acid chains, which can vary in length, functionalization and degree of saturation (13).

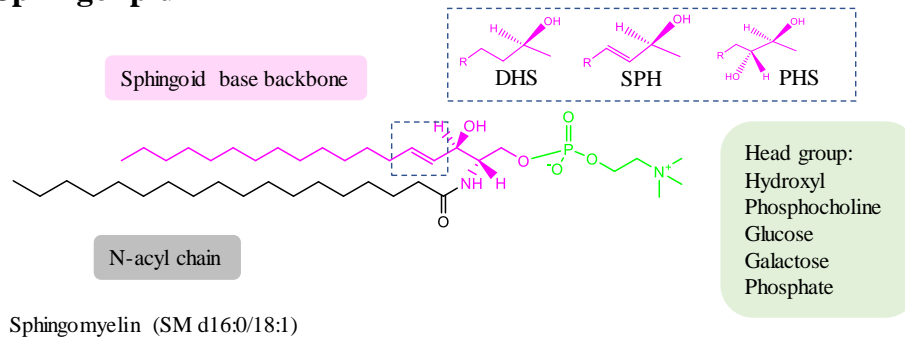
Fatty acyl



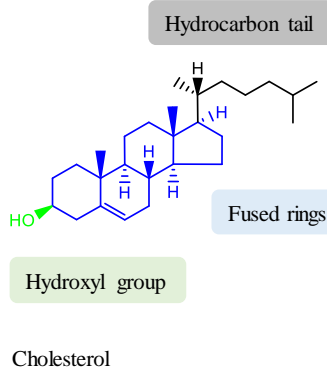
Glycerophospholipid



Sphingolipid



Sterol



Glycerolipid

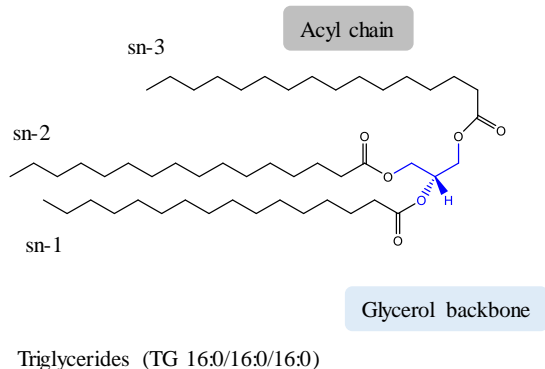


Figure 1. Structural diversity of membrane lipids in mammals. DHS, Sphinganine; SPH, sphingosine; DHS, PHS, 4-hydroxy-sphinganine. Adapted from (2)

1.2. Biological function of lipids

Lipids have several major functions in cells, including as membrane structural components (2), energy storage (14), signaling molecules (15), protein recruitment platforms (16) and substrates for posttranslational protein–lipid modification (17). Lipids are used for energy storage, principally as triglycerides and stearyl esters, in lipid droplets. They serve primarily as anhydrous reservoirs for the efficient storage of caloric reserves and as supply of fatty acid and sterol components that are needed for membrane biogenesis. The matrix of cellular membranes is formed by polar lipids, which consist of a hydrophobic and a hydrophilic portion. This fundamental principle of amphipathic molecules is an essential chemical property that cells required to segregate their internal constituents (cytosol and organelles) from the external environment. In addition to the barrier function, lipids provide membranes with the potential for budding tubulation, fission and fusion, characteristics that are essential for cell division, biological reproduction and intracellular membrane trafficking (3).

Lipids also regulate proteins function and structure. They recruit lipid-binding proteins or can be ligands for proteins, such as nuclear receptors thereby regulating protein activity. Lipids can act as first and second messengers in signal transduction and molecular recognition processes (3). The lipid mediators, such as prostaglandins, leukotrienes, lipoxins, eicosanoids, platelet-activating factor, lysophosphatidic acid, sphingosine 1-phosphate, for example, are produced by multistep enzymatic pathways, which are initiated by the de-esterification of membrane phospholipids by phospholipase A₂s or sphingomyelinase. Subsequently, lipid mediators exert their biological effects by binding to cognate receptors. In concert with others type of signaling molecules, such as neurotransmitters, hormones, and cytokines, lipid mediators are known to play important role in the regulation of cell proliferation and differentiation, inflammatory and immune responses (16).

Despite the fact that head groups of lipid categories determines their function, the molecular characteristics of fatty acids bonded to glycerophospholipids and sphingolipids may affect the biophysics properties of membranes and also could exerts signaling function (2). For instance, glycerophospholipids linked to polyunsaturated or short chain fatty acids provide more membrane fluidity than those esterified to monounsaturated or long chain fatty acids (18). As mentioned above, polyunsaturated fatty acid is classified as omega-6 and omega-3 fatty acids. Omega-6 fatty acids are represented by linoleic acid (C18:2) and omega-3 fatty acids by alpha-linolenic acid (C18:3). Both essential fatty acids are metabolized to longer-chain fatty acids of 20 and 22 carbon atoms. Linoleic acid is metabolized to arachidonic acid (C20:4) while alpha-linolenic acid is metabolized to eicosatetraenoic acid (C20:5) and docosahexaenoic acid (C22:6). Increasing the chain length and degree of unsaturation is achieved by adding extra double bond to the carboxyl end of the fatty acid molecule (Figure 2). There is competition between omega-6 and omega-3 fatty acids for the desaturation enzymes. Both fatty acid desaturase 1 (FADS1) and fatty acid desaturase 2 (FADS2) interferes with the desaturation and elongation of alpha-linolenic (19). Omega-3 and omega-6 fatty acids are not interconvertible, but they are metabolically and functionally distinct, and often have important opposing physiological effects, therefore their balance in the diet is important (19). The eicosanoid metabolic products from arachidonic acid, specifically prostaglandins, thromboxanes, leukotrienes, hydroxy fatty acids, and lipoxins, are formed enzymatically by cyclooxygenases, lipoxygenases and members of the cytochrome P450 (20). Those metabolites contribute to the formation of thrombi and atheroma; the development of allergic and inflammatory disorders, particularly in susceptible people, and cell proliferation (20). Thus, omega-6 fatty acids shifts the physiological state to one that is proinflammatory, prothrombotic, and proaggregatory, with increases in blood viscosity, vasospasm, vasoconstriction and cell proliferation (19). Moreover, these polyunsaturated fatty acids and

their hydroperoxy metabolites can be non-enzymatically converted by radical-induced peroxidation to bioactive mediators such as hydroxyalkenals (21).

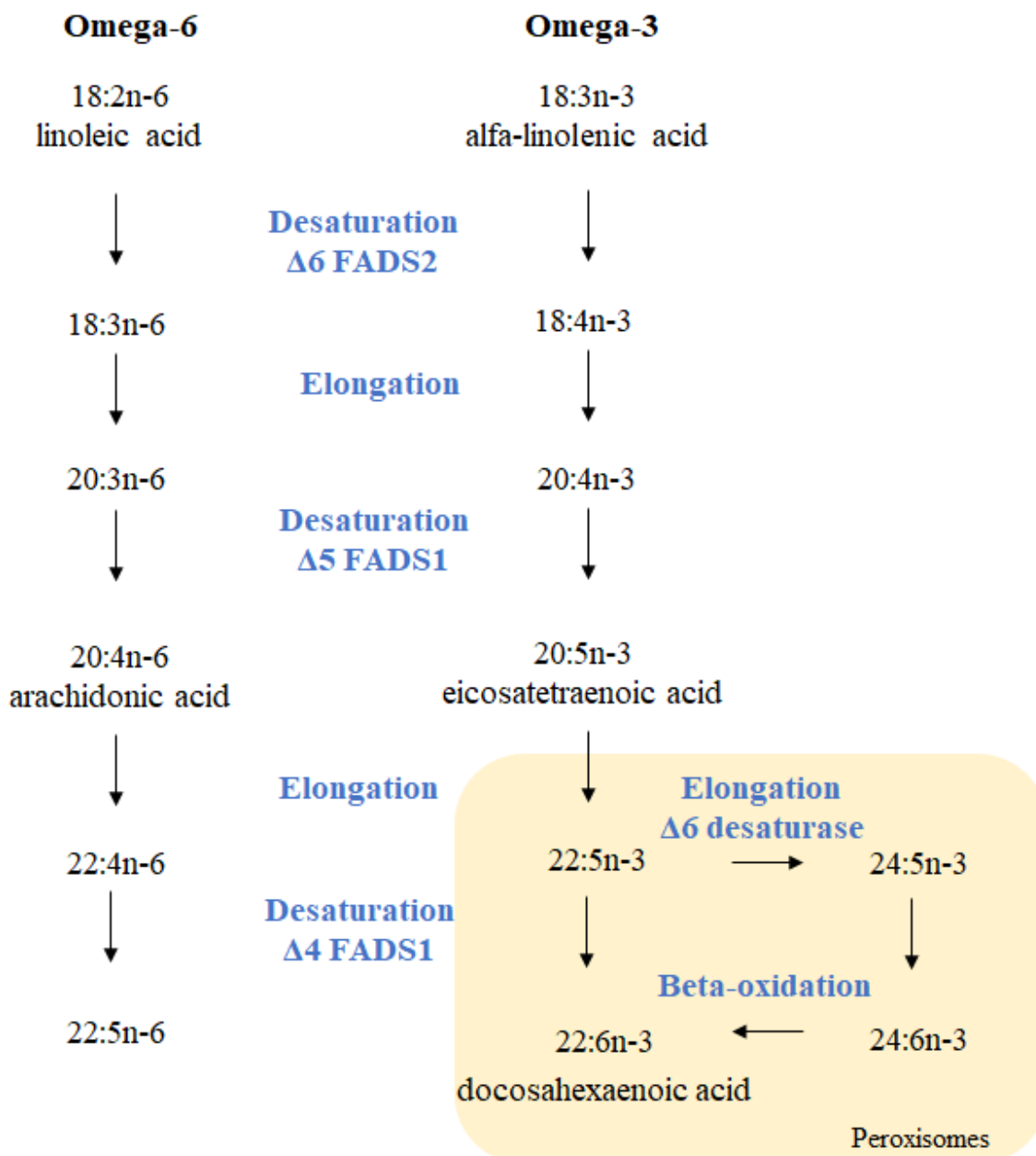


Figure 2. Desaturation and elongation of essential omega-3 (n-3) and omega-6 (n-6) fatty acids by the enzyme fatty acids desaturases FADS2 ($\Delta 6$) and FADS1 ($\Delta 5$).

1.3 Subcellular localization and synthesis of lipids

Lipids are distributed heterogeneously in several ranges: subcellular organelles show varied lipid arrangements, furthermore plasma membrane and organelle membrane present foci of

specific lipid domains, and finally lipid distribution shows lateral differences and/or transversal asymmetry (22). Although the endoplasmic reticulum is the main site of cholesterol and ceramide synthesis, these lipids are rapidly transported to other organelles. Indeed, the endoplasmic reticulum displays only low concentrations of sterol and complex sphingolipids and more unsaturated glycerophospholipids (2, 23). Mammalian Golgi is the main producer of sphingolipids: sphingomyelin, glucosylceramide and galactosylceramide, whose destination is the plasma membrane (24). In contrast to the endoplasmic reticulum, sterols are abundant in trans-Golgi (2).

Both sphingolipids and sterol are concentrated on the plasma membrane, which are packed at higher density than glycerophospholipids and resist to mechanical stress (2). Plasma membrane does not participate in autonomous synthesis of structural lipids. However, numerous reactions for either synthesizing or degrading lipids that are involved in signaling cascade have been described for the organelle (25). For sphingomyelin turnover, for example, the plasma membrane contains sphingomyelin synthase 2 (SM2), which allow the (re)synthesis of sphingomyelin from ceramide at plasma membranes (26). Furthermore, in eukaryotes, both leaflets of the plasma membrane contain specific lipid compositions. The outer leaflet of the plasma membrane mostly contains phosphatidylcholine and sphingolipids. The inner leaflet, in contrast, involves phosphatidylethanolamine, the negatively charged phosphatidylserine, and phosphatidylinositol (26). Plasma membrane nanodomains are enriched in cholesterol, sphingolipids and probably phosphatidylserine (3).

Early endosomes are similar to plasma membranes, but on maturation to late endosomes there is a decrease in sterol and phosphatidylserine followed by a significant increase in bis(monoacylglycerol)phosphate (27). A dedicate collection of kinases and phosphatases generate and terminate specific phosphoinositide (PI), among then phosphatidylinositol 3,4,5-triphosphate (PIP3) on early endosomes and phosphatidylinositol 3,5-biphosphate (PIP2) on

late endosomes (28). Lysosomal lipids are fully obtained by lipid transport from other organelles particularly through the budding and fusion of membrane vesicles. Low amounts of cholesterol and high amounts of sphingolipids characterize the lysosomal lipid signature (26).

Significant levels of lipid synthesis occur in the mitochondria. Lipids autonomously synthesized by mitochondria include phosphatidylglycerol, phosphatidic acid, cardiolipin, cytidine diphosphate diacylglycerol and in part phosphatidylethanolamine (29). These lipids are synthesized in a specific subfraction of endoplasmic reticulum called mitochondrial associated membrane (MAM). Mitochondrial lipid composition is mostly shared by all different mammalian cells and tissues and is characterized by low phospholipid to protein ratio and sterol to protein ratio versus other subcellular fractions. In addition, high levels of phosphatidylcholine and phosphatidylethanolamine (80% of total phospholipid), and high content of cardiolipin (10%–15% of total lipid composition) are found in mitochondrial membranes. In contrast, mitochondria are characterized by low sphingolipids and sterols amounts. Other exceptions are mitochondria from heart, brain and other tissue, which additionally contain 5% to 30% of phosphatidylcholine and phosphatidylethanolamine plasmalogens (26).

1.4 Lipid damage by reactive oxygen species

A free radical is any molecular species capable of independent existence and containing one or more unpaired electrons (30). Many free radicals exist in living systems, although most molecules *in vivo* are nonradicals. Reactive oxygen species (ROS) is a collective term that includes not only the oxygen radicals but also some nonradical derivatives of O₂ (30). These reactive species include among others hydroxyl radicals (OH[•]), peroxy radicals (ROO[•]), singlet oxygen (¹O₂), and peroxynitrite (ONOO⁻) formed from nitrogen oxide (NO). The ROS can be produced from either endogenous or exogenous sources. The endogenous source of

ROS includes mitochondria, peroxisomes and endoplasmic reticulum, whereas the exogenous source includes ionizing radiation, ultraviolet rays, tobacco smoke, pathogen infections, environmental toxins, and exposure to herbicide/insecticides. Since these free radicals are highly reactive, they can damage all three important classes of biological molecules including nucleic acids, protein and lipids (31). The membrane lipids, especially the polyunsaturated fatty acid residues of phospholipids are highly susceptible to oxidation by free radicals (32). The lipid peroxidation is very important *in vivo* because of its involvement in various pathological conditions. The lipid peroxidation results in loss of membrane functioning, for example, decreased fluidity, inactivation of membranes bound enzymes and receptors (33). The overall process of lipid peroxidation consists of three steps: initiation, propagation, and termination (34, 35). The lipid peroxidation is initiated, when any free radical attacks (e.g. OH^\bullet or $^1\text{O}_2$) and abstract hydrogen from a methylene groups (CH_2) from a polyunsaturated fatty acid (LH) which results in the formation of a carbon-centered lipid radical (L^\bullet). The lipid radical can react with molecular oxygen to form a lipid peroxy radical (LOO^\bullet) which is reactive enough to both oxidize membrane proteins and attack adjacent polyunsaturated side chains, propagating a chain reaction (36) (Figure 3). When the polyunsaturated chain has more than two double bonds, the resultant lipid peroxy radical undergo rearrangement via cyclization reactions and further oxygen addition and chain breaking reactions to form several reactive aldehydes, such as malondialdehyde (MDA) and 4-hydroxynonenal (4-HNE) (37).

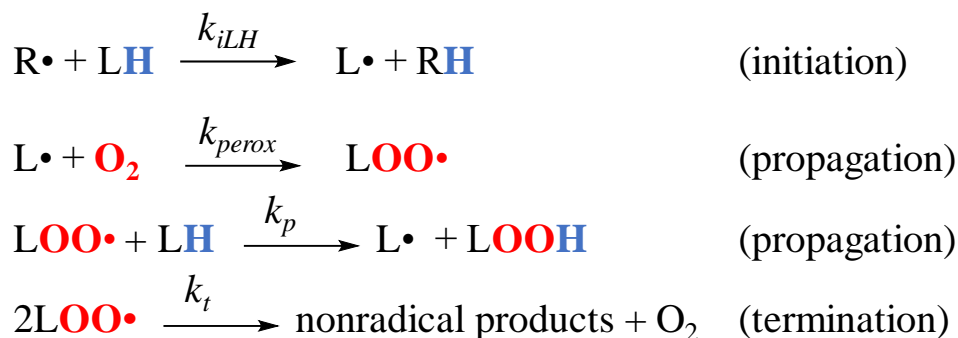


Figure 3. The lipid peroxidation reaction. There are three steps involved in nonenzymatic lipid peroxidation. The first step is the generation of lipid radicals (initiation). LH represents a polyunsaturated fatty acid moiety, and R• the highly energetic electron oxidant, such as a hydroxyl radical (OH•). The second step is the creation of new lipid radicals (propagation). Carbon-centered radical (L•) reacts rapidly with dioxygen producing lipid peroxy radical (LOO•). The final step is termination, either by antioxidants or another radical. $k_{iLH} = 6 \times 10^1 \text{M}^{-1}\text{s}^{-1}$; $k_{perox} = 10^9 \text{M}^{-1}\text{s}^{-1}$; $k_p = 6 \times 10^1 \text{M}^{-1}\text{s}^{-1}$ for linoleate; $k_t = 1 \times 10^5$ to $10^7 \text{M}^{-1}\text{s}^{-1}$. Adapted from (35).

Lipid peroxidation produces a wide variety of oxidation products. The main primary products of lipid peroxidation are lipid hydroperoxides (LOOH). The initial hydrogen abstraction from polyunsaturated fatty acid can occur at different points on the carbon chain, giving complex mixtures of peroxides. The lipid hydroperoxide may decompose *in vivo* through two-electron reduction, which can inhibit the peroxidative damage. The major enzymes responsible for two-electron reduction of hydroperoxides to corresponding alcohols are selenium-dependent glutathione peroxidases (GPx) and selenoprotein P (SeP) (38, 39), as well as peroxiredoxins (Prx) (40). Lipid hydroperoxides may also decompose *in vivo* through one-electron reduction and take part in initiation/propagation steps (34, 35), induce new lipid hydroperoxides, and feed the lipid peroxidation process. Lipid hydroperoxides can be converted to oxygen radical intermediates such as lipid peroxy radical (LOO•) and/or alkoxy (LO•) by redox cycling of transition metal ions, resulting in lipid hydroperoxide decomposition and the oxidized or reduced form of these metal, respectively (41). The continued oxidation of fatty acid side chains and the fragmentation of peroxides produce a huge number of secondary products (42),

which eventually can easily diffuse across membranes and can covalently modify any protein in the cytoplasm and nucleus, far from their site of origin (43).

1.5 Lipid in amyotrophic lateral sclerosis

Amyotrophic lateral sclerosis (ALS) is a fatal neurodegenerative disorder that is characterized by the progressive degeneration of both upper and lower motor neurons. The motor symptoms including muscle weakness, fasciculation, spasticity, dysphagia, and eventually respiratory dysfunction. Death occurs typically 3-5 years after diagnosis (44). ALS has long been recognized as a disease of motor neurons; however, increasing evidences suggest the involvement of extra-motor neurons and extraneural tissue in the pathogenesis of ALS (45). Consideration of incidence (frequency of new cases per year) and prevalence (the proportion of affected individuals in the population 1-2 and 4-6 per 100,000, respectively) understated the impact of ALS, with the lifetime risk at about 1 in 1000 (46). There are only a few clinical-epidemiological studies about ALS in Brazil. The incidence and prevalence rates (0.4 case/100,000 persons/year and 0.9-1.5 cases/100,000 persons, respectively) were estimated on data provided by a study performed in São Paulo City (47).

Most incidences of ALS are sporadic but ~10% of patients have a familial history. The first genetic mutations found to cause ALS, the gene superoxide dismutase or *SOD1*, was reported in 1993, with more than 50 additional potential ALS genes published since, although validating the causality of specific variants remains a challenge (44). As an important antioxidant, the normal function of SOD1 is to catalyze the conversion of highly reactive superoxide to hydrogen peroxide or oxygen. In familial ALS, cytotoxicity of motor neurons appears to result from a gain of toxic SOD1 function, rather than loss of dismutase activity (48). While the exact molecular mechanisms underlying mutant-SOD1-mediated motor neuron degeneration are unclear, prevailing hypotheses suggest a role for mutation-induced

conformational changes that lead to SOD1 misfolding and subsequent aggregation (49). The more than 170 ALS-causing mutations that have now been identified (<http://alsod.iop.kcl.ac.uk/>) lie in almost every region of the 153-aminoacid SOD1 polypeptide.

The identification of molecular mechanisms by which motor neurons degenerate in ALS is crucial for understanding disease progression and for the development of new therapeutic approaches. Although SOD1 mutations have been linked to ALS for more than two decades, the mechanisms underlying the mode of action of mutant SOD1 and the subsequent neurodegeneration/neurotoxicity are still unclear. The pathophysiological mechanism of the disease appears to be multifactorial and several mechanisms contribute to neurodegeneration. It is believed that mutant SOD1 stimulates oxidative stress and induces mitochondrial dysfunction, excitotoxicity, inflammation, and protein aggregation (50).

A growing number of *in vitro* and *in vivo* studies have begun to investigate metabolism as a means of explaining the neuropathology observed in ALS. While a number of metabolic hallmarks have been observed in ALS patients (51-53), interesting alterations in lipid handling mechanisms have also been noted to occur (52, 54). A major site of interest for lipid studies in ALS is skeletal muscle. Many studies have suggested that skeletal muscle is a major source of dysregulated lipid metabolism (55-57). Indeed, a defined switch from glucose-based to lipid-based metabolism is an early pathological event in ALS muscle (55). Furthermore, significant alterations in glycosphingolipid metabolism in the muscle of ALS mice impacts muscle innervation and motor recovery (56, 57). Thus, dysregulation in lipid metabolism in skeletal muscle has been linked to pathological outcomes. Similarly, altered levels of sphingomyelin, ceramides, cholesterol esters and omega-3 fatty acids have been observed in spinal cord of ALS patient and mutant SOD1 mice (56, 58). In accordance to these studies, our group found cholesterol esters and cardiolipin altered in spinal cord of mutant SOD1 rats

(Chaves-Filho et al., manuscript submitted). Additionally, recent study reported an extensive lipid remodeling involving phosphatidylcholine, ceramide and glucosylceramide in cerebrospinal fluid of ALS (59). Altogether, these findings strongly suggest intimate relationships between changes in lipid metabolism and ALS pathology.

Given the consistent observations of altered lipid metabolism in skeletal muscle, spinal cord and cerebrospinal fluid, research has begun to consider that systemic metabolism may correlate with ALS progression. Indeed, in mouse models of ALS, lipid catabolism and clearance to peripheral tissues are significantly increased (60). In ALS patients, several indices of dyslipidemia, including a high LDL/HDL cholesterol ratio, elevated total cholesterol or triglycerides and a high palmitoleic-to-palmitic fatty acid ratio, have been associated with a better prognosis (61). Nevertheless, it is clear that a more detailed characterization of the lipidome in plasma will be required for a deeper understanding of alterations in lipid metabolism linked to ALS.

1.6 Mass spectrometry-based lipidomics

Lipidomics is a newly emerged discipline that studies cellular lipids on a large scale based on analytical chemistry principles and technological tools, particularly mass spectrometry (62). The development of mass spectrometry (MS) techniques marked the beginning of a new era for the study of lipids, opening a series of unprecedented experimental opportunities. Indeed, the implementation of atmospheric-pressure ionization techniques such as electrospray ionization (ESI) and atmospheric pressure chemical ionization (APCI), capable of coupling liquid chromatography (LC) with MS, made it possible to separate and analyze even the most hydrophobic lipids with much greater accuracy than ever before possible (63).

A number of strategies have been introduced for the comprehensive analysis of cellular lipidomes, including targeted lipidomics, which focuses on the identification and

quantification of a single lipid or subset of lipids in a tissue or cellular extract, and so-called global lipidomics, which aims to identify and quantify all the lipids in a system (64). Such methods should have high mass accuracy and resolution, characteristics that can be obtained with time-of-flight and Orbitrap mass spectrometry. Both approaches have been advanced by innovations in MS and the parallel evolution of associated tools for data analysis (65, 66).

The ultimate goal of lipidomics is to understand the role of lipids in the biology of living organisms. It represents a rapidly evolving tool in system biology, which integrates multidisciplinary sets of data derived from molecular-profiling techniques such as genomics, transcriptomics, and proteomics. Therefore, there is a growing scientific interest in using lipidomics to answer various biological questions arising from living organisms with all degree of biological complexity, such as animals, plants, fungi, protists, bacteria, archaea, and viruses (63)

Since the emergence of the lipidomics discipline in 2003, the advancing analytical technologies have greatly driven the field to essentially all biological and biomedical areas. Lipidomics is a tool for investigation of clinical application, such as diabetes, obesity, arteriosclerosis, coronary heart disease and brain injuries, and so on (67). Therefore, this approach has led us to identify new signaling molecules, reveal the underlying mechanisms responsible for pathophysiological conditions, discover potential biomarkers for early diagnosis and prognosis of diseases, screen drug targets and/or test drug efficacy, guide nutritional intervention, and achieve personalized medicine (62). These accomplishments are due to not only technique development, but also to the nature of lipidomics in being able to comprehensively analyze hundreds to thousands of lipid species to study lipid metabolism (62).

References

1. Fahy E, Subramaniam S, Brown HA, Glass CK, Merrill AH, Murphy RC, et al. A comprehensive classification system for lipids. *Journal of Lipid Research*. 2005;46(5):839-62.
2. van Meer G, Voelker DR, Feigenson GW. Membrane lipids: where they are and how they behave. *Nature Reviews Molecular Cell Biology*. [Review Article]. 2008;9:112.
3. Harayama T, Riezman H. Understanding the diversity of membrane lipid composition. *Nature Reviews Molecular Cell Biology*. [Review Article]. 2018;19:281.
4. Tracey TJ, Steyn FJ, Wolvetang EJ, Ngo ST. Neuronal Lipid Metabolism: Multiple Pathways Driving Functional Outcomes in Health and Disease. *Frontiers in Molecular Neuroscience*. 2018;11:10.
5. Yamashita A, Hayashi Y, Matsumoto N, Nemoto-Sasaki Y, Oka S, Tanikawa T, et al. Glycerophosphate/Acylglycerophosphate Acyltransferases. *Biology*. 2014;3(4).
6. Braverman NE, Moser AB. Functions of plasmalogen lipids in health and disease. *Biochimica et Biophysica Acta (BBA) - Molecular Basis of Disease*. 2012;1822(9):1442-52.
7. Daum G. Lipids of mitochondria. *Biochimica et Biophysica Acta (BBA) - Reviews on Biomembranes*. 1985;822(1):1-42.
8. van Meer G, Lisman Q. Sphingolipid Transport: Rafts and Translocators. *Journal of Biological Chemistry*. 2002;277(29):25855-8.
9. Pruett ST, Bushnev A, Hagedorn K, Adiga M, Haynes CA, Sullards MC, et al. Biodiversity of sphingoid bases ("sphingosines") and related amino alcohols. *Journal of lipid research*. 2008;49(8):1621-39.
10. Pinto SN, Silva LC, Futerman AH, Prieto M. Effect of ceramide structure on membrane biophysical properties: The role of acyl chain length and unsaturation. *Biochimica et Biophysica Acta (BBA) - Biomembranes*. 2011;1808(11):2753-60.
11. Stith JL, Velazquez FN, Obeid LM. Advances in determining signaling mechanisms of ceramide and role in disease. *Journal of Lipid Research*. 2019;60(5):913-8.
12. Bukiya AN, Dopico AM. Common structural features of cholesterol binding sites in crystallized soluble proteins. *Journal of lipid research*. 2017;58(6):1044-54.
13. Karupaiah T, Sundram K. Effects of stereospecific positioning of fatty acids in triacylglycerol structures in native and randomized fats: a review of their nutritional implications. *Nutrition & Metabolism*. 2007;4(1):16.
14. Nakamura MT, Yudell BE, Loor JJ. Regulation of energy metabolism by long-chain fatty acids. *Progress in Lipid Research*. 2014;53:124-44.
15. Shimizu T. Lipid Mediators in Health and Disease: Enzymes and Receptors as Therapeutic Targets for the Regulation of Immunity and Inflammation. *Annual Review of Pharmacology and Toxicology*. 2009;49(1):123-50.
16. Saliba A-E, Vonkova I, Gavin A-C. The systematic analysis of protein–lipid interactions comes of age. *Nature Reviews Molecular Cell Biology*. [Perspective]. 2015;16:753.

17. Resh MD. Fatty acylation of proteins: The long and the short of it. *Progress in Lipid Research*. 2016;63:120-31.
18. Maulucci G, Cohen O, Daniel B, Sansone A, Petropoulou PI, Filou S, et al. Fatty acid-related modulations of membrane fluidity in cells: detection and implications. *Free Radical Research*. 2016;50(sup1):40-50.
19. Simopoulos AP. An Increase in the Omega-6/Omega-3 Fatty Acid Ratio Increases the Risk for Obesity. *Nutrients*. 2016;8(3):128.
20. Simopoulos AP. The Importance of the Omega-6/Omega-3 Fatty Acid Ratio in Cardiovascular Disease and Other Chronic Diseases. *Experimental Biology and Medicine*. 2008;233(6):674-88.
21. Roy J, Le Guennec J-Y, Galano J-M, Thireau J, Bultel-Poncé V, Demion M, et al. Non-enzymatic cyclic oxygenated metabolites of omega-3 polyunsaturated fatty acid: Bioactive drugs? *Biochimie*. 2016;120:56-61.
22. Hullin-Matsuda F, Taguchi T, Greimel P, Kobayashi T. Lipid compartmentalization in the endosome system. *Seminars in Cell & Developmental Biology*. 2014;31:48-56.
23. Antonny B, Vanni S, Shindou H, Ferreira T. From zero to six double bonds: phospholipid unsaturation and organelle function. *Trends in Cell Biology*. 2015;25(7):427-36.
24. Futerman AH, Riezman H. The ins and outs of sphingolipid synthesis. *Trends in Cell Biology*. 2005;15(6):312-8.
25. Di Paolo G, De Camilli P. Phosphoinositides in cell regulation and membrane dynamics. *Nature*. 2006;443(7112):651-7.
26. Casares D, Escriba PV, Rossello CA. Membrane Lipid Composition: Effect on Membrane and Organelle Structure, Function and Compartmentalization and Therapeutic Avenues. *Int J Mol Sci*. 2019;20(9).
27. Chevallier J, Chamoun Z, Jiang G, Prestwich G, Sakai N, Matile S, et al. Lysobisphosphatidic Acid Controls Endosomal Cholesterol Levels. *Journal of Biological Chemistry*. 2008;283(41):27871-80.
28. Platta HW, Stenmark H. Endocytosis and signaling. *Current Opinion in Cell Biology*. 2011;23(4):393-403.
29. Horvath SE, Daum G. Lipids of mitochondria. *Progress in Lipid Research*. 2013;52(4):590-614.
30. Halliwell B. Reactive Species and Antioxidants. Redox Biology Is a Fundamental Theme of Aerobic Life. *Plant Physiology*. 2006;141(2):312-22.
31. Dröge W. Free Radicals in the Physiological Control of Cell Function. *Physiological Reviews*. 2002 2002/01/01;82(1):47-95.
32. Siems WG, Grune T, Esterbauer H. 4-Hydroxynonenal formation during ischemia and reperfusion of rat small intestine. *Life Sciences*. 1995 1995/07/14;57(8):785-9.
33. Burton GJ, Jauniaux E. Oxidative stress. *Best Pract Res Clin Obstet Gynaecol*. 2011;25(3):287-99.

34. Girotti AW. Lipid hydroperoxide generation, turnover, and effector action in biological systems. *Journal of Lipid Research*. 1998;39(8):1529-42.
35. Yin H, Xu L, Porter NA. Free Radical Lipid Peroxidation: Mechanisms and Analysis. *Chemical Reviews*. 2011 2011/10/12;111(10):5944-72.
36. Aruoma OI. Free radicals, oxidative stress, and antioxidants in human health and disease. *Journal of the American Oil Chemists' Society*. 1998 1998/02/01;75(2):199-212.
37. Marnett LJ. Lipid peroxidation—DNA damage by malondialdehyde. *Mutation Research/Fundamental and Molecular Mechanisms of Mutagenesis*. 1999 1999/03/08;424(1):83-95.
38. Brigelius-Flohé R, Maiorino M. Glutathione peroxidases. *Biochimica et Biophysica Acta (BBA) - General Subjects*. 2013 2013/05/01;1830(5):3289-303.
39. Steinbrenner H, Sies H. Protection against reactive oxygen species by selenoproteins. *Biochimica et Biophysica Acta (BBA) - General Subjects*. 2009 2009/11/01;1790(11):1478-85.
40. Rhee SG. Overview on Peroxiredoxin. *Mol Cells*. 2016;39(1):1-5.
41. Valko M, Morris H, Cronin MTD. Metals, Toxicity and Oxidative Stress. *Current Medicinal Chemistry*. 2005;12(10):1161-208.
42. Esterbauer H, Schaur RJ, Zollner H. Chemistry and biochemistry of 4-hydroxynonenal, malonaldehyde and related aldehydes. *Free Radical Biology and Medicine*. 1991 1991/01/01;11(1):81-128.
43. Negre-Salvayre A, Coatrieux C, Ingueneau C, Salvayre R. Advanced lipid peroxidation end products in oxidative damage to proteins. Potential role in diseases and therapeutic prospects for the inhibitors. *British Journal of Pharmacology*. 153(1):6-20.
44. Taylor JP, Brown RH, Jr., Cleveland DW. Decoding ALS: from genes to mechanism. *Nature*. 539(7628):197-206.
45. Kim S-M, Kim H, Kim J-E, Park KS, Sung J-J, Kim SH, et al. Amyotrophic Lateral Sclerosis Is Associated with Hypolipidemia at the Presymptomatic Stage in Mice. *PLOS ONE*. 2011;6(3):e17985.
46. Boillée S, Vande Velde C, Cleveland Don W. ALS: A Disease of Motor Neurons and Their Nonneuronal Neighbors. *Neuron*. 2006;52(1):39-59.
47. Prado LdGR, Bicalho ICS, Vidigal-Lopes M, Ferreira CJA, Mageste Barbosa LS, Gomez RS, et al. Amyotrophic lateral sclerosis in Brazil: Case series and review of the Brazilian literature. *Amyotrophic Lateral Sclerosis and Frontotemporal Degeneration*. 2016;17(3-4):282-8.
48. Valentine JS, Doucette PA, Zittin Potter S. Copper -Zinc Superoxide Dismutase and amyotrophic lateral Sclerosis. *Annual Review of Biochemistry*. 2005;74(1):563-93.
49. Chattopadhyay M, Valentine JS. Aggregation of Copper–Zinc Superoxide Dismutase in Familial and Sporadic ALS. *Antioxidants & Redox Signaling*. 2009;11(7):1603-14.
50. Bonafede R, Mariotti R. ALS Pathogenesis and Therapeutic Approaches: The Role of Mesenchymal Stem Cells and Extracellular Vesicles. *Frontiers in cellular neuroscience*. 2017;11:80.

51. Jesús P, Fayemendy P, Nicol M, Lautrette G, Sourisseau H, Preux PM, et al. Hypermetabolism is a deleterious prognostic factor in patients with amyotrophic lateral sclerosis. *European Journal of Neurology*. 2018;25(1):97-104.
52. Dupuis L, Corcia P, Fergani A, Gonzalez De Aguilar JL, Bonnefont-Rousselot D, Bittar R, et al. Dyslipidemia is a protective factor in amyotrophic lateral sclerosis. *Neurology*. 2008;70(13):1004.
53. Desport JC, Torny F, Lacoste M, Preux PM, Couratier P. Hypermetabolism in ALS: Correlations with Clinical and Paraclinical Parameters. *Neurodegenerative Diseases*. 2005;2(3-4):202-7.
54. Dorst J, Kühnlein P, Hendrich C, Kassubek J, Sperfeld AD, Ludolph AC. Patients with elevated triglyceride and cholesterol serum levels have a prolonged survival in amyotrophic lateral sclerosis. *Journal of Neurology*. 2011;258(4):613-7.
55. Palamiuc L, Schlagowski A, Ngo ST, Vernay A, Dirrig-Grosch S, Henriques A, et al. A metabolic switch toward lipid use in glycolytic muscle is an early pathologic event in a mouse model of amyotrophic lateral sclerosis. *EMBO Molecular Medicine*. 2015;7(5):526.
56. Henriques A, Croixmarie V, Priestman DA, Rosenbohm A, Dirrig-Grosch S, D'Ambra E, et al. Amyotrophic lateral sclerosis and denervation alter sphingolipids and up-regulate glucosylceramide synthase. *Human Molecular Genetics*. 2015;24(25):7390-405.
57. Henriques A, Huebeker M, Blasco H, Keime C, Andres CR, Corcia P, et al. Inhibition of β -Glucocerebrosidase Activity Preserves Motor Unit Integrity in a Mouse Model of Amyotrophic Lateral Sclerosis. *Scientific Reports*. 2017;7(1):5235.
58. Cutler RG, Pedersen WA, Camandola S, Rothstein JD, Mattson MP. Evidence that accumulation of ceramides and cholesterol esters mediates oxidative stress-induced death of motor neurons in amyotrophic lateral sclerosis. *Annals of Neurology*. 2002;52(4):448-57.
59. Blasco H, Veyrat-Durebex C, Bocca C, Patin F, Vourc'h P, Kouassi Nzoughet J, et al. Lipidomics Reveals Cerebrospinal-Fluid Signatures of ALS. *Scientific Reports*. 2017;7(1):17652.
60. Fergani A, Oudart H, Gonzalez De Aguilar J-L, Fricker B, René F, Hocquette J-F, et al. Increased peripheral lipid clearance in an animal model of amyotrophic lateral sclerosis. *Journal of lipid research*. 2007;48(7):1571-80.
61. González De Aguilar J-L. Lipid Biomarkers for Amyotrophic Lateral Sclerosis. *Frontiers in Neurology*. 2019;10:284.
62. Yang K, Han X. Lipidomics: Techniques, Applications, and Outcomes Related to Biomedical Sciences. *Trends Biochem Sci*. 2016;41(11):954-69.
63. Astarita G, Ahmed F, Piomelli D. Lipidomic Analysis of Biological Samples by Liquid Chromatography Coupled to Mass Spectrometry. In: Armstrong D, editor. *Lipidomics: Volume 1: Methods and Protocols*. Totowa, NJ: Humana Press; 2009. p. 201-19.
64. Han X. Lipidomics: Developments and applications. *Journal of Chromatography B*. 2009;877(26):2663.
65. Wenk MR. The emerging field of lipidomics. *Nature Reviews Drug Discovery*. 2005;4(7):594-610.
66. Blanksby SJ, Mitchell TW. Advances in mass spectrometry for lipidomics. *Annu Rev Anal Chem (Palo Alto Calif)*. 2010;3:433-65.

67. Shamim A, Mahmood T, Ahsan F, Kumar A, Bagga P. Lipids: An insight into the neurodegenerative disorders. *Clinical Nutrition Experimental*. 2018 2018/08/01/;20:1-19.

2. Objective

2.1 General objective

In the present study, we investigated the role of lipids in protein aggregation and in amyotrophic lateral sclerosis.

2.2 Specific objectives

Chapter 1: To investigate the interaction between cytochrome c with cardiolipin hydroperoxide in a mimetic mitochondrial membrane.

Chapter 2: To investigate the interaction between cytochrome c with cholesterol hydroperoxide in a mimetic mitochondrial membrane.

Chapter 3: To characterize the plasma lipidome alterations of a rodent model of amyotrophic lateral sclerosis.

Chapter 4: To evaluate the effect of high fat diet on plasma lipidome of a rodent model of amyotrophic lateral sclerosis.

CHAPTER 1

Cytochrome c Modification and Aggregation Induced by Cardiolipin Hydroperoxides in a Mimetic Membrane Model

Isabella F D Pinto[†], Daniela da Cunha[†] and Sayuri Miyamoto*

Department of Biochemistry, Institute of Chemistry, University of Sao Paulo, Sao Paulo, Brazil.

[†]These authors contributed equally to this work.

* Corresponding Author: Sayuri Miyamoto. E-mail address: miyamoto@iq.usp.br

Institutional address: Departamento de Bioquímica, Instituto de Química, Av. Prof. Lineu Prestes 1524, CP 26077, CEP 05313-970, Butantã, São Paulo, SP. Brazil. Phone: + 55 11 30911413

Highlights

- Cardiolipin hydroperoxide reacts with cytochrome c at a reaction rate of $9.58 \pm 0.16 \times 10^2 \text{ M}^{-1} \text{ s}^{-1}$, which is two orders faster than with hydrogen peroxide.
- Binding analysis suggest that cardiolipin hydroperoxide may induce covalent binding of cytochrome c to liposomes.
- Using nLC-MS/MS, we have identified both 4-ONE and 4-HNE modification at lysine residues (K27, K72, K73 and K88) and histidine residue (H26), as well as dityrosine cross-links (Y48-Y74, Y48-Y97 and Y74-Y97).

Abstract

Cytochrome c (cytc) is a heme protein of 12 kDa that transfers electrons in the mitochondrial respiratory chain. Increased cytc peroxidase activity leads to cardiolipin oxidation, a hallmark of early apoptosis stage. Here we aimed to investigate the interaction between cytc with cardiolipin hydroperoxide (CLOOH) in a mimetic mitochondrial membrane. We estimated that cytc reacts with CLOOH at a reaction rate of $9.58 \pm 0.16 \times 10^2 \text{ M}^{-1}\text{s}^{-1}$, which is two orders faster than with H_2O_2 . Binding analysis revealed that most of cytc (ca. 96%) remains strongly attached to membranes containing cardiolipin CLOOH. Interestingly, cytc was only partly released from liposomes containing CLOOH by increasing the ionic strength of the medium. This result suggests that CLOOH may induce the covalent bind of the protein to the liposomes. Moreover, this binding was further demonstrated to be time-dependent SDS-PAGE analysis with dimeric and trimeric species observed in the first 15 min and increased high molecular weight aggregates formation afterwards. Using nLC-MS/MS, we have identified K72 and H26 consistently modified by 4-HNE, while K27, K73 and K88 were modified by 4-ONE. Further, dityrosine cross-linked peptides were characterized at residues Y48-Y74, Y48-Y97 and Y74-Y97. These covalent modifications may play a role in cytc oligomerization. Collectively, our findings suggest cytc-CLOOH reaction induce covalent binding of cytochrome c to membranes and protein cross-linking. Furthermore, H26, K27, K72, K73 and K88 represent potential sites for lipid electrophile-protein interaction.

Keywords: cytochrome c, cardiolipin monohydroperoxide, aggregation, dityrosine, aldehydes

Abbreviations

Amplex red: 10-acyl-3,7-dihydroxyphenoxazine

Bis-ANS: bis-anilinonaphthalene sulfonate

Cytc: cytochrome c

CL: cardiolipin

CLOOH: cardiolipin hydroperoxide

DPPC: dipalmitoyl phosphatidylcholine

H₂O₂: hydrogen peroxide

KCl: chloride potassium

TOCL: tetraoleoyl-cardiolipin

TLCL: tetralinoleoyl-cardiolipin

nLC-MS/MS: nano-liquid chromatography coupled to mass spectrometer

13(S)-HpODE: linoleic acid hydroperoxide

4-HNE: 4-hydroxynonenal

4-ONE: 4-oxo-nonenal

1. Introduction

Lipid-protein interactions are currently regarded as a key factor determining the structural and functional characteristics of membrane proteins. Cytochrome c (cytc), a small heme protein, is a component of the electron transport chain in the inner mitochondrial membrane (1, 2). During the last years, studies revealed the distinct affinity of cytc for anionic lipids (3). Among the different phospholipids capable of forming complexes with cytc, particular attention has been given to cardiolipin, which is responsible for the attachment of cytc to the inner mitochondrial membrane. Cardiolipin (CL), a unique phospholipid containing two phosphate group and four acyl chains (4). To date, the mechanisms underlying cytc-cardiolipin binding are rather well characterized by several techniques as nuclear magnetic resonance (5), surface plasmon resonance (6), infrared spectroscopy (7), atomic force microscopy (3) and fluorescence spectroscopy (8).

The interaction between cytc and cardiolipin is not only mediated by electrostatic, but also hydrogen bonding and hydrophobic interactions (9, 10). At least three cardiolipin binding sites on the cytc protein surface have been described. A-site accounts for electrostatic interactions between cytc and deprotonated phospholipids. C-site is responsible for the protein binding to the protonated phospholipids via hydrogen (8). And L-site, an additional electrostatic binding site on cytc (10). Hydrophobic interactions mediated C-site has been suggested to facilitated interaction of cytc between nonpolar acyl residues of lipid molecules (11) Interactions of cytc with anionic phospholipids are complex, and multiple factors can contribute to the unfolding capacity of the lipid but the molecular description is not complete (12)

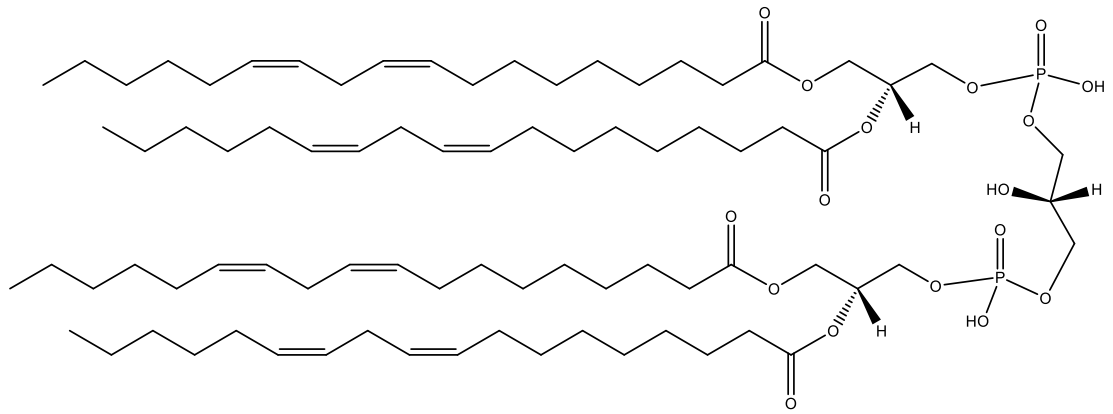
Physiological consequences of the association of cytc with cardiolipin are not restricted to its functioning as a component of the mitochondrial respiratory chain, but also are connected with ability of this protein to trigger apoptosis through a mechanism involving cardiolipin

oxidation and cytc release to cytosol (1, 13, 14). Despite the wealth of knowledge about the nature of cytc-cardiolipin interaction, key details of this process still remain unclear, especially in relation to its interaction with oxidized cardiolipin.

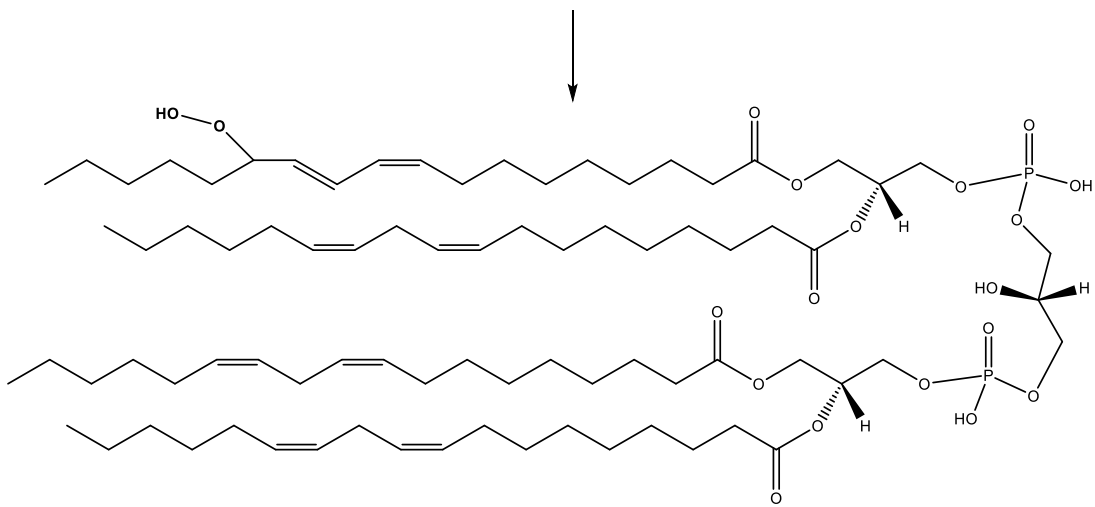
Several studies have described cytc modification induced by aldehydes derived from lipid peroxidation (15-18). For instance, the covalent addition of 4-hydroxynonenal (HNE) (16, 17), 4-oxo-nonenal (ONE), 4,5-epoxy-2-decenal (EDE), 9,12-dioxo-10-dodecenoic acid (DODE) (17) and 2,4-decadienal (DDE) (18) to cytc was reported. In addition, previous studies described cytc oligomerization via dityrosine cross-linking when cytc-CL complexes were incubated in presence of H₂O₂ (19-21).

Cardiolipin peroxidation generates, as primary products, several reactive hydroperoxides (Figure 1) (12). In a scenario where cardiolipin is oxidized, the appearance of such hydroperoxides seems to be a key triggering event of apoptosis (12). However, there has been a lack of information on cytc modifications resulting from its interaction with cardiolipin hydroperoxides.

In view of this, our study examined the interaction between cytc and cardiolipin hydroperoxides (CLOOH) in a mimetic membrane model. Our data showed that cytc reacts with CLOOH faster than H₂O₂. Conversely, the presence of CLOOH species in liposomal membranes led to cytc aggregation and sedimentation with the membrane fraction. In addition, we characterized the cytc modifications caused by electrophilic products derived from CLOOH breakdown or decomposition. Thus, we demonstrated 4-ONE and 4-HNE adducts on lysine and histidine residues as well as dityrosine cross-link.

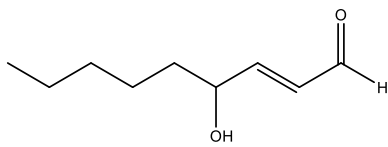


Tetralinoleoyl cardiolipin (TLCL)

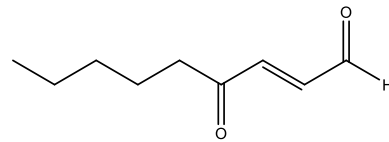


Monohydroperoxides

↓ decomposition



4-hydroxy-nonenal (4-HNE)



4-oxo-nonenal (4-ONE)

Figure 1. Chemical structures of tetralinoleoyl cardiolipin, cardiolipin monohydroperoxides and lipid electrophiles products.

2. Material and Methods

2.1. Materials

Bovine heart cytochrome c (Fe^{3+}), bovine cardiolipin, diethylenetriaminepentaacetic acid (DTPA), potassium chloride (KCl), hydrogen peroxide (H_2O_2), bicinchoninic acid (BCA), formic acid, methylene blue and HEPES were obtained from Sigma (St Louis, MO, USA). Tetraoleoyl cardiolipin (TOCL), dipalmitoyl phosphatidylcholine (DPPC) were purchased from Avanti Polar Lipids Inc (Alabaster, AL, USA). Amplex Red was acquired from Invitrogen (Eugene, Oregon, USA). Acetonitrile and methanol were purchased from J. T. Baker. All other reagents were analytical grade. All solutions were prepared using deionized water (Millipore, Mili-Q). Stock solutions of cytochrome c were prepared with deionized water and the concentration was calculated using molar absorptivity of $\epsilon_{409} = 1.06 \times 10^5 \text{ M}^{-1} \cdot \text{cm}^{-1}$ (22).

2.2. Synthesis and purification of cardiolipin hydroperoxide

Tetralinoleoyl-cardiolipin monohydroperoxide (CLOOH) was synthesized by photooxidation (23). Briefly, bovine cardiolipin (50 mg) was dissolved in 10 mL of chloroform in 50 mL round-bottomed flask followed by addition of 2 μL of methylene blue solution (100 mM in methanol). The solution was ice-cooled and irradiated using one tungsten lamp (500 W) for 1 h under continuous stirring in an oxygen-saturated atmosphere. After photooxidation the solution containing oxidized TLCL was evaporated, resuspended in methanol and loaded on a C8 reverse phase HPLC column (Luna C8, 250 x 6 mm, 5 μm ; Phenomenex, Torrance, CA, USA) for purification step. The column was eluted at flow rate of 5 mL/min. A gradient of solvent A (10 mM ammonium formate in water) and solvent B (methanol) was used as follows: 5 min, 90% B; 20 min, 97%B; 26 min, 97% B; 27 min, 90% B; 35 min, 90%B. The run was monitored at 205 nm for TLCL and 235 nm for CLOOH detection. Fractions of

eluent containing CLOOH were collected and dried by rotary evaporation. The dried residue was resuspended in methanol and quantified by iodometry (Buege & Aust, 1978). CLOOH was stored at -80°C for further use.

2.3. Liposome preparation

Large unilamellar liposomes containing DPPC, TOCL, TLCL(OOH)₁ or 13-(S)-HpODE were prepared by an extrusion technique (23). Briefly, individual phospholipids from stock solution in methanol were mixed followed by solvent evaporation under nitrogen atmosphere and vacuum to remove traces of solvent for 1h. The lipid film was hydrated in 5 mM HEPES buffer (pH 7.4) containing 100 μM of DTPA by vortexing for 1 min and extruded 21 times through a polycarbonate membrane with 100 nm pore size. Different liposome compositions were prepared according to the analysis to be performed (Supplementary Table S1-S4). The final concentration of liposomes in all experiments was 0.5 mM. All liposomes were prepared immediately before the experiment.

2.4. Cytochrome c-liposome binding assay

The following assay was used to evaluate cytc binding in liposome containing CLOOH. Thus, DPPC:TOCL:CLOOH liposomes (80:20, DPPC:CL_{total} proportion) containing variable concentration of CLOOH (0-200 μM) was incubated with cytochrome c (5 μM) in 5 mM HEPES buffer (pH 7.4) for 15 min at 25°C . The samples were centrifuged for 1h using a Beckman Coulter ultracentrifuge at 160,000 g for 1h at 4°C (9). After centrifugation, the supernatant was immediately removed, and its absorption spectrum measured at 410 nm. The measured absorption was converted to concentration of cytc using a standard curve (15).

To evaluate cytc binding to liposome containing CLOOH on high ionic strength buffer (250 mM KCl), DPPC:TOCL:CLOOH liposomes containing 5% and 20% of CLOOH were incubated with cytochrome c (5 μM) in 5 mM HEPES buffer (pH 7.4) for 15 min and 24 h at

25°C. After ultracentrifugation (160,000 g for 1h at 4°C) in absence or presence of 250 mM KCl, the supernatant was immediately separated from pellet and quantified by soret band absorption at 410 nm and by bicinchoninic acid (BCA) method (Stoscheck, 1990). CL total was considered as sum of TOCL and CLOOH.

2.5. Kinetics of the reaction of cytochrome c with lipid hydroperoxides

Determination of reaction rate of cytc with lipid hydroperoxides was performed using a spectrofluorimeter at 25°C. This assay was made using three different liposomes compositions: 1) DPPC:TOCL (80:20 proportion); 2) DPPC:TOCL:13-(S)-HpODE (variable concentrations, see Supplementary Table S3); 3) DPPC:TOLC: CLOOH (variable concentrations, see Supplementary Table S4). The final concentration of all liposomes was 0.5 mM.

For assays with H₂O₂, cytc (0.5 μM) was incubated with DPPC:TOCL liposome for 2 min followed by addition of 100 μM Amplex Red and H₂O₂ at 25 μM, 35 μM, 45 μM, 55 μM and 70 μM. The H₂O₂ concentration was calculated using $\epsilon_{240\text{nm}} = 39.4 \text{ M}^{-1} \text{ cm}^{-1}$. Immediately after H₂O₂ addition the reaction rate was monitored by resorufin formation using an excitation wavelength of 575 nm and emission wavelength of 585 nm.

For assays with 13-(S)-HpODE and TLCL(OOH)₁ were added 100 μM Amplex Red and cytc (0.5 μM) to liposomes containing DPPC:TOCL:13-(S)-HpODE and DPPC:TOLC:CLOOH. Reaction rate was monitored immediately after cytc addition for resorufin formation using an excitation wavelength of 575 nm and emission wavelength of 585 nm. The calculation was performed as previous described (24).

2.6. SDS Polyacrylamide gel electrophoresis (SDS-PAGE)

SDS-PAGE electrophoresis was performed to check the formation of cytc oligomers. Briefly, the samples diluted in Laemmli buffer (62 mM Tris-HCl buffer pH 6.8, 10% glycerol, 2%

SDS and 0.01% bromophenol blue) were loaded into a 15% acrylamide gel under nonreducing or reducing conditions after having been heated for 5 min. Gels were prepared containing acrylamide (15%), Tris-HCl buffer pH 8.8 (0.4 M), ammonium persulfate (0.1%) and SDS (0.1%) (Laemmli, 1970). Gels were run for 15 min at 80 V and for 75 min at 110 V. After electrophoresis run, the gels were stained with Coomassie or silver stains.

2.7. Size exclusion chromatography (SEC)

The incubated samples were loaded into Hiload 75 100/300 column. The size exclusion column was eluted with 50 mM PBS buffer at flow rate of 0.5 ml/min, and the absorption value monitored at 280 nm.

2.8. nLC MS/MS analysis

Cytochrome c (final concentration 25 μ M) was incubated with DPPC:CLOOH liposomes (80:20 proportion) for 1h30min at 25°C. After reaction an aliquot was analyzed by SDS-PAGE and another aliquot was submitted to digestion. For tryptic digestion 20 μ L of reaction was mixed to 20 μ L 0.2% Rapigest SF (Waters, Milford, MA, USA) at 56°C for 30 min. After cooling at room temperature, trypsin (Trypsin Gold, Mass spectrometry Grade, Pormega, USA) at 1:100 (trypsin:protein) was added and incubated overnight at 37°C. Hydrochloride acid (final concentration 200 mM) was added before an incubation for 45 min at 37°C followed by centrifugation at 14,000 g for 10 min at 4°C. Supernatant was separated in a clear tube, stored at -80°C until analyzed by nLC-ESI-MS/MS.

Tryptic peptides were injected into a reversed-phase nano-column BEH C18 1.7 μ m (100 μ m x 100 mm; Waters, Milford, MA, USA) coupled to nanoACQUITY UPLC System (Waters, Milford, MA, USA) and eluted at a flow rate of 400 nL/min (25). A gradient of solvent A (0.1% formic acid in water, v/v) and solvent B (acetonitrile containing 0.1% formic acid, v/v) was used as follows: 2% B initial condition run, 2% to 35% B in 60 min, 35% to 85% B in 1

min, 85% B for 4 min and 85% to 2% B in 4 min. ESI-MS/MS was performed with a Triple TOF 6600 instrument (Sciex, Concord, ON) equipped with a nanoSpray ion source. Mass spectra was acquired in positive mode set at 5kV source voltage, 100°C source temperature and 2 psi nebulizer gas (GS1) with declustering potential of 80 V. The instrument performed a survey TOF-MS acquisition from m/z 300-2000 (250 ms accumulation time) followed by MS/MS of the 25 most intense precursor ions charged of 2 to 5 from m/z 100-2000 (excluded for 4 s after occurrences) using data-dependent mode with total cycle time of 2.802 s. Each MS/MS was obtained by dynamic collision energy.

2.9. Data Analysis

Raw data as .wiff files were converted to .mgf files by Mascot Distiller software (Matrix Science Ltd, London) and then searched against Swiss-Prot protein database by MASCOT software (Matrix Science Ltd, London). The following parameters were specified: (i) enzyme trypsin, (ii) missed cleavage 3, (iii) variable modifications methionine oxidation, 4-HNE and 4-ONE modified histidine and lysine residue (shift mass 156.222 Da and 154.009 Da respectively), (iv) peptide tolerance 20 ppm, (v) MS/MS tolerance 0.3 Da. The peptide containing 4-HNE and 4-ONE modifications amino acids with $p < 0.05$ and peptide ion score were further confirmed by manually checking the MS/MS spectra. Dityrosine was searched using SIM-XL software (Lima et al., 2015). Data .mgf files were loaded into software and the parameters specified were: (i) dityrosine cross-link (-2.0156 Da), (ii) MS and MS/MS tolerance 20 ppm, (iii) enzyme trypsin, (iv) missed cleavage 3, (v) fragmentation method CID. The peptides cross-linked with score > 2 were manually sequenced using PeakView software (version 2.2, Sciex, Concord, ON) for visual inspection of MS/MS data.

2.10. Statistical analysis

Data are expressed as means \pm SD of at least three independent experiments. Changes in variables were analyzed by t test for two comparisons or by one-way ANOVA for multiple comparisons using GraphPad Prism 5 software. Statistical significance was considered for a p-value less than 0.05.

3. Results

3.1. Cytochrome c reacts with cardiolipin hydroperoxide faster than with hydrogen hydroperoxide

To study the reaction of cytc with CLOOH, we first determined the rate constants of cytc-CLOOH interaction at 25°C using a spectrofluorimeter (Table 1 and Supplementary Figure S1). We found that CLOOH was a better substrate for cytochrome c than H₂O₂. For instance, the rate constant for the reaction between cytc-CL complexes is quite low, $5.9 \times 10^1 \text{ M}^{-1} \cdot \text{s}^{-1}$, compared with reaction in presence of CLOOH, which is two orders of magnitude higher, $9.5 \times 10^2 \text{ M}^{-1} \cdot \text{s}^{-1}$. Similarly, the rate constant for cytc-CL complexes in presence of 13-(S)-HpODE, $6.9 \times 10^2 \text{ M}^{-1} \cdot \text{s}^{-1}$ was higher than H₂O₂.

Table 1. Rate constants (k_1) for cytochrome c/cardiolipin complex oxidation by R-OOH

R-OOH	$k_1 (\text{M}^{-1} \cdot \text{s}^{-1})$
H ₂ O ₂	$5.91 \pm 0.18 \times 10^1$
13(S)-HpODE	$6.91 \pm 0.30 \times 10^2$
CLOOH	$9.58 \pm 0.16 \times 10^2$

The calculation was done as described by Belikova et al., 2009.

3.2. Cytochrome c release from liposomes depends on cardiolipin hydroperoxide concentration

Cytc binding to a mitochondrial mimetic membrane was evaluated by measuring the amount of soluble protein (i.e., free cytc not bound to liposomes) in the supernatant obtained after ultracentrifugation (160,000 g for 1h at 4°C). Consistent with previous findings, cytc was scarcely associated to liposomes containing only phosphatidylcholine (without cardiolipin) (26). In contrast, almost all cytc became attached to membranes when liposomes contained cardiolipin (DPPC:CL; 80:20 mol%), confirming that cytc-membrane association was of electrostatic nature (Figure 2). In the presence of increasing percentages of synthetic cardiolipin hydroperoxides (CLOOH, 15%-100%), we observed that membranes containing 15%-50% CLOOH did not induce cytc detachment. A small increase in the unbound form of cytc was observed only when all cardiolipin was replaced by CLOOH (Figure 2).

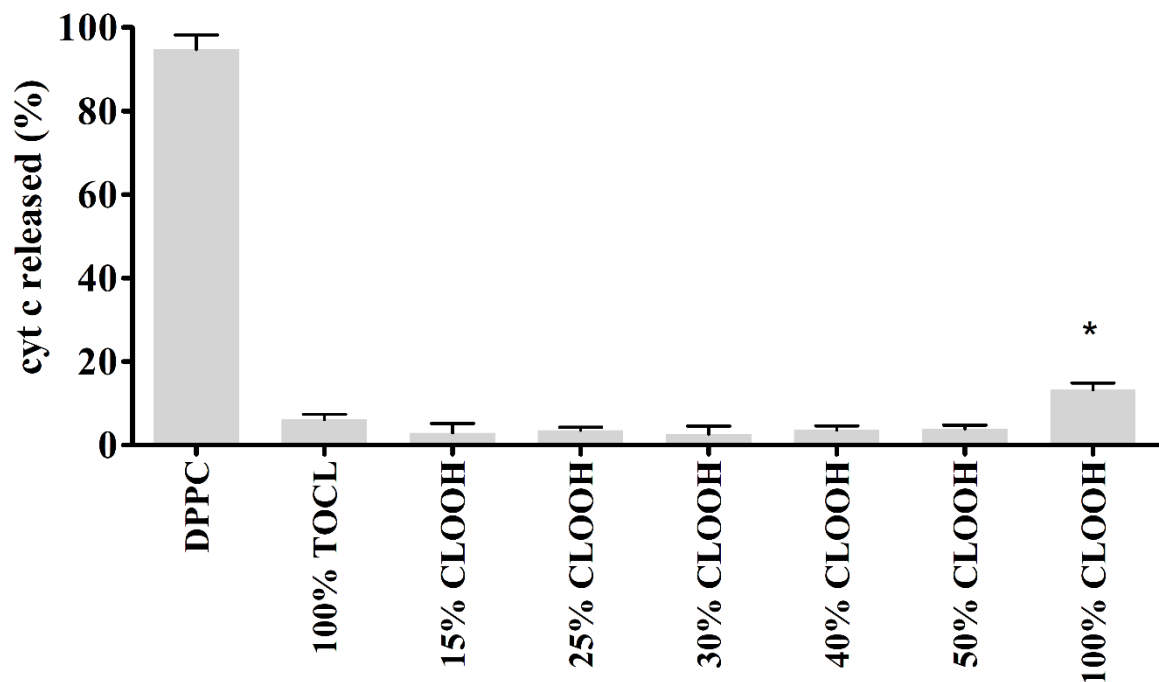
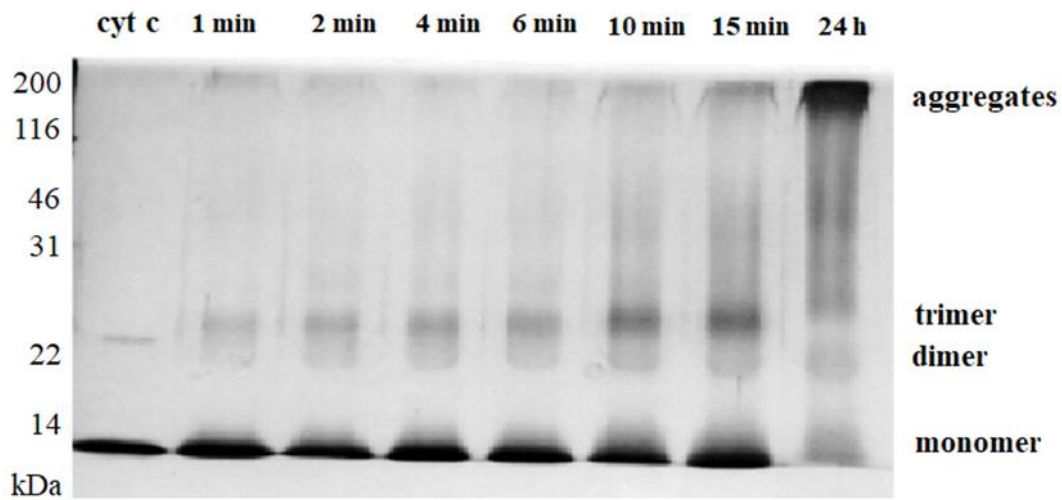


Figure 2. Cytochrome c is kept strongly bound to membranes containing up to 50 % CLOOH. Unilamellar liposomes containing non-oxidized cardiolipin (TOCL) and increasing percentages of cardiolipin hydroperoxide (CLOOH) were used as model for mitochondrial membranes. Membranes containing 15%, 25%, 30%, 40%, 50% and 100 % of cardiolipin in its oxidized form (CLOOH) were prepared by mixing DPPC:TOCL:CLOOH at the following ratios 80:20:0, 80:17:3, 80:15:5, 80:13:7, 80:11:9, 80:10:10 and 80:0:20. Free cytochrome c was determined by measuring cytc absorption at 410 nm. One-way ANOVA followed by Bonferroni post-hoc test was used. Values are the means \pm SD (n=3). *p<0.01 *versus* DPPC, 100% TOCL and 15%-50% CLOOH.

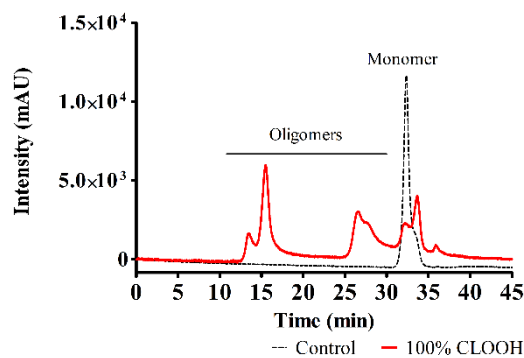
To better characterize the nature of membrane-bound cytc population formed in the presence of CLOOH, both the supernatant (S) and the liposomal pellet (P) fractions obtained after ultracentrifugation were analyzed by SDS-PAGE (Supplementary Figure 2). As expected, cytc monomers were observed in the supernatant fraction of samples containing only cytc or cytc+DPPC liposomes, as well as in the pellet fraction of DPPC:TOCL liposomes. In contrast, an intense band of high molecular weight cytc aggregates were observed in the presence of 25% or 100% of CLOOH. Cytc aggregates were mostly detected in the pellet fractions of membranes containing 25% CLOOH as well as in the supernatant fractions of incubations containing 100% CLOOH. Thus, it can be concluded that CLOOH promotes extensive cytc aggregation.

The aggregation kinetics was evaluated by SDS-PAGE at 1 min, 2 min, 4 min, 6 min, 10 min, 15 min and 24 h of reaction (Figure 3A). Interestingly, cytc dimers, trimers and high molecular aggregates were formed consecutively in a time-dependent manner. The cytc oligomers formed at 15 min incubation were also checked by size exclusion chromatography (Figure 3B). Three major peaks were observed in the chromatogram: cytc monomer at 32 min, dimer and trimer species at 25-30 min, and high molecular aggregates at 15 min. Besides the formation of high molecular aggregates, we also checked alterations in the overall protein hydrophobicity (Figure 3C). Bis-ANS was used as hydrophobic fluorescence probe to evaluate changes in protein structure occurring upon cytc binding to CLOOH-containing liposomes. CLOOH promoted an increase in fluorescence intensity of bis-ANS when compared to control. These results suggest an extended change in cytc structure in presence of CLOOH.

A



B



C

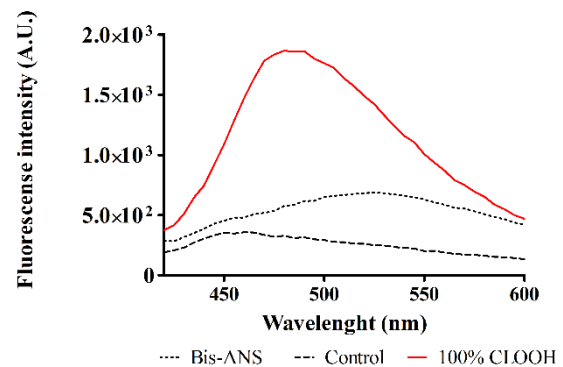


Figure 3. Cardiolipin hydroperoxides promotes cytc oligomerization to dimer, trimer and high molecular weight aggregates. (A) Time-dependent analysis of cytc oligomerization by SDS-PAGE. Cytc (5 μ M) was quickly mixed with liposomes containing cardiolipin hydroperoxide (DPPC:CLOOH; 80:20 mol%) at 25°C for 1-15 min and 24 h. Samples were loaded onto the gel and electrophoresis was run in 15% SDS-PAGE with 5% stacking gel. The gel was stained with silver stains. (B) Size-exclusion chromatography analysis cytc oligomers formed after 15 min incubation. Cytc and its oligomers were separated on Hiloal 75 100/300 column, eluted with 50 mM PBS buffer at flow rate of 0.5 ml/min., and monitored at 280 nm. (C) CLOOH-containing liposomes promotes an increase of cytc hydrophobicity. Fluorescence quenching spectra of bis-ANS bound to cytc in presence of 100% CLOOH-containing liposomes as described in Materials and Methods.

3.3. Oxidized cardiolipin promotes cytochrome c covalent modifications

To characterize cytc post-translational modifications formed in the presence of CLOOH, we performed a proteomic analysis using trypsin to digest the modified protein. Trypsin typically

cleaves at lysine and arginine amino acids residues. Thus, the peptides obtained were analyzed by high resolution nLC-MS/MS. Incubation of cytc with CLOOH-containing liposomes resulted in eight major modified peptides by 4-HNE and 4-ONE adducted at lysine and histidine residues. Besides that, we also characterized dityrosine cross-linking at Y97, Y74 and Y48 residues (Table 2).

4-ONE modified peptides at lysine residue were identified at K27, K73 and K88 (Supplementary Figure S4). We found an increase of 154 Da in the b7 and b9 ion in the peptide $^{88}\text{KGEREDLIAYLKK}^{100}$ with 4-ONE adduct at K88 (Supplementary Figure S4A). Similarly, an increase of 154 Da was observed in the b1, b3 and b6 ion in the peptide $^{73}\text{KYIPGTK}^{79}$ with 4-ONE adduct at K73 (Supplementary Figure S4B). Finally, 4-ONE adduction was observed in the b8 and b9 ion in the peptide $^{26}\text{HKTGPNLHGLFGR}^{38}$ at K27 with increase of 154 Da (Supplementary Figure S4C).

Besides 4-ONE modified peptides, we also identified 4-HNE induced modifications (Supplementary Figure S5). 4-HNE-modified peptides contained diagnostic product ion at m/z 139.11 and 266.19, in case of histidine modification, related to the dehydrated protonated 4-HNE and immonium ion of 4-HNE-modified histidine, respectively. We found an increase of 156 Da in the b8 and b12 ion in tryptic peptide $^{26}\text{HKTGPNLHGLFGR}^3$ for 4-HNE adduct at H26 (Supplementary Figure S5A). Similarly, we found an increase of 156 Da in the y2, y3, y4, y5, y6, y7, y8, y10, y11, y13 ion fragmentation of tryptic peptide $^{56}\text{GITWGEETLMEYLENPK}^{72}$ for Michael adduct at K72 (Supplementary Figure S5B).

Considering the propensity of tyrosine residues to undergo crosslinking reactions we also searched for this modification. We identified three major cross-links involving tyrosine residues Y48, Y74 and Y97: Y48-Y97, Y48-Y74 and Y74-Y97 (Table 2). Fragments y3, y4, y5 and y6 ions contained the cross-linking Y74-Y97 (Supplementary Figure S6A), whereas fragments y6 and y7 ions contained the cross-linking Y48-Y74 (Supplementary Figure S6B)

and fragments y7, y10 and y11 contained the cross-linking Y48-Y97 (Supplementary Figure S6C). Thus, this data demonstrates that cytc oligomerization observed in the presence of CLOOH probably involves dityrosine cross-linking. However, additional mechanisms, possibly including cross-linking by bifunctional secondary products of lipid peroxidation (e.g. dialdehydes) can be considered (19)

Table 2. Cytochrome c modifications formed after incubation with liposomes containing cardiolipin hydroperoxide (CLOOH).

Peptides	Theor. m/z	Obs. m/z	Modif.	Error (ppm)
²⁶ HKTGPNLHGLFGR ³⁸	1432.768	398.228(4+)	4-HNE (H26) ¹	0.4
²⁶ HKTGPNLHGLFGR ³⁸	1432.768	397.728(4+)	4-ONE (K27)	1.4
⁵⁶ GITWGEETLMEYLENPK ⁷²	2008.945	722.6903(3+)	4-HNE (K72) ¹	2.3
⁷³ KYIPGTK ⁷⁹	805.469	480.793(2+)	4-ONE (K73)	2.0
⁸⁸ KGEREDLIAYLKK ¹⁰⁰	1561.882	430.002(4+)	4-ONE (K88)	0.3
⁹² EDLIAYLK ⁹⁹ - ⁷³ KYIPGTK ⁷⁹	1767.989	442.752(4+)	DiTyr (Y97-Y74)	1.3
⁴⁰ TGQAPGFSTYDANK ⁵³ - ⁷⁴ YIPGTK ⁷⁹	2132.030	533.761(4+)	DiTyr (Y48-Y74)	3.1
⁴⁰ TGQAPGFSTYDANK ⁵³ - ⁹² EDLIAYLK ⁹⁹	2418.182	806.731(3+)	DiTyr (Y48-Y97)	1.1

Data were obtained as described in the Materials and Methods. The residue number is based on the sequence of mature protein minus methionine initial residue.

Mass spectra of peptide are showed in the Supporting Information.

Theoretical mass corresponds to unmodified peptide.

¹MA: Michael addition

Dityr: Dityrosine.

4. Discussion

Cytochrome c is an electron carrier between mitochondrial respiratory complexes III and IV, but under certain conditions interactions of cytc with cardiolipin are important for apoptotic

functions of this protein. When bound to cardiolipin, cytc catalyzes cardiolipin peroxidations, which contributes to the protein release into the cytosol and initiate the caspases cascade of proteolytic reactions designated as apoptosis (27, 28). However, their specific mechanism of binding is still not completely understood. Since cardiolipin peroxidation plays an important role in cytc release into the cytosol (13), this finding encouraged us to study the interaction of cytc between CLOOH in a mitochondrial mimetic membrane model.

Here we have demonstrated that CLOOH was better substrate for cytc than H_2O_2 (Table 1). Overall the rates of amplex red oxidation by cytc complex were about 1.1-1.6 orders of magnitude higher in the presence of linoleic acid hydroperoxide (13(S)-HpODE) and CLOOH than H_2O_2 . The difference between CLOOH and H_2O_2 may be associated with a distinct reaction mechanism. Cytc may split CLOOH predominantly via heterolytic mechanism as proposed for the reaction of cytc-CL complexes with fatty acid hydroperoxides (24), whereas H_2O_2 undergo homolytic cleavage (24, 29), whereas. The homolytic mechanism involves one-electron reduction of hydroperoxide and yields an O-centered radical from peroxide. Conversely, two-electron reduction of peroxide via the heterolytic pathway produces alcohol and no free-radical intermediates. Heterolytic peroxidase catalysis commonly involves participation of histidine and arginine residues (30, 31).

Moreover, given the rate constant of cytc-CLOOH reaction, we also showed *in vitro* that CLOOH keeps cytc strongly attached to the membrane (Figure 2). This attachment could not be reversed in the presence of ionic strength buffer containing 250 mM of KCl (Supplementary Figure S2). Cytc interacts electrostatically with membranes containing acidic phospholipids (such as CL that bears two negative charges) due to its net positive charge +8e at neutral pH, and this interaction is very sensitive to ionic strength (24). Analysis of the effects of ionic strength and mutations suggest that cytc binding to CL containing membranes is guided by electrostatic forces but hydrophobic interactions also play a role (9, 26, 32-34).

This study also showed that CLOOH-containing liposomes induced cytc oligomerization that ultimately leads to protein aggregation. Oligomeric species of cytc as dimers, trimers and high molecular weight aggregates were detected using SDS-PAGE and size exclusion chromatography (Figure 3). Due to high local concentration of cytc in mitochondria (0.5 to 5 mM in the intermembrane space), protein oligomerization and aggregation are important to consider (32). Cyt c oligomerization has been previously identified upon cytc reaction with non-oxidizable cardiolipin (TOCL), TLCL (19), H₂O₂ (15, 29) and cholesterol hydroperoxide (77). Tyurina et al. demonstrated that peroxidase reaction of cytc/cardiolipin complexes in presence of H₂O₂ increased fluorescence characteristic of dityrosine suggesting these oligomers can be formed through cross-linking via dityrosine formation (19). However, oxidative oligomerization involves not only dityrosine cross-linking, but also additional mechanism, possibly including cross-linking by dysfunctional secondary product of lipid peroxidation (19). It is important to mention that protein oligomers could also result from protein hydrophobic interaction, generating non-covalent species resistant to SDS treatment (15). Non-covalent cytc oligomers are known to be formed when the protein is treated with ethanol 60% (v/v), but this species seem to be stable only at low temperature, being converted back to the monomers when heated at 70 °C for 5 min (35).

Thus, to get more insights into the mechanisms involved in CLOOH induced cytc aggregation, mass spectrometry experiment was conducted to characterize the nature of cytc oligomers. We identified peptides from cytc adducted with electrophiles products from CLOOH decomposition (Table 2). The predominant adduct resulting from modification of peptides by 4-HNE and 4-ONE had a mass of 156 and 154 Da, respectively. These lipid aldehydes were probably derived from CLOOH breakdown. The reaction of cytc with 4-HNE had been examined previously by Isom et al. and confirmed by Williams et al., they showed that HNE forms several adducts including a Michael adduct on H33 (16, 17). We did not see

HNE adduction on H33 but on H26 and K72. The reaction of cyt c with 4-OONE was performed by Williams et al., who showed that 4-OONE forms several adducts on K5, K7, K8, K99 and K100. In contrast, here we identified covalent modification by 4-OONE on K27, K73 and K88. Different to previously reported, we did not use isolated aldehydes, but rather these lipid electrophiles were generated *in situ* from CLOOH decomposition in the presence of cyt c. Many studies have examined the site of cyt c and cardiolipin interactions. Three distinct sites on the cyt c surface have been suggested for interaction with cardiolipin: the A-site, formed by K72, K73, K86 and K87; the C-site, located near N52 (8); and L site involving K22, K27, H33, K25 and H26, that operates at low pH (10). Thus, our results can help to understand the site at which bifunctional electrophilic products are probably formed through lipid and protein interaction, as well as the site on the cyt c that occurs this interaction (Figure 4).

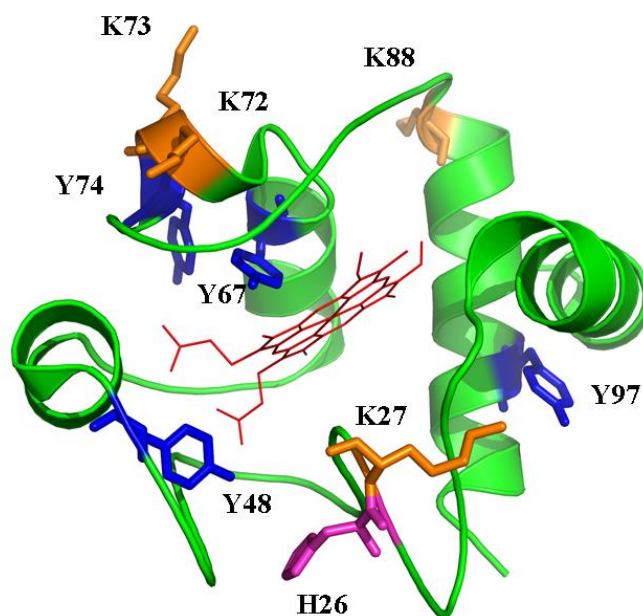


Figure 4. Native structure of bovine cytochrome c showing modified amino acid residues. Tyrosine (blue), lysine (orange) and histidine (pink) residues are highlighted in the structure of cyt c (PDB code 2B4Z). Residues numbers are given.

Besides the identification of protein alkylation sites, three major dityrosine cross-linked peptides were detected (Table 2). Tyrosine residues – via the generation of tyrosyl radicals – are linked reactive intermediates of the peroxidase cycle leading to cardiolipin peroxidation. A protein-derived tyrosyl radical formed during peroxidase reaction of cytc-cardiolipin complex can isomerize and combine with another tyrosyl radical with subsequent enolization. As a result, a stable, covalent, carbon-carbon bond is generated, yielding 1,3-dityrosine (19). Cyt c has four tyrosine residues some of which are located close to heme moiety and some are present on the surface of the protein. In interaction of cytc with cardiolipin results in partial unfolding of the protein and tyrosine residues in the complex formed may readily interact with both heme and polyunsaturated fatty acid chains (19). The highly conserved Y67 was found as the primary electron-donor (radical acceptor) in the oxygenase half-reaction of the cytochrome c/cardiolipin peroxidase complex (36). Several oxidizing systems were found to produce dityrosines during oxidant exposure of both purified proteins *in vitro* and intact cells (37, 38).

In summary, our results showed that cytc reacts with cardiolipin hydroperoxides faster than with H₂O₂. In addition, our data showed that cytc reacts with CLOOH producing electrophiles capable to form covalent adducts with the protein, as well as protein radical tyrosyl radicals responsible for protein aggregation by dityrosine cross-linking. The covalent modifications in lysine and tyrosine residues of cytc may contribute to protein aggregation and improve binding of cytc to the mitochondrial membrane. Physiological role(s) of cytc aggregates warrant further studies.

5. Acknowledgments

This study was supported by Fundação de Amparo à Pesquisa do Estado de São Paulo [FAPESP, CEPID–Redoxoma Grant 13/07937-8], Conselho Nacional de Desenvolvimento Científico e Tecnológico [CNPq, Universal 424094/2016-9], Coordenação de

Aperfeiçoamento de Pessoal de Nível Superior [CAPES, Finance Code 001] and Pro-Reitoria de Pesquisa da Universidade de São Paulo [PRPUSP]. The PhD scholarship of Isabella F. D. Pinto was supported by FAPESP [Grant 2014/11556-2].

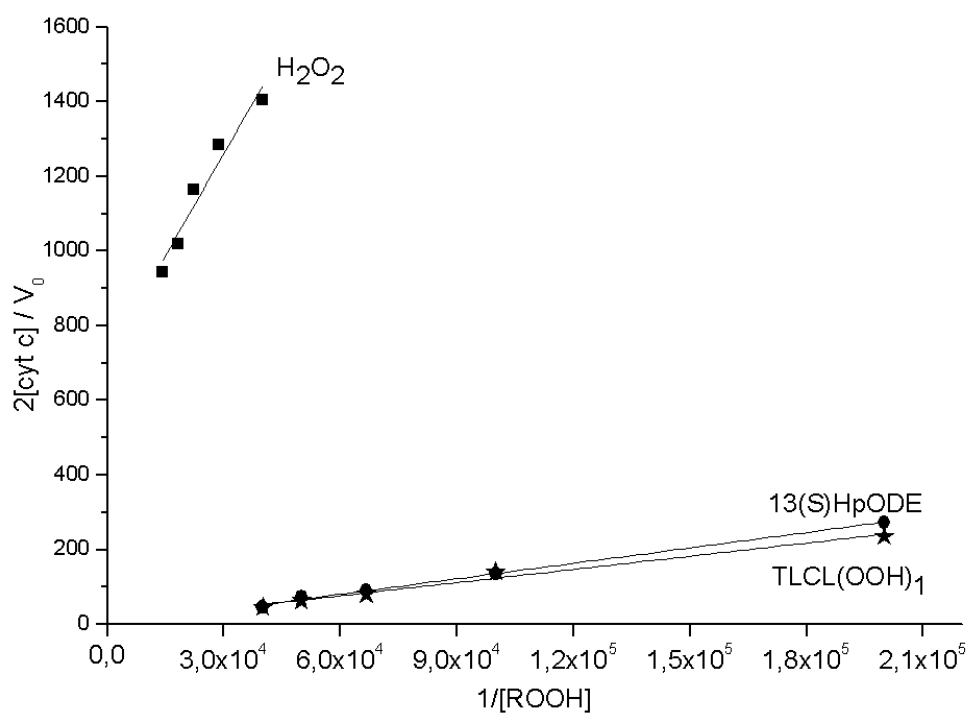
6. References

1. Ow Y-LP, Green DR, Hao Z, Mak TW. Cytochrome c: functions beyond respiration. *Nature Reviews Molecular Cell Biology*. [Review Article]. 2008;9:532.
2. Hüttemann M, Pecina P, Rainbolt M, Sanderson TH, Kagan VE, Samavati L, et al. The multiple functions of cytochrome c and their regulation in life and death decisions of the mammalian cell: From respiration to apoptosis. *Mitochondrion*. 2011;11(3):369-81.
3. Choi EJ, Dimitriadis EK. Cytochrome c Adsorption to Supported, Anionic Lipid Bilayers Studied via Atomic Force Microscopy. *Biophysical Journal*. 2004;87(5):3234-41.
4. Hübner W, Mantsch HH, Kates M. Intramolecular hydrogen bonding in cardiolipin. *Biochimica et Biophysica Acta (BBA) - Biomembranes*. 1991;1066(2):166-74.
5. Brown LR, Wüthrich K. NMR and ESR studies of the interactions of cytochrome c with mixed cardiolipin-phosphatidylcholine vesicles. *Biochimica et Biophysica Acta (BBA) - Biomembranes*. 1977;468(3):389-410.
6. Salamon Z, Tollin G. Surface plasmon resonance studies of complex formation between cytochrome c and bovine cytochrome c oxidase incorporated into a supported planar lipid bilayer. II. Binding of cytochrome c to oxidase-containing cardiolipin/phosphatidylcholine membranes. *Biophysical Journal*. 1996;71(2):858-67.
7. Choi S, Swanson JM. Interaction of cytochrome c with cardiolipin: an infrared spectroscopic study. *Biophysical Chemistry*. 1995;54(3):271-8.
8. Rytömaa M, Kinnunen PKJ. Reversibility of the Binding of Cytochrome c to Liposomes: Implications for Lipid-Protein Interactions. *Journal of Biological Chemistry*. 1995;270(7):3197-202.
9. Hanske J, Toffey JR, Morenz AM, Bonilla AJ, Schiavoni KH, Pletneva EV. Conformational properties of cardiolipin-bound cytochrome c. *Proceedings of the National Academy of Sciences*. 2012;109(1):125.
10. Kawai C, Prado FM, Nunes GLC, Di Mascio P, Carmona-Ribeiro AM, Nantes IL. pH-dependent Interaction of Cytochrome c with Mitochondrial Mimetic Membranes: The Role of an Array of Positively Charged Amino Acids. *Journal of Biological Chemistry*. 2005;280(41):34709-17.
11. Tuominen EKJ, Wallace CJA, Kinnunen PKJ. Phospholipid-Cytochrome c Interaction: Evidence for the Extended Lipid Anchorage. *Journal of Biological Chemistry*. 2002;277(11):8822-6.
12. Kagan VE, Bayır HA, Belikova NA, Kapralov O, Tyurina YY, Tyurin VA, et al. Cytochrome c/cardiolipin relations in mitochondria: a kiss of death. *Free Radical Biology and Medicine*. 2009;46(11):1439-53.

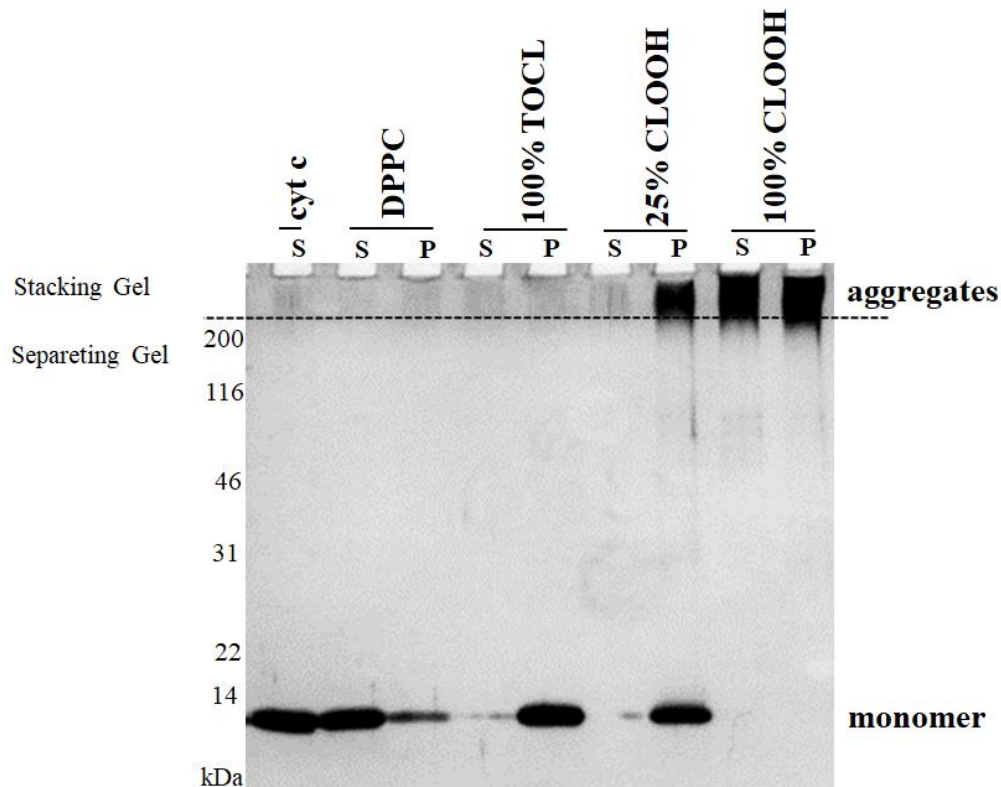
13. Belikova NA, Vladimirov YA, Osipov AN, Kapralov AA, Tyurin VA, Potapovich MV, et al. Peroxidase Activity and Structural Transitions of Cytochrome c Bound to Cardiolipin-Containing Membranes. *Biochemistry*. 2006;45(15):4998-5009.
14. Liu X, Kim CN, Yang J, Jemmerson R, Wang X. Induction of Apoptotic Program in Cell-Free Extracts: Requirement for dATP and Cytochrome c. *Cell*. 1996;86(1):147-57.
15. Genaro-Mattos TC, Appolinário PP, Mugnol KCU, Bloch Jr C, Nantes IL, Di Mascio P, et al. Covalent Binding and Anchoring of Cytochrome c to Mitochondrial Mimetic Membranes Promoted by Cholesterol Carboxyaldehyde. *Chemical Research in Toxicology*. 2013;26(10):1536-44.
16. Isom AL, Barnes S, Wilson L, Kirk M, Coward L, Darley-Usmar V. Modification of Cytochrome c by 4-hydroxy- 2-nonenal: Evidence for histidine, lysine, and arginine-aldehyde adducts. *Journal of the American Society for Mass Spectrometry*. 2004;15(8):1136-47.
17. Williams MV, Wishnok JS, Tannenbaum SR. Covalent adducts arising from the decomposition products of lipid hydroperoxides in the presence of cytochrome c. *Chemical research in toxicology*. 2007;20(5):767-75.
18. Sigolo CAO, Mascio PD, Medeiros MHG. Covalent Modification of Cytochrome c Exposed to trans,trans-2,4-Decadienal. *Chemical Research in Toxicology*. 2007;20(8):1099-110.
19. Tyurina YY, Kini V, Tyurin VA, Vlasova II, Jiang J, Kapralov AA, et al. Mechanisms of Cardiolipin Oxidation by Cytochrome c: Relevance to Pro- and Antiapoptotic Functions of Etoposide. *Molecular Pharmacology*. 2006;70(2):706.
20. Bayır H, Kapralov AA, Jiang J, Huang Z, Tyurina YY, Tyurin VA, et al. Peroxidase Mechanism of Lipid-dependent Cross-linking of Synuclein with Cytochrome c: Protection Against Apoptosis Versus Delayed Oxidative Stress in Parkinson Disease. *Journal of Biological Chemistry*. 2009;284(23):15951-69.
21. Vlasova II, Tyurin VA, Kapralov AA, Kurnikov IV, Osipov AN, Potapovich MV, et al. Nitric Oxide Inhibits Peroxidase Activity of Cytochrome c- Cardiolipin Complex and Blocks Cardiolipin Oxidation. *Journal of Biological Chemistry*. 2006;281(21):14554-62.
22. Margoliash E, Frohwirt N. Spectrum of horse-heart cytochrome c. *The Biochemical journal*. 1959;71(3):570-2.
23. Miyamoto S, Nantes IL, Faria PA, Cunha D, Ronsein GE, Medeiros MHG, et al. Cytochrome c-promoted cardiolipin oxidation generates singlet molecular oxygen. *Photochemical & Photobiological Sciences*. 2012;11(10):1536-46.
24. Belikova NA, Tyurina YY, Borisenko G, Tyurin V, Samhan Arias AK, Yanamala N, et al. Heterolytic Reduction of Fatty Acid Hydroperoxides by Cytochrome c/Cardiolipin Complexes: Antioxidant Function in Mitochondria. *Journal of the American Chemical Society*. 2009/08/19;131(32):11288-9.
25. Dantas LS, Chaves-Filho AB, Coelho FR, Genaro-Mattos TC, Tallman KA, Porter NA, et al. Cholesterol secosterol aldehyde adduction and aggregation of Cu,Zn-superoxide dismutase: Potential implications in ALS. *Redox biology*. 2018;19:105-15.
26. Abe M, Niibayashi R, Koubori S, Moriyama I, Miyoshi H. Molecular Mechanisms for the Induction of Peroxidase Activity of the Cytochrome c-Cardiolipin Complex. *Biochemistry*. 2011;50(39):8383-91.

27. Chen Q, Crosby M, Almasan A. Redox Regulation of Apoptosis before and after Cytochrome C Release. *Korean journal of biological sciences*. 2003;7(1):1-9.
28. Bossy-Wetzel E, Newmeyer DD, Green DR. Mitochondrial cytochrome c release in apoptosis occurs upstream of DEVD-specific caspase activation and independently of mitochondrial transmembrane depolarization. *The EMBO journal*. 1998;17(1):37-49.
29. Barr DP, Gunther MR, Deterding LJ, Tomer KB, Mason RP. ESR Spin-trapping of a Protein-derived Tyrosyl Radical from the Reaction of Cytochrome c with Hydrogen Peroxide. *Journal of Biological Chemistry*. 1996;271(26):15498-503.
30. Hiner ANP, Raven EL, Thorneley RNF, García-Cánovas F, Rodríguez-López JN. Mechanisms of compound I formation in heme peroxidases. *Journal of Inorganic Biochemistry*. 2002;91(1):27-34.
31. Poulos TL, Kraut J. The stereochemistry of peroxidase catalysis. *Journal of Biological Chemistry*. 1980;255(17):8199-205.
32. Muenzner J, Pletneva EV. Structural transformations of cytochrome c upon interaction with cardiolipin. *Chemistry and Physics of Lipids*. 2014;179:57-63.
33. Sinibaldi F, Fiorucci L, Patriarca A, Lauceri R, Ferri T, Coletta M, et al. Insights into Cytochrome c-Cardiolipin Interaction. Role Played by Ionic Strength. *Biochemistry*. 2008;47(26):6928-35.
34. Sinibaldi F, Milazzo L, Howes BD, Piro MC, Fiorucci L, Polticelli F, et al. The key role played by charge in the interaction of cytochrome c with cardiolipin. *JBIC Journal of Biological Inorganic Chemistry*. 2017;22(1):19-29.
35. Hirota S, Hattori Y, Nagao S, Taketa M, Komori H, Kamikubo H, et al. Cytochrome c polymerization by successive domain swapping at the C-terminal helix. *Proceedings of the National Academy of Sciences*. 2010;107(29):12854.
36. Maguire JJ, Tyurina YY, Mohammadyani D, Kapralov AA, Anthonymuthu TS, Qu F, et al. Known unknowns of cardiolipin signaling: The best is yet to come. *Biochimica et biophysica acta Molecular and cell biology of lipids*. 2017;1862(1):8-24.
37. Giulivi C, Davies KJ. Dityrosine and tyrosine oxidation products are endogenous markers for the selective proteolysis of oxidatively modified red blood cell hemoglobin by (the 19 S) proteasome. *Journal of Biological Chemistry*. 1993;268(12):8752-9.
38. Mayer F, Pröpper S, Ritz-Timme S. Dityrosine, a protein product of oxidative stress, as a possible marker of acute myocardial infarctions. *International Journal of Legal Medicine*. 2014;128(5):787-94.

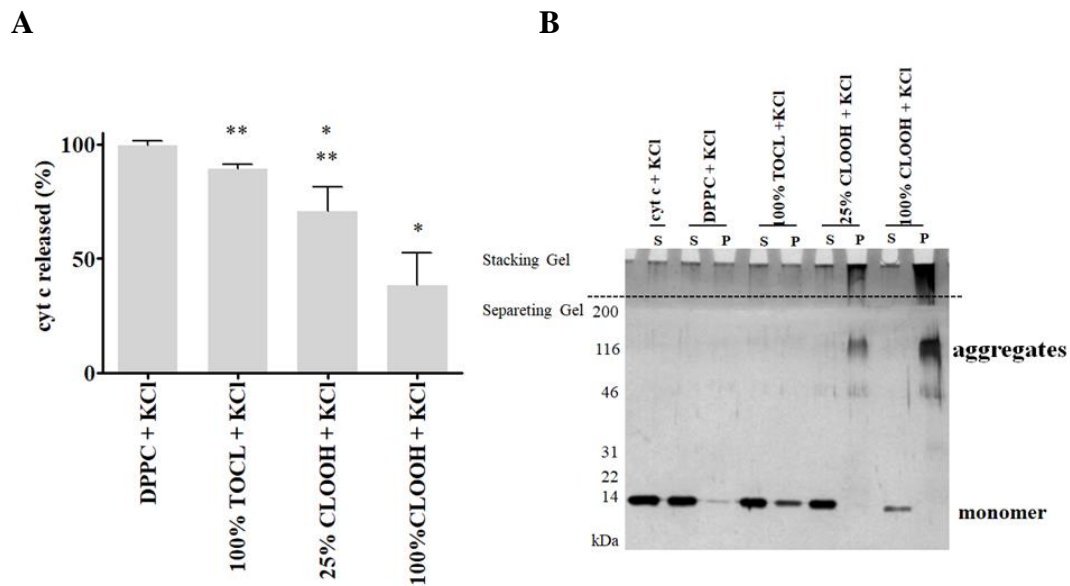
Supplementary figures



Supplementary Figure S1. Linear plot representing used for ratio rates calculation (k_1) of cytochrome c (cyt c) between hydrogen hydroperoxide (H_2O_2), linolec acid hydroperoxide (13-(S)-HpODE) and tetraoleoyl-cardiolipin hydroperoxide ($\text{TLCL}(\text{OOH})_1$).

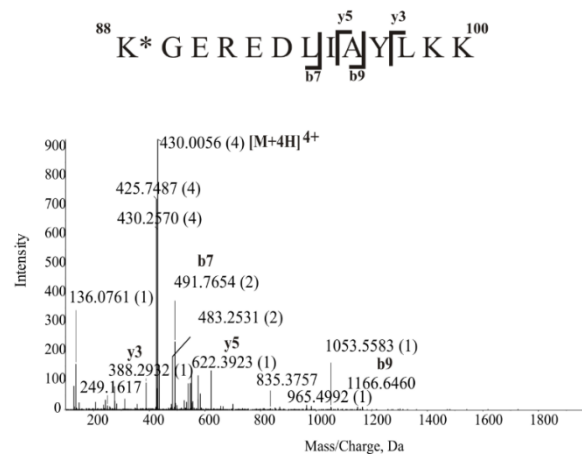


Supplementary Figure S2. Cytochrome c undergoes aggregation in the presence membranes containing cardiolipin hydroperoxides. SDS-PAGE analysis of cytc-cardiolipin complexes after incubation of cytc with liposomes containing 25, and 100 % of cardiolipin in the oxidized form. Liposomes at 0.5 mM final concentration were incubated with 5 μ M cytc for 15 min at 25°C and then sedimented by ultracentrifugation at 160,000 g for 1h at 4 °C. Both the pellet (P) and supernatant (S) fractions were analyzed by SDS-PAGE. Cytc is found mostly in its monomeric form when incubated with DPPC or DPPC:TOCL membranes. In contrast, addition of either 25% or 100 % cardiolipin in its oxidize form (CLOOH) induces the formation of high molecular weight aggregates (detected in the stacking gel). Electrophoresis was run in 15% SDS-PAGE and 5% stacking gel. Silver staining was used to visualized protein on gels.

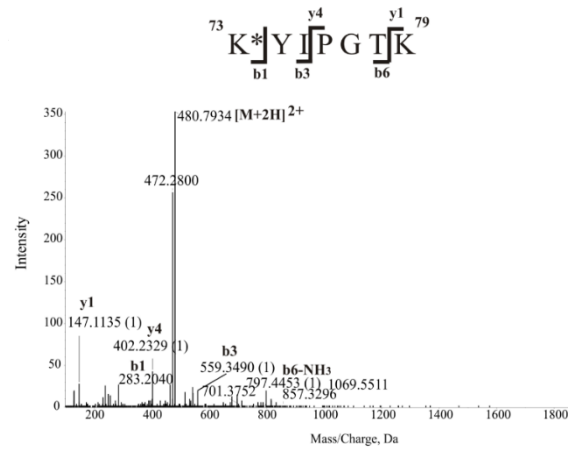


Supplementary Figure S3. High ionic strength is less effective to disturbing cytochrome c/CLOOH complex. (A) Percentage of cytochrome c released measuring at 410 nm after incubation with CL-containing liposomes. (B) Electrophoresis gel of cytochrome c/CL complexes after binding assay. DPPC only, DPPC:TOCL, DPPC:TOCL:CLOOH and DPPC:CLOOH liposomes (0.5 mM total lipid) were prepared by extrusion in 5 mM HEPES buffer (pH7.4) containing 0.1 mM DTPA. The liposomes were incubated with 5 μ M cyt c for 15 min at 25°C in presence of 250 mM KCl and then sedimented by ultracentrifugation at 160,000 g for 1h at 4 °C. Samples were loaded onto the gel and electrophoresis was run in 15% SDS-PAGE with 5% stacking gel. The gel was stained with silver stains. One-way ANOVA followed by Bonferroni post-hoc test was used. Values are the means \pm SD (n=3), and *p<0.01: different from DPPC, **p<0.01 different from DPPC:CLOOH.

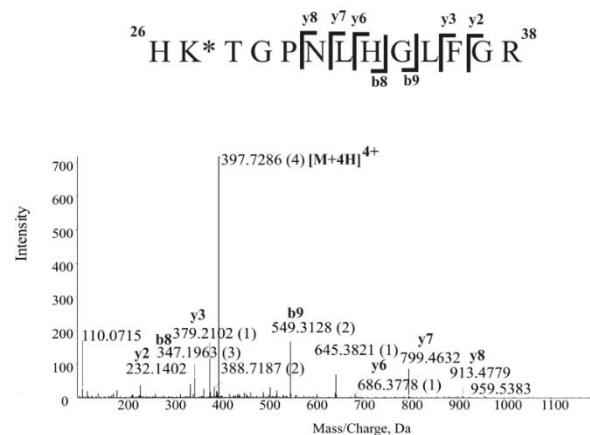
A



B

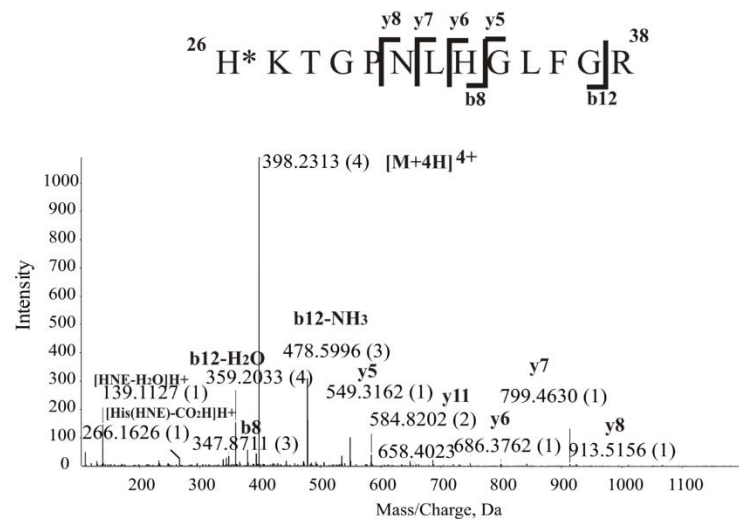


C

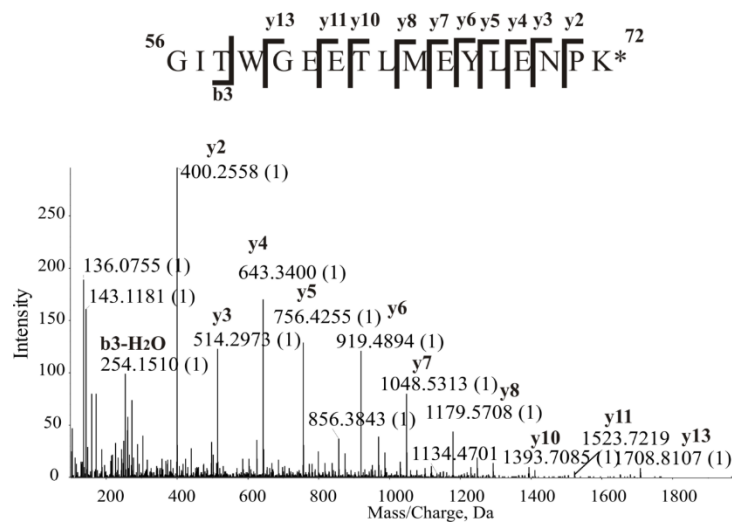


Supplementary Figure S4. nLC-MS/MS sequencing of 4-ONE modified peptides derived from the tryptic digestion of cytochrome c incubated with CLOOH in presence of liposome. (A) MS/MS of the peptide containing 4-ONE adduct at K88. (B) MS/MS of the peptide containing 4-ONE adduct at K73. An asterisk after the one-letter code of amino acid residue denotes its modification. Fragments b1, b2 and b6 ions confirming the adducted peptide. (C) MS/MS of the peptide containing 4-ONE adduct at K27. Fragments b8 and b9 ions confirming the adducted peptide. An asterisk after the one-letter code of amino acid residue denotes its modification.

A

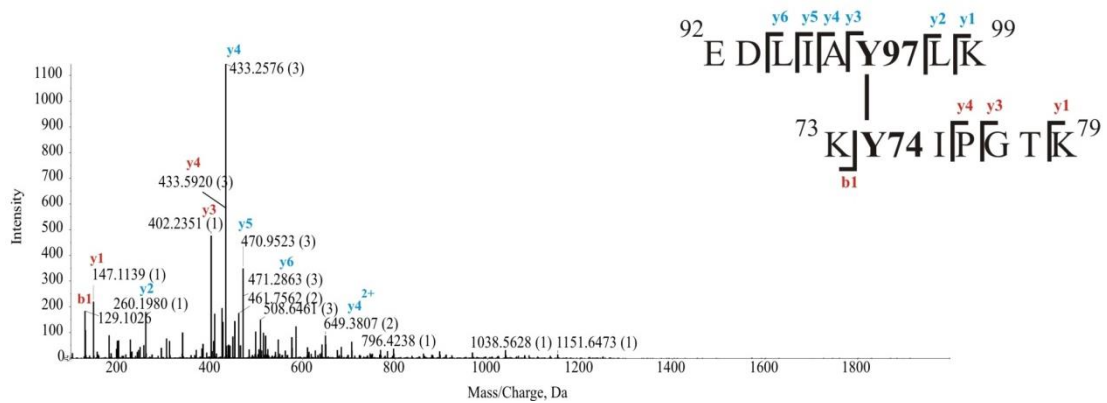


B

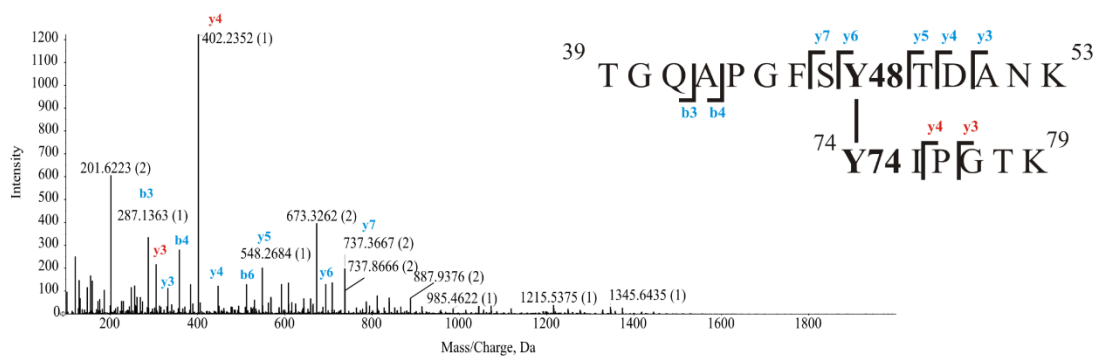


Supplementary Figure S5. nLC-MS/MS sequencing of 4-HNE modified peptides derived from the tryptic digestion of cytochrome c incubated with CLOOH in presence of liposome. (A) MS/MS of the peptide containing 4-HNE adduct at K26 (Michael adduct). HNE-related product ions at m/z 139.11 and 266.16 relating to dehydrated HNE and immonium ion, respectively. (B) MS/MS of the peptide containing 4-HNE adduct at K72 (Michael adduct). Fragments y2, y3, y4, y5, y6, y7, y8, y10, y11, y13 ions confirming the adducted peptide. An asterisk after the one-letter code of amino acid residue denotes its modification.

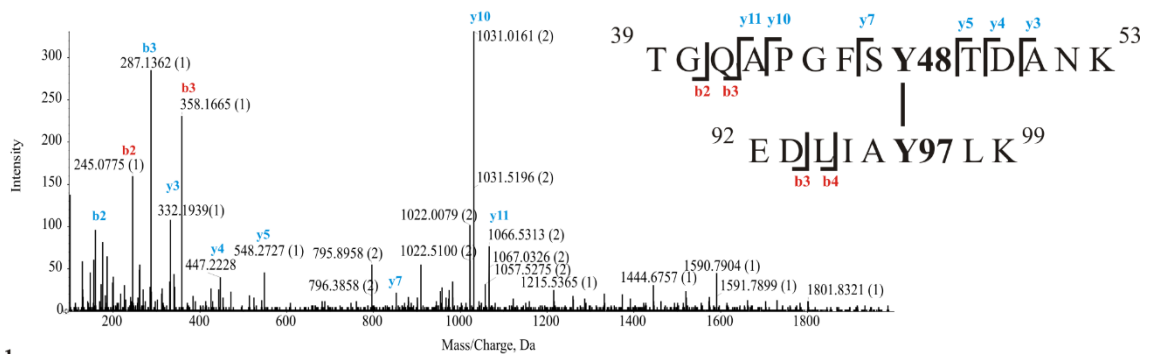
A



B



C



Supplementary Figure S6. nLC-MS/MS sequencing of dityrosine cross-linked peptides derived from the tryptic digestion of cytochrome c incubated with CLOOH in presence of liposome. (A) MS/MS of the cross-linked peptide at Y97 and Y74. Fragments y3, y4, y5 and y6 ions containing the cross-linked residue. (B) MS/MS of the cross-linked peptide at Y48 and Y74. Fragments y6 and y7 ions containing the cross-linked residue. (C) MS/MS of the cross-linked peptide at Y97 and Y48. Fragments y7, y10 and y11 ions containing the cross-linked residue.

Supplementary tables

Supplementary Table S1. Liposomes composition for cytochrome c-liposome binding assay without high ionic strength.

DPPC (μM)	TOCL (μM)	CLOOH (μM)	PL total proportion (%)
1000	0	0	100
800	200	0	80:20:0
800	170	30	80:17:3
800	150	50	80:15:5
800	140	60	80:13:7
800	120	80	80:11:9
800	100	100	80:10:10
800	0	200	80:0:20

PL: phospholipid

Supplementary Table S2. Liposome composition for cytochrome c-liposome binding assay with high ionic strength.

DPPC (μM)	TOCL (μM)	CLOOH (μM)	PL total proportion (%)
800	200	0	80:20:0
800	150	50	80:15:5
800	0	200	80:0:20

PL: phospholipid

Supplementary Table S3. Liposome composition for kinetics of the reaction of cytochrome c with 13-(S)-HpODE.

DPPC (μM)	TOCL (μM)	13-(S)-HpODE (μM)
500	0	0
500	100	0
500	100	10
500	100	20
500	100	30
500	100	40
500	100	50

Supplementary Table S4. Liposome composition for kinetics of the reaction of cytochrome c with CLOOH

DPPC (μM)	TOCL (μM)	CLOOH (μM)
400	90	10
400	80	20
400	70	30
400	60	40
400	50	50

CHAPTER 2

Characterization of Dityrosine Cross-Linked Sites in Cytochrome c Induced by Cholesterol Hydroperoxide

Isabella F D Pinto, Alex Inague, Lucas S Dantas, Sayuri Miyamoto*

Department of Biochemistry, Institute of Chemistry, University of Sao Paulo, Sao Paulo, Brazil

*Corresponding Author: Sayuri Miyamoto. E-mail address: miyamoto@iq.usp.br
Institutional address: Departamento de Bioquímica, Instituto de Química, Av. Prof. Lineu Prestes 1524, CP 26077, CEP 05313-970, Butantã, São Paulo, SP. Brazil. Phone: + 55 11 30911413

Highlights

- Cholesterol hydroperoxide promotes an increase of cytochrome c hydrophobicity and a rapid conversion of protein monomer into dimer and trimer.
- Mass spectrometry analysis revealed dityrosine cross-linked peptides (Y48-Y48, Y48-Y74 and Y48-Y97).

Abstract

Protein oligomerization is a well-known process that has been implicated in many diseases. Under pathological conditions, accumulation of mitochondrial cholesterol can lead to generation of cholesterol hydroperoxides, which react with cytochrome c (cytc). Cytc is an abundant mitochondrial protein that acts as electron carrier in the respiratory chain and also in apoptosis pathway. Previous study revealed the formation of lipid and protein-derived radicals in the reaction between cytc and cholesterol hydroperoxide (ChOOH), a mechanism that could be associated with protein oligomerization. However, protein oligomers are not completely elucidated in this process. Here we characterized dityrosine cross-links formed through the reaction between cytc and 7 α -ChOOH. The oligomerization was checked by SDS-PAGE, and it showed a rapid and an efficient conversion of cytc monomer into dimer and trimer in a concentration-dependent manner. Importantly, mass spectrometry analysis revealed dityrosine cross-linked peptides involving Y48, Y74 and Y97 residues (i.e., Y48-Y48, Y48-Y74 and Y48-Y97). Overall, our data support the potential involvement of ChOOH in reactions leading to protein tyrosyl radical formation that subsequently recombines giving dimers and trimers.

Keywords: Cytochrome c, Cholesterol hydroperoxide, Dityrosine cross-linking, LC-MS/MS

Abbreviations

Bis-ANS: bis-anilinonaphtalene sulfonate

Cytc: cytochrome c

ChOOH: cholesterol hydroperoxide

nLC-MS/MS: nano-liquid chromatography coupled to mass spectrometer

SDS: sodium dodecyl sulfate

1. Introduction

Cholesterol is an essential component of cell plasma membrane. Due to its chemical composition (long rigid hydrophobic chain and a small polar hydroxyl group), it fits most of its structure into the lipid bilayer (1, 2). Cholesterol is synthesized in the endoplasmic reticulum (ER) and then distributed to organelles. Mitochondrial cholesterol content, for instance, is generally low, except for cells involved in steroid hormone synthesis or synthesis of bile acids, in which the mitochondria import and metabolize cholesterol in concert with ER (1, 3). In pathological condition the accumulation of cholesterol in mitochondria alters membrane organization, which regulates membrane permeability and function of resident proteins (3). Of relevance, recent evidence indicated that accumulation of mitochondrial cholesterol may be a key step in disease progression including cancer, Alzheimer's disease, atherosclerosis and steatohepatitis (1, 4, 5).

As mitochondria are the main source of radical generation, and cholesterol has a susceptible structure to free radical damage, pathological accumulation of mitochondrial cholesterol may increase the formation of oxidized cholesterol species (6). Oxidation of cholesterol can occur by non-enzymatic or enzymatic mechanism and generates as primary products hydroperoxides. Non-enzymatically, cholesterol can be oxidized by free radical-mediated reaction generating 7α -ChOOH and 7β -ChOOH as the most predominant hydroperoxide products (Figure 1), with less amounts of dihydroxy-derivatives (7α -ChOH, 7β -ChOH, 7-ketone, 5,6-epoxides, etc.) (7, 8). Therefore, highly reactive products of lipid peroxidation display marked biological effects, which cause alterations in cell signaling, protein and DNA damage, and cytotoxicity (9).

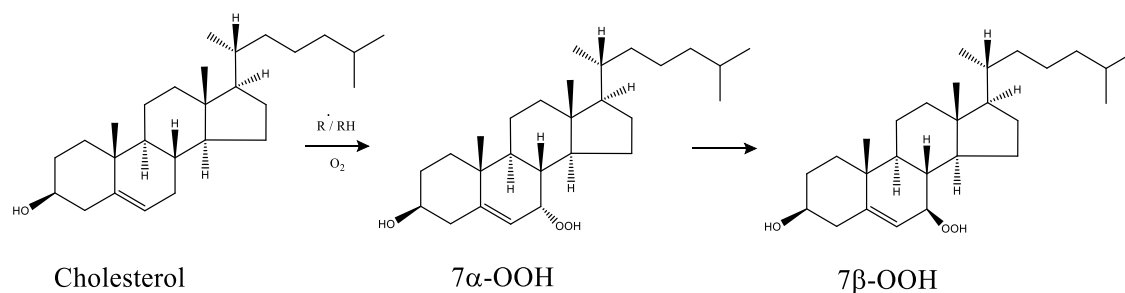


Figure 1. Cholesterol hydroperoxide produced by cholesterol oxidation mediated by free radicals.

The reaction of cholesterol hydroperoxide (ChOOH) with mitochondrial proteins, such as cytochrome c (cytc), can play an important role in the generation of free radicals in the organelle. Cytc is a highly-conserved protein with 104 amino acids residues, approximately 12 kDa, located at inner mitochondrial membrane (10). Its play a crucial role in the electron carrier between complex III to IV (11). Cytc can acts as a peroxidase catalyzing the oxidation of cardiolipin in mitochondrial membrane and carries to apoptosis pathway (12, 13). In addition, *in vitro* studies have been demonstrated that hydrogen peroxide (14), cholesterol carboxaldehyde (15) and cholesterol hydroperoxide (16) can promote cytc oligomerization. The proposed mechanism for protein oligomerization by free radicals involves generation of protein carbon-centered and lipid radicals. However, a detailed characterization of cytc oligomerization mediated by ChOOH has not been clearly characterized yet.

The oxidation of most protein residues is irreversible, and includes several covalent modifications, such as protein cleavage, carbonylation, nitration, hydroxylation, halogenation and protein cross-linking (17). An important example is the dityrosine cross-link, which is formed through a carbon-carbon bond between two proximal tyrosine residues. A variety of oxidative systems, including peroxidases and other heme proteins such as cytc can generates dityrosine (18-21). Dityrosine is known to occur in

amyloid fibril formation (22), Parkinson's disease (23), atherosclerosis caused by hemodialysis (24), cataract of the eye lens (25), aging (26) and oxidative stress during exercise (27). While the formation of dityrosine linkages in proteins has been documented, its consequences on the structure and biological function of the modified proteins are yet to be fully understood. In some cases, dityrosine is believed to be beneficial in terms of structural rigidity and strength, in other cases, they could lead to alterations in conformation, ligand binding, and biological activity.

Considering its potential significance for oxidative modification by ChOOH, we have sought to characterize the cross-linking of 7α -ChOOH-mediated cytc oligomerization. MS analysis showed four potential dityrosine cross-linked peptides involving Y48, Y74 and Y97. Our findings are in accordance with previous studies that reported formation of protein carbon-centered radical as mechanism to give dimeric and trimeric species (16).

2. Materials and methods

2.1 Materials

Bovine heart cytochrome c, ammonium bicarbonate (NH_4HCO_3), cholesterol (Cholest-5-en-3-ol), sodium dodecyl sulfate (SDS), methylene blue, dye bis-ANS (4,4'-dianilino-1,1'-binaphthyl-5,5'-disulphonic acid), rose bengal, pyridine, glycerol, bromophenol blue, Tris-HCl, formic acid MS grade, trifluoroacetic acid (TFA), diethylenetriaminepenta-acetic acid (DTPA) were purchased from Sigma (St. Louis, MO). Isopropanol, acetonitrile, chloroform, ethyl ether and ethyl acetate were purchased from J. T. Baker. All solvents employed were HPLC grade. Stock solutions of ammonium bicarbonate buffer (pH 7.4) were freshly prepared in ultrapure water (Millipore Milli-Q system), and the pH was adjusted to 7.4 prior to use. Cytochrome c

concentration was checked prior to each experiment as previously described ($\epsilon=106.1 \text{ mM}^{-1}\text{cm}^{-1}$) (15, 28).

2.2 Synthesis and purification of cholesterol hydroperoxide

Cholesterol hydroperoxide was synthesized by photooxidation. Briefly, cholesterol (0,7999 g) was dissolved in 7 mL of pyridine in a round-bottomed flask, and 9.3 mg of rose Bengal were added. The solution was irradiated using one tungsten lamp (500 W) for approximately 34 h under continuous stirring in a cold room (16°C). The mixture of ChOOH isomers was purified in the first step by silica gel column chromatography. The column was equilibrated with hexane and a gradient of hexane: ethyl ether was used. The second step of purification was performed by reverse phase HPLC using a C18 semi-preparative column and mobile phase composed by water (A) and methanol (B). After collecting fractions containing isolated ChOOH isomers, the solvent was evaporated, and the hydroperoxides were resuspended in isopropanol, quantified by iodometry (29). The hydroperoxides were stored at -80°C for further use.

2.3 Cytochrome c reaction with SDS micelles

The reaction was performed as described previously (15). Briefly, 10 mM ammonium bicarbonate buffer (pH 7.4) containing 0.1 mM DTPA was mixed with SDS (8 mM final concentration) followed by mixture of ChOOH isomers (150 μM) or isolated 7 α -ChOOH (150 μM). After 5 min, cytc (30 μM final concentration) was added to the solution, and the reaction was carried out at 37°C for 1h under continuous stirring.

2.4 Sodium dodecyl sulfate polyacrylamide gel electrophoresis (SDS-PAGE)

SDS-PAGE electrophoresis was performed in gel comprising 5% stacking gel (w/v) and 15% separating gel (w/v) under non-reducing conditions. The samples were diluted four times in the Laemmli buffer (8% SDS, 40% glycerol, 0.04% bromophenol blue and 200

mM Tris-HCl, pH 6.8) and heated to 95°C for 5 min. After the electrophoretic run, the gel was stained with Thermo Scientific PageBlue Protein Staining Solution.

2.5 Bis-ANS binding

Exposure of hydrophobic sites of protein was verified by reaction with the dye 4,4'-dianilino-1,1'-binaphthyl-5,5'-disulfonic acid (bis-ANS) using a fluorescence plate reader (TECAN, Switzerland). Briefly, stock solution of bis-ANS (2.9 mM) was prepared in ethanol. An aliquot of reaction containing 10 μ M of cyt c was incubated with 10 mM sodium phosphate buffer (pH 7.4) and 60 μ M bis-ANS for 30 min at 37°C. The fluorescence was measured using excitation wavelength at 390 nm and emission wavelength at 400-600 nm. Bis-ANS contained no protein served as negative control.

2.6 In-gel tryptic digestion of cytochrome c

The bands were excised from gel and destained twice with a solution containing 50% acetonitrile in 50 mM ammonium bicarbonate buffer (pH 7.4) for 45 min at 37°C. The gel pieces were dehydrated using 100% acetonitrile for 5 min at room temperature. Then they were rehydrated in 0.02 μ g/mL trypsin (Promega Sequence Grade Modified) in 40 mM ammonium bicarbonate buffer with 10% acetonitrile (pH 8.1) for 1h at ice-bath. The digestion was performed overnight at 37°C. Peptides were extracted twice with 1% TFA for 10 min under stirring at room temperature, followed by third extraction with 60% acetonitrile in 0.1% TFA. The peptides were transferred to a new tube, dried in a vacuum centrifuge and reconstituted in 0.1% TFA. Before LC-MS/MS analysis peptides were cleaned-up using a ZipTip-C18 column (Milipore, Bedford, MA).

2.7 nLC-MS/MS analysis

The analysis was performed using a Waters® nanoAcquity UPLC system coupled to a TripleTOF 6600 mass spectrometer (SCIEX, Concord, ON). The analysis was conducted under trap and elute mode using a nanoAcquity UPLC-Symmetry C18 trap column (20 mm x 180 μ m; 5 μ m) and separation column (75 μ m x 150 mm; 3.5 μ m) (30). Trapping was done at 10 μ L/min with 1% of solvent B (0.1% formic acid in acetonitrile). The peptides were separated using a mobile phase A (0.1% formic acid in water) and B (0.1% formic acid in acetonitrile) at flow rate of 400 nL/min in the following gradient: 2-35% B in 60 min, 35-85% B in 1 min, 85% B for 4 min, and 85-2% B in 4 min. Nano-electrospray ion source was operated at 2.4 kV (ion spray voltage floating, ISVF), curtain gas 20, interface heater (IHT) 120, ion source gas 1 (GS1) 3, ion source gas 2 (GS2) zero, declustering potential (DP) 80 V. TOFMS and MS/MS data were acquired using information-dependent acquisition (IDA) mode. For IDA parameters, a 100 ms survey scan in the m/z range of 300-2000 was followed by 25 MS/MS ions in the m/z range of 100-2000 acquired with an accumulation time of 50 ms (total cycle time 1.4 s). Switch criteria included, intensity greater than 150 counts and charge state 3-5. Former target ions were excluded for 20 s. Software used for acquisition and data processing were Analyst TF 1.7 and PeakView 2.1, respectively. For the protein coverage and modifications, MASCOT software (Matrix Science, London, UK) was used against SWISS-PROT database with a precursor mass tolerance of 15 ppm and a fragment ion mass tolerance of 0.03 Da. Oxidation of methionine was searched as variable modifications. Dityrosine cross-linking search was performed using SIM-XL software (31) with a precursor ion and fragment ion mass tolerance of 20 ppm, oxidation of methionine as variable modification and trypsin as proteolytic enzyme. All MS/MS spectra were manually inspected for validation, and b- and y- ions fragments annotation.

3. Results

3.1 7α -ChOOH promotes an increase of cytochrome c hydrophobicity and a rapid conversion into dimer and trimer

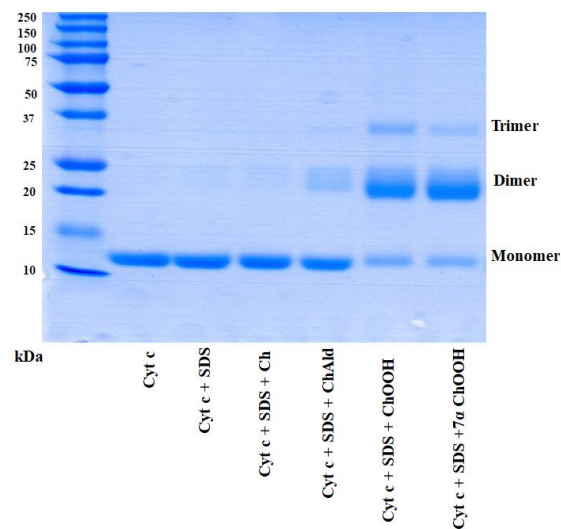
In order to investigate ChOOH-induced aggregation on cytc, incubation between 7α -ChOOH and protein was conducted for 1h at 37°C in the presence of SDS micelles, and then analyzed by SDS-PAGE (Figure 2A). Cytc showed monomer bands in agreement with their molecular mass (approximately 12 kDa). Control reactions incubated with cholesterol (Ch) did not reveal any change in the monomeric band of cytc. However, incubation with ChOOH mixture or isolated 7α -ChOOH decreased the intensity of monomeric band of cytc. In contrast, we observed a marked increase in the intensity of the band assigned to a dimer, as well as, the appearance at the band corresponding to trimeric species. A similar trend was observed in incubation containing cholesterol aldehyde (ChAld), although this reaction resulted in a low formation of dimers and trimers. *In vitro* dimerization of cytc is known to occur in the presence of ChAld and ChOOH mixture (15, 16).

In addition, 7α -ChOOH induced concentration-dependent cyt c dimerization (Supplementary Figure S1A). Cytc dimers were formed at 1:0.5 proportion (protein: 7α -ChOOH), and gradually became evident at 1:5 proportion. Importantly, our data supports that SDS-PAGE analysis did not induced artefact in the cytc oligomerization. Time-dependent analysis showed a rather fast oligomerization kinetics reaching a plateau within 30 seconds (Supplementary Figure S1B). Thus, formation of dimeric, trimeric and aggregates of cytc started at very short incubation times

To examine cytc hydrophobicity, we conducted dye binding experiments with bis-ANS, which binds hydrophobic regions (Figure 2B). Increased fluorescence intensity, and emission maximum blue shift to 490 nm were observed in presence of 7α -ChOOH after

30 min of incubation (Figure 2B; red line). Note that the presence of SDS also induces exposure of hydrophobic residues of protein (Figure 1B; filled black line). Alterations in protein conformation can lead to exposure of their hydrophobic residues (32, 33). As expected ChAld promote a large exposure of hydrophobic residues of protein due alterations in Lys residues (15). Collectively, these results suggest that alteration of cytochrome c conformation by 7α -ChOOH involving heme rearrangement followed by formation of covalent oligomers (Figure 2). In contrast, oligomers (e.g. dimer) formed by SDS only was readily destabilized in presence of denaturation condition during SDS-PAGE analysis.

A



B

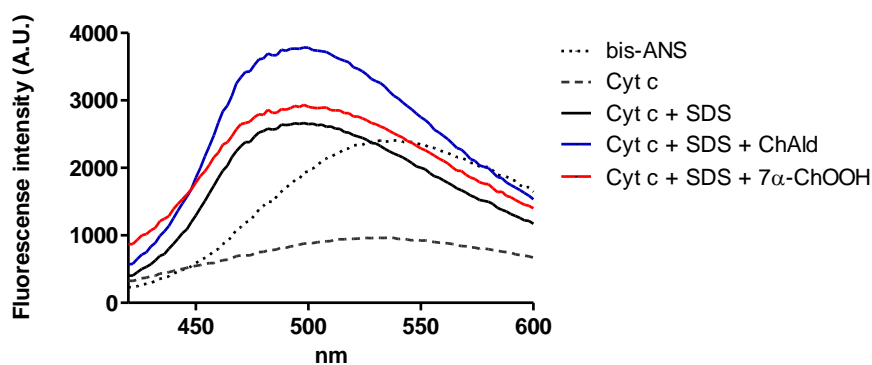


Figure 2. 7α -ChOOH induces cytochrome c oligomerization and increased hydrophobicity in presence of SDS micelles. (A) Non reducing SDS-PAGE gel. Samples were loaded into the gel and electrophoresis was performed in 15% separating gel under non-reducing conditions. Control was performed in presence of SDS. (B). Bis-ANS binding. Cyt c (10 μ M) was incubated with 7α -ChOOH (150 μ M) in presence of SDS micelles for 1 h at 37°C. Then 60 μ L of the reaction was incubated with bis-ANS (60 μ M), and fluorescence measured after 30 min of incubation at 37°C as described in Materials and Methods.

3.2 7α -ChOOH induces of dityrosine cross-links leading to cytochrome c dimerization

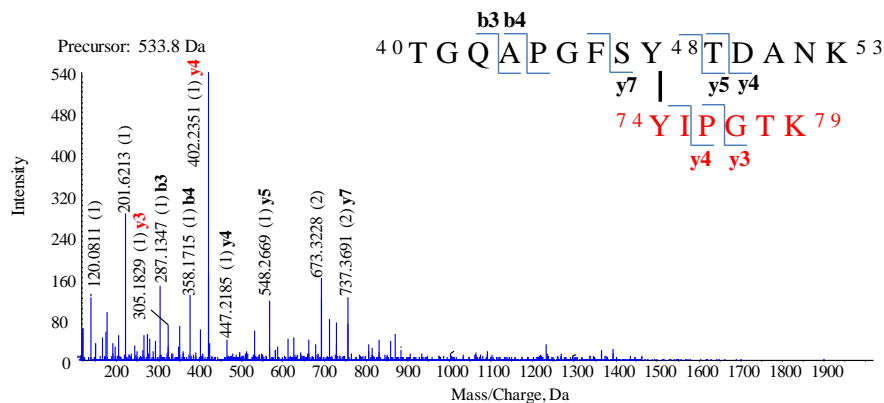
Considering the significant extent of protein oligomers detected by SDS-PAGE, and the potential importance of dityrosine in generation of these species, we examined the dityrosine cross-links using a mass spectrometry approach. Cyt c dimers was isolated from SDS-PAGE gels and subjected to trypsin digestion followed by nano-LC-MS/MS analysis. Four major peptides containing dityrosine cross-links were identified involving Y48, Y74 and Y97 (Table 1).

Table 1. Dityrosine characterization of cytochrome c dimers induced by cholesterol hydroperoxide.

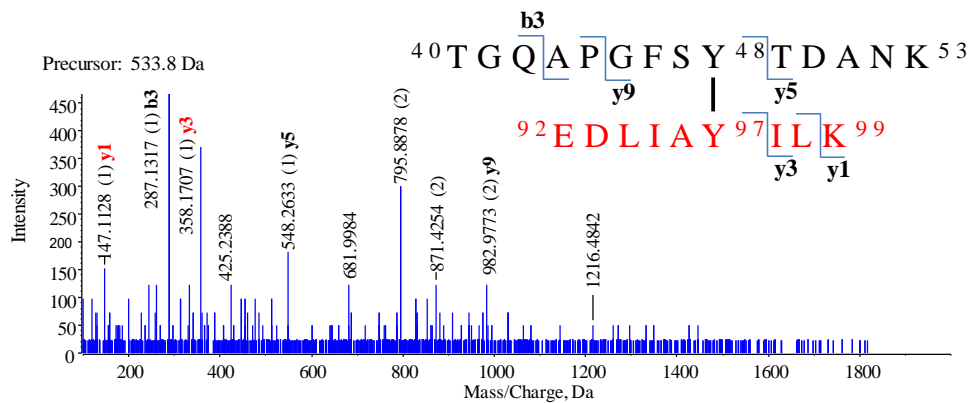
Peptide sequence 1	Peptide sequence 2	m/z	diTyr	Error (ppm)	Sample
⁴⁰ TGQAPGFSYTDANK ⁵³⁴⁰	⁵³⁴⁰ TGQAPGFSYTDANK ⁵³	971.4447 (3+)	Y48 - Y48	1.84	ChOOH
⁴⁰ TGQAPGFSYTDANK ⁵³⁷⁴	⁵³⁷⁴ YIPGTK ⁷⁹	533.7609 (4+)	Y48 - Y74	3.86	
⁴⁰ TGQAPGFSYTDANK ⁵³⁹²	⁵³⁹² EDLIAYLK ⁹⁹	605.2990 (4+)	Y48 - Y97	3.11	7α - ChOOH
⁴⁰ TGQAPGFSYTDANK ⁵³⁴⁰	⁵³⁴⁰ TGQAPGFSYTDANK ⁵³	728.3311 (4+)	Y48 - Y48	5.20	

The MS/MS spectra of each cross-link were manually examined for further confirmation (Figure 3). The spectra of heterodimeric dityrosine cross-link between $^{40}\text{TGQAPGFSYTDANK}^{53}$ and $^{74}\text{YIPGTK}^{79}$ peptides revealed possible dityrosine cross-linking between Y48 and Y74 at m/z 533.7609 (4+) (Figure 3A). The presence of the $y7^{2+}$ lead to the successful identification and assignment of the dityrosine cross-link position. A similar fragmentation behavior was observed for the heterodimeric peptide formed by $^{40}\text{TGQAPGFSYTDANK}^{53}$ and $^{92}\text{EDLIAYILK}^{99}$ cross-linked via Y48 and Y97 at m/z 605.2990 (4+) (Figure 3B). The presence of the ion $y9^{2+}$ confirmed the dityrosine cross-link position. Additionally, we identified only one homodimeric dityrosine cross-link $^{40}\text{TGQAPGFSYTDANK}^{53}$ peptides linked via Y48 at m/z 728.3311 (4+) (Figure 3C and Supplementary Figure S2). MS/MS spectra indicated a cleavage of the C-C bond between the aromatic ring of dityrosine and a hydrogen transfer yielding the protoned peptides. Taken together, our results suggest the formation of dityrosine cross-linked peptides as potential mechanism involved in oligomerization of cytc after exposure to ChOOH-containing SDS micelles.

A



B



C

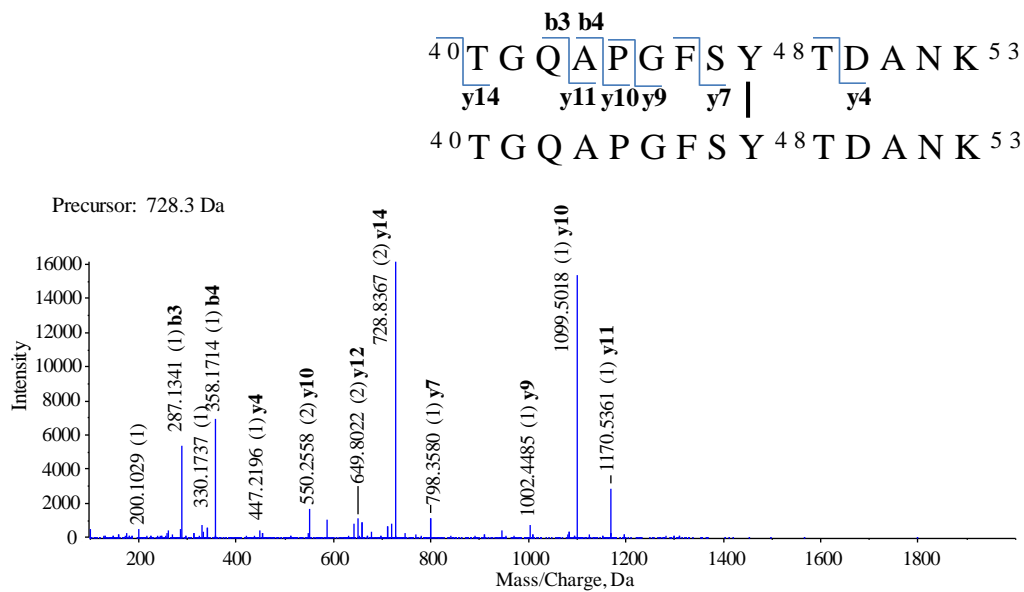


Figure 3. Nano-LC-ESI-MS/MS analysis of dityrosine cross-linked peptides from cytochrome c dimers induced by 7 α -ChOOH. (A) MS/MS spectra of the dityrosine cross-link between ⁴⁰TGQAPGFSTYDANK⁵³ and ⁷⁴YIPTK⁷⁹ with [M + 4H]⁴⁺ at m/z 533.7609, cross-linked between Y48 and Y74. (B) MS/MS spectra of the dityrosine cross-link between ⁴⁰TGQAPGFSTYDANK⁵³ and ⁹²EDLIAYILK⁹⁹ with [M + 4H]⁴⁺ at m/z 605.2990, cross-linked between Y48 and Y97. (C) MS/MS spectra of the dityrosine cross-linked ⁴⁰TGQAPGFSTYDANK⁵³ homodimer with [M + 4H]⁴⁺ at m/z 728.3311 cross-linked between Y48 and Y48.

4. Discussion

In the present study, we characterized cyt c covalent oligomerization induced by mixture of ChOOH isomers and isolated 7 α -ChOOH. Our data showed that cytc oligomerization required low amounts of 7 α -ChOOH (1:0.5; proportion protein: cholesterol hydroperoxide). Dimers were formed within 30 s, and further oligomerization occurred over 24 h. In addition, 7 α -ChOOH promoted alteration in protein conformation leading to increase of protein hydrophobicity. Based on previous results we expected that protein oligomerization by 7 α -ChOOH would involve covalent dityrosine cross-linking. Evidence from MS indicated the presence of two heterodimeric peptides cross-linked between Y48 and Y74 or Y97, and one homodimeric peptide cross-linked through Y48.

A previous *in vitro* study has shown that reaction between cytc and ChOOH produces lipid and protein-derived radicals (16). This reaction could occur by one electron mechanism (16, 34), which induces the hemolytic cleavage of the O-O bond in ChOOH producing lipid radicals (16). It is probably the preferential mechanism of reaction between cytc and ChOOH. Note of that the formation of lipid and protein-derived radicals could occur also by two-electron mechanism, which consists of the heterolytic cleavage of the O-O bond, reducing the hydroperoxide group to the corresponding alcohol (34). This is the catalytic mechanism of several peroxidase enzymes (35). However, as demonstrated by Genaro-Mattos et al., it fails to explain the formation of

epoxyl-alkyl radicals (16). In addition to lipid radical formation, the protein radicals were formed by the production of high-valent heme intermediates ($\text{Fe}^{4+}=\text{O}$ porphyrin π -cation radical) in both hetero- and homolytic cleavages of the hydroperoxide O-O bond (16, 36).

Cytc oligomers can be formed by recombination of protein-centered radicals. Although it is known that reaction between cytc and ChOOH induces protein oligomerization (16), here we are able to characterize the amino acid residues involved in oligomerization process. Previous studies have identified oxidized and dimerized tyrosine residues upon cytc reaction with peroxides (36-38). Oxidation of tyrosine residues generates phenoxyl radical, which, in turn, resonates in the aromatic ring, giving carbon-centered radicals (39). These radicals could be recombining to produce protein dimers and, subsequently, oligomers, as observed by the formation of cytc trimers and tetramers (36, 39). There are differences between the covalent and non-covalent oligomerization of cytc. Previous study has been reported non-covalent oligomerization of cytc induced by SDS (0.1%) or ethanol (60%, v/v) through hydrophobic interactions (40, 41). Non-covalent oligomers can be disrupted after boiling in the presence of 2% SDS, a treatment it is known to disrupt non-covalent interactions. Cytc oligomerization induced by ChOOH was not disrupted by heat and it is mostly likely due to the formation of covalent cytc oligomers involving dityrosine cross-links.

Oxidative stress an endogenous mechanism can result in the covalent cross-link between two tyrosine residues resulting in the formation of a dityrosine post translational modification (42). Dityrosine cross-linking in proteins can be performed by oxidizing agents such as hydroperoxyl radical, peroxy nitrite, nitrosoperoxy carbonate, and lipid hydroperoxides as well as UV and γ -irradiation (43). Enzymatic oxidation of tyrosine residues in protein by peroxidase-catalyzed mechanism has been found to

promote dityrosine cross-links. *In vitro*, dityrosine cross-linking of proteins such as lysozyme, calmodulin, myoglobin, hemoglobin, insulin, and RNase is known to occur as a product of oxidative stress (44).

Dityrosine cross-linked peptides and proteins have been associated with neurotoxic roles in Alzheimer's and Parkinson's diseases, but little molecular detail is available (45, 46). The major limitation in dityrosine research is the inability to determine the location of the dityrosine cross-link proteins. Here, we addressed these limitations and difficulties in the identification of dityrosine cross-linked peptides using mass spectrometry in a bottom-up proteomic workflow. Native cytc contains four tyrosine residues (i.e., Y48, Y67, Y74 and Y97) in their structure as are shown in the Figure 3. The -OH groups of Y48 and Y67 residues are 4Å from the heme moiety. They are, therefore, considerably closer to heme moiety when compared to the surface accessible Y74 and Y97. However, only Y67 lies in close proximity to the iron co-ordination site (36). This structural proximity may favor the generation of tyrosine radicals from Y67 as opposed to Y48, Y74 and Y97. It is tempting to speculate that the covalent cytc oligomers are produced, most likely, through the formation of dityrosine cross-links generated by the recombination of protein-immobilized tyrosine radicals (36). Our result revealed three major dityrosine cross-linking in cytc dimer induced by 7 α -ChOOH comprising Y48, Y74 and Y97. Interesting, we did not observe dityrosine cross-link involving Y67 residue. Since Y67 is highly conserved, and it plays a role in stabilizing the cytc structure, the preservation of Y67 could be associated with protein function (47).

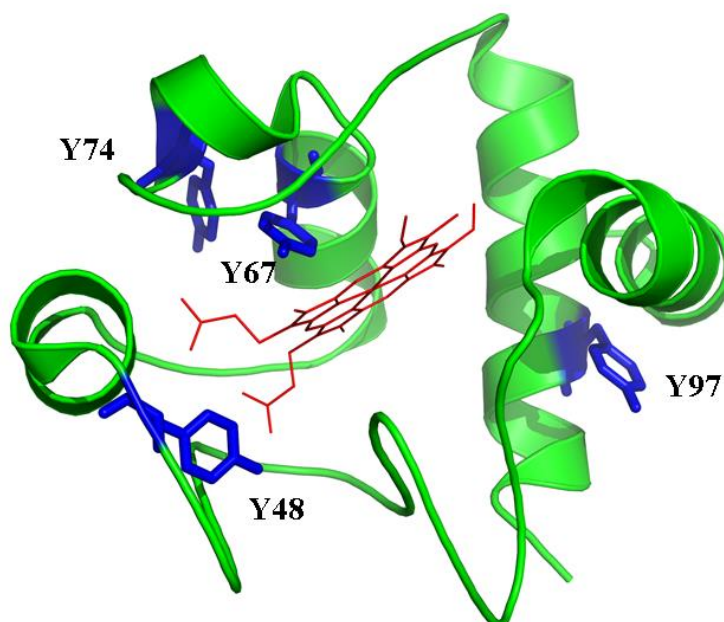


Figure 3. Native structure of bovine cytochrome c showing the locations of Y48, Y67, Y74 and Y97 (in blue). Tyrosine residues are indicated as letter Y highlighted in the protein sequence (PDB code 2B4Z).

The exact physiological role of cytc dimers has not been completely elucidated. An *in vitro* study showed enhanced peroxidase activity of equine cytc dimer relative to monomeric species, which has led to the suggestion that the dimer might mediate peroxidase activity early in apoptosis (48). Peroxidase activity of cytc has been reported by the increase of the rupture of the Met80-heme iron bond in the dimer (48). Therefore, pathological conditions could favor the formation of lipid hydroperoxides may contribute to the mitochondrial stress via a process that is enhanced by cytc peroxidase activity (49).

Mitochondria are cholesterol-poor organelles compared to other cell bilayers (e.g. plasma membrane). Nevertheless, the limited availability of cholesterol in the inner mitochondrial membrane plays an important physiological role, including the synthesis of hepatic bile acids, oxysterols and steroid hormones. In addition, both mitochondrial membranes must be supplied with cholesterol for membrane maintenance. The

trafficking of cholesterol to mitochondria involves multiples routes, from endolysosomes, plasma membrane and endoplasmic reticulum (50). Transfer of endolysosomes cholesterol to mitochondria is thought to occur in a non-vesicular manner between closely apposed membranes and mediated by steroidogenic acute regulatory (StAR)-related lipid transfer (START) domain proteins (51). Similarly, StARD1, with its sterol-binding domain and mitochondrial-targeting sequences, has been shown to promote cholesterol uptake into the mitochondrial outer membrane (52). On the other hand, the molecular basis for transfer of endoplasmic reticulum cholesterol to mitochondria, which may occur at contact site in mitochondria-associated membranes (53).

In pathological conditions, however, the accumulation of cholesterol in mitochondria alters membrane organization and the coexistence of liquid-disordered and liquid-ordered phases, which regulates membrane permeability and function of resident proteins (3). Of relevance, the increased mitochondrial cholesterol levels have been observed in diverse types of cancer, atherosclerosis, hepatic steatosis and Alzheimer's disease. Each of these conditions is associated with increased oxidative stress, impaired oxidative phosphorylation, and changes in the susceptibility to apoptosis, among other alterations in mitochondrial functions (4, 5, 54). Under oxidative stress conditions, steroidogenic cells may deliver not only cholesterol to mitochondrial compartments, but also cholesterol hydroperoxides such as $7\alpha/7\beta$ -ChOOH, thereby setting the stage for free radical damage, metabolic dysfunction and even apoptotic cell death (55).

In summary, the reaction between cytc and 7α -ChOOH increases the overall protein hydrophobicity, disrupts the heme configuration and leads to cytc oligomerization. Our results corroborate with available data showing that cytc reacts with 7α -ChOOH through a homolytic mechanism producing lipid- and protein-derived radicals. We demonstrated

that cytc oligomerization occurs via dityrosine cross-links formation. Additional studies are necessary to evaluate the presence of cytc oligomers *in vivo* and to identify their biological role under oxidative stress condition. Furthermore, we speculate that under these circumstances 7α -ChOOH may contribute to increase the oxidative stress in the mitochondria and, ultimately, to apoptosis signaling.

5. Acknowledgements

This study was supported by Fundação de Amparo à Pesquisa do Estado de São Paulo [FAPESP, CEPID–Redoxoma Grant 2013/07937-8], Conselho Nacional de Desenvolvimento Científico e Tecnológico [CNPq, Universal 424094/2016-9], Coordenação de Aperfeiçoamento de Pessoal de Nível Superior [CAPES, Finance Code 001] and Pro-Reitoria de Pesquisa da Universidade de São Paulo [PRPUSP]. The PhD scholarship of Isabella F. D. Pinto was supported by FAPESP [grant 2014/11556-2]. The PhD scholarship of Alex Inague was supported by FAPESP [grant 2017/13804-1]. The PhD scholarship of Lucas S Dantas was supported by CNPq.

6. References

1. Basañez G, Caballero F, Colell Riera A, Fernández-Checa JC, García-Ruiz C, Marí M, et al. Mitochondrial cholesterol in health and disease. *Histology and Histopathology*. 2009;24:117-32.
2. Ikonen E. Cellular cholesterol trafficking and compartmentalization. *Nature Reviews Molecular Cell Biology*. [Review Article]. 2008;9:125.
3. Maxfield FR, Tabas I. Role of cholesterol and lipid organization in disease. *Nature*. 2005;438:612.
4. Colell A, Fernández A, Fernández-Checa JC. Mitochondria, cholesterol and amyloid β peptide: a dangerous trio in Alzheimer disease. *Journal of Bioenergetics and Biomembranes*. 2009;41(5):417.
5. Montero J, Morales A, Llacuna L, Lluís JM, Terrones O, Basañez G, et al. Mitochondrial Cholesterol Contributes to Chemotherapy Resistance in Hepatocellular Carcinoma. *Cancer Research*. 2008;68(13):5246.
6. Ribas V, García-Ruiz C, Fernández-Checa JC. Mitochondria, cholesterol and cancer cell metabolism. *Clinical and translational medicine*. 2016;5(1):22-.

7. Miyoshi N. Biochemical properties of cholesterol aldehyde secosterol and its derivatives. *Journal of clinical biochemistry and nutrition*. 2018;62(2):107-14.
8. Murphy RC, Johnson KM. Cholesterol, reactive oxygen species, and the formation of biologically active mediators. *The Journal of biological chemistry*. 2008;283(23):15521-5.
9. Higdon A, Diers AR, Oh JY, Landar A, Darley-Usmar VM. Cell signalling by reactive lipid species: new concepts and molecular mechanisms. *The Biochemical journal*. 2012;442(3):453-64.
10. Ow Y-LP, Green DR, Hao Z, Mak TW. Cytochrome c: functions beyond respiration. *Nature Reviews Molecular Cell Biology*. [Review Article]. 2008;9:532.
11. Hüttemann M, Pecina P, Rainbolt M, Sanderson TH, Kagan VE, Samavati L, et al. The multiple functions of cytochrome c and their regulation in life and death decisions of the mammalian cell: From respiration to apoptosis. *Mitochondrion*. 2011;11(3):369-81.
12. Li P, Nijhawan D, Budihardjo I, Srinivasula SM, Ahmad M, Alnemri ES, et al. Cytochrome c and dATP-Dependent Formation of Apaf-1/Caspase-9 Complex Initiates an Apoptotic Protease Cascade. *Cell*. 1997;91(4):479-89.
13. Zou H, Li Y, Liu X, Wang X. An APAF-1·Cytochrome c Multimeric Complex Is a Functional Apoptosome That Activates Procaspase-9. *Journal of Biological Chemistry*. 1999;274(17):11549-56.
14. Nam Hoon K, Moon Sik J, Soo Young C, Jung Hoon K. Oxidative Modification of Cytochrome c by Hydrogen Peroxide. *Mol Cells*. 2006;22(2):220-7.
15. Genaro-Mattos TC, Appolinário PP, Mugnol KCU, Bloch Jr C, Nantes IL, Di Mascio P, et al. Covalent Binding and Anchoring of Cytochrome c to Mitochondrial Mimetic Membranes Promoted by Cholesterol Carboxyaldehyde. *Chemical Research in Toxicology*. 2013;26(10):1536-44.
16. Genaro-Mattos TC, Queiroz RF, Cunha D, Appolinario PP, Di Mascio P, Nantes IL, et al. Cytochrome c Reacts with Cholesterol Hydroperoxides To Produce Lipid- and Protein-Derived Radicals. *Biochemistry*. 2015;54(18):2841-50.
17. Paviani V, Galdino GT, Prazeres JNd, Queiroz RF, Augusto O. Dityryptophan Cross-Links as Novel Products of Protein Oxidation. *Journal of the Brazilian Chemical Society*. 2018;29:925-33.
18. Catalano CE, Choe YS, Ortiz de Montellano PR. Reactions of the protein radical in peroxide-treated myoglobin. Formation of a heme-protein cross-link. *Journal of Biological Chemistry*. 1989;264(18):10534-41.
19. Barr DP, Gunther MR, Deterding LJ, Tomer KB, Mason RP. ESR Spin-trapping of a Protein-derived Tyrosyl Radical from the Reaction of Cytochrome c with Hydrogen Peroxide. *Journal of Biological Chemistry*. 1996;271(26):15498-503.
20. Heinecke JW, Li W, Daehnke HL, Goldstein JA. Dityrosine, a specific marker of oxidation, is synthesized by the myeloperoxidase-hydrogen peroxide system of human neutrophils and macrophages. *Journal of Biological Chemistry*. 1993;268(6):4069-77.
21. McCormick ML, Gaut JP, Lin T-S, Britigan BE, Buettner GR, Heinecke JW. Electron Paramagnetic Resonance Detection of Free Tyrosyl Radical Generated by Myeloperoxidase,

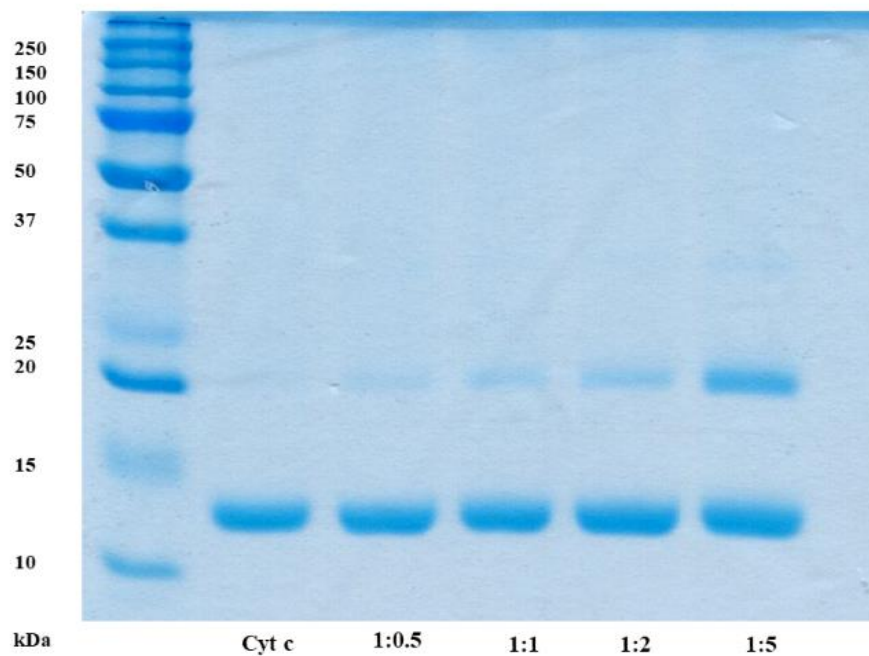
- Lactoperoxidase, and Horseradish Peroxidase. *Journal of Biological Chemistry*. 1998;273(48):32030-7.
22. Galeazzi L, Ronchi P, Fau - Franceschi C, Franceschi C Fau - Giunta S, Giunta S. In vitro peroxidase oxidation induces stable dimers of beta-amyloid (1-42) through dityrosine bridge formation. 1999(1350-6129 (Print)).
 23. Pennathur S, Jackson-Lewis V, Przedborski S, Heinecke JW. Mass Spectrometric Quantification of 3-Nitrotyrosine, ortho-Tyrosine, and o,o'-Dityrosine in Brain Tissue of 1-Methyl-4-phenyl-1,2,3,6-tetrahydropyridine-treated Mice, a Model of Oxidative Stress in Parkinson's Disease. *Journal of Biological Chemistry*. 1999;274(49):34621-8.
 24. Ziouzenkova O, Asatryan L, Akmal M, Tetta C, Wratten ML, Loseto-Wich G, et al. Oxidative Cross-linking of ApoB100 and Hemoglobin Results in Low Density Lipoprotein Modification in Blood: Relevance to a Atherogenesis Caused by Hemodialysis. *Journal of Biological Chemistry*. 1999;274(27):18916-24.
 25. Bodaness RS, Leclair M, Zigler JS. An analysis of the H₂O₂-mediated crosslinking of lens crystallins catalyzed by the heme-undecapeptide from cytochrome c. *Archives of Biochemistry and Biophysics*. 1984;231(2):461-9.
 26. Onorato JM, Thorpe SR, Baynes JW. Immunohistochemical and ELISA Assays for Biomarkers of Oxidative Stress in Aging and Disease. *Annals of the New York Academy of Sciences*. 1998;854(1):277-90.
 27. Leeuwenburgh C, Hansen PA, Holloszy JO, Heinecke JW. Hydroxyl radical generation during exercise increases mitochondrial protein oxidation and levels of urinary dityrosine. *Free Radical Biology and Medicine*. 1999;27(1):186-92.
 28. Oellerich S, Lecomte S, Paternostre M, Heimburg T, Hildebrandt P. Peripheral and Integral Binding of Cytochrome c to Phospholipids Vesicles. *The Journal of Physical Chemistry B*. 2004 2004/03/01;108(12):3871-8.
 29. Buege JA, Aust SD. [30] Microsomal lipid peroxidation. In: Fleischer S, Packer L, editors. *Methods in Enzymology*: Academic Press; 1978. p. 302-10.
 30. Dantas LS, Chaves-Filho AB, Coelho FR, Genaro-Mattos TC, Tallman KA, Porter NA, et al. Cholesterol secosterol aldehyde adduction and aggregation of Cu,Zn-superoxide dismutase: Potential implications in ALS. *Redox biology*. 2018;19:105-15.
 31. Lima DB, de Lima TB, Balbuena TS, Neves-Ferreira AGC, Barbosa VC, Gozzo FC, et al. SIM-XL: A powerful and user-friendly tool for peptide cross-linking analysis. *Journal of Proteomics*. 2015;129:51-5.
 32. Banci L, Bertini I, Boca M, Calderone V, Cantini F, Girotto S, et al. Structural and dynamic aspects related to oligomerization of apo SOD1 and its mutants. *Proceedings of the National Academy of Sciences*. 2009;106(17):6980.
 33. Münch C, O'Brien J, Bertolotti A. Prion-like propagation of mutant superoxide dismutase-1 misfolding in neuronal cells. *Proceedings of the National Academy of Sciences*. 2011;108(9):3548.
 34. Belikova NA, Tyurina YY, Borisenko G, Tyurin V, Samhan Arias AK, Yanamala N, et al. Heterolytic Reduction of Fatty Acid Hydroperoxides by Cytochrome c/Cardiolipin Complexes: Antioxidant Function in Mitochondria. *Journal of the American Chemical Society*. 2009 2009/08/19;131(32):11288-9.

35. Rodriguez-Lopez JN, Smith AT, Thorneley RNF. Role of Arginine 38 in Horseradish Peroxidase: A Critical residue for Substrate Binding and Catalysis. *Journal of Biological Chemistry*. 1996;271(8):4023-30.
36. Kapralov AA, Yanamala N, Tyurina YY, Castro L, Samhan-Arias A, Vladimirov YA, et al. Topography of tyrosine residues and their involvement in peroxidation of polyunsaturated cardiolipin in cytochrome c/cardiolipin peroxidase complexes. *Biochimica et Biophysica Acta (BBA) - Biomembranes*. 2011;1808(9):2147-55.
37. Chen Y-R, Gunther MR, Mason RP. An Electron Spin Resonance Spin-trapping Investigation of the Free Radicals Formed by the Reaction of Mitochondrial Cytochrome c Oxidase with H₂O₂. *Journal of Biological Chemistry*. 1999;274(6):3308-14.
38. Qian SY, Chen Y-R, Deterding LJ, Fann YC, Chignell CF, Tomer KB, et al. Identification of protein-derived tyrosyl radical in the reaction of cytochrome c and hydrogen peroxide: characterization by ESR spin-trapping, HPLC and MS. *Biochemical Journal*. 2002;363(2):281.
39. Shchepin R, Möller MN, Kim H-yH, Hatch DM, Bartesaghi S, Kalyanaraman B, et al. Tyrosine-Lipid Peroxide Adducts from Radical Termination: Para Coupling and Intramolecular Diels-Alder Cyclization. *Journal of the American Chemical Society*. 2010;132(49):17490-500.
40. Hirota S, Hattori Y, Nagao S, Taketa M, Komori H, Kamikubo H, et al. Cytochrome c polymerization by successive domain swapping at the C-terminal helix. *Proceedings of the National Academy of Sciences*. 2010;107(29):12854.
41. Margoliash E, Lustgarten J. Interconversion of Horse Heart Cytochrome c Monomer and Polymers. *Journal of Biological Chemistry*. 1962;237(11):3397-405.
42. Giulivi C, N.J. T, Davies KJ. Tyrosine oxidation products: analysis and biological relevance. *Amino Acids*. 2003;25(3-4):227-32.
43. Aeschbach R, Amadoò R, Neukom H. Formation of dityrosine cross-links in proteins by oxidation of tyrosine residues. *Biochimica et Biophysica Acta (BBA) - Protein Structure*. 1976 1976/08/09;439(2):292-301.
44. Giulivi C, Davies KJ. Dityrosine and tyrosine oxidation products are endogenous markers for the selective proteolysis of oxidatively modified red blood cell hemoglobin by (the 19 S) proteasome. *Journal of Biological Chemistry*. 1993;268(12):8752-9.
45. Al-Hilaly YK, Williams TL, Stewart-Parker M, Ford L, Skaria E, Cole M, et al. A central role for dityrosine crosslinking of Amyloid- β in Alzheimer's disease. *Acta Neuropathologica Communications*. 2013;1(1):83.
46. Krishnan S, Chi EY, Wood SJ, Kendrick BS, Li C, Garzon-Rodriguez W, et al. Oxidative Dimer Formation Is the Critical Rate-Limiting Step for Parkinson's Disease α -Synuclein Fibrillogenesis. *Biochemistry*. 2003;42(3):829-37.
47. Ying T, Wang Z-H, Lin Y-W, Xie J, Tan X, Huang Z-X. Tyrosine-67 in cytochrome c is a possible apoptotic trigger controlled by hydrogen bonds via a conformational transition. *Chemical Communications*. 2009(30):4512-4.
48. Wang Z, Matsuo T, Nagao S, Hirota S. Peroxidase activity enhancement of horse cytochrome c by dimerization. *Organic & Biomolecular Chemistry*. 2011;9(13):4766-9.

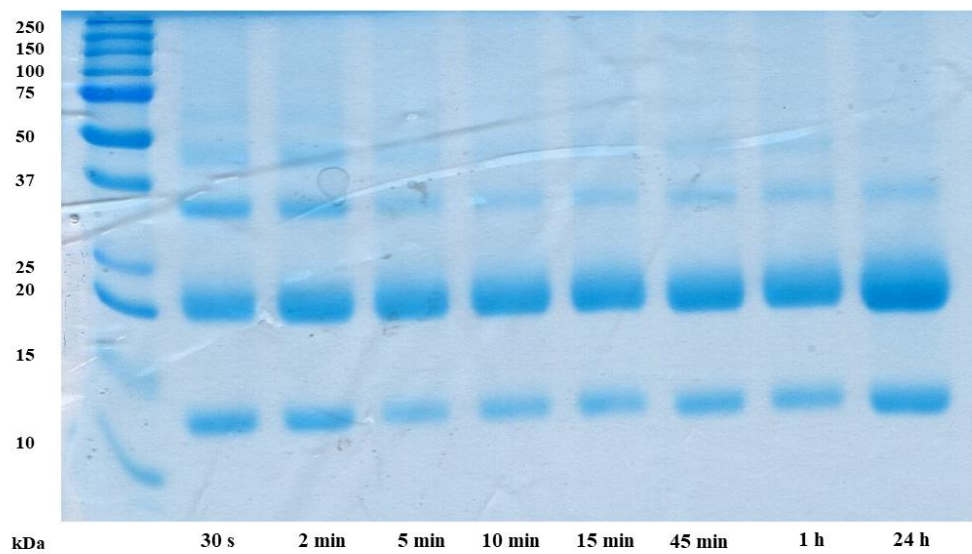
49. Turrens JF. Mitochondrial formation of reactive oxygen species. *The Journal of physiology*. 2003;552(Pt 2):335-44.
50. Jinn S, Brandis Katrina A, Ren A, Chacko A, Dudley-Rucker N, Gale Sarah E, et al. snoRNA U17 Regulates Cellular Cholesterol Trafficking. *Cell Metab*. 2015;21(6):855-67.
51. Alpy F, Tomasetto C. Give lipids a START: the StAR-related lipid transfer (START) domain in mammals. *Journal of Cell Science*. 2005;118(13):2791.
52. Bose HS, Lingappa VR, Miller WL. The Steroidogenic Acute Regulatory Protein, StAR, Works Only at the Outer Mitochondrial Membrane. *Endocrine Research*. 2002 2002/01/01;28(4):295-308.
53. Rowland AA, Voeltz GK. Endoplasmic reticulum–mitochondria contacts: function of the junction. *Nature Reviews Molecular Cell Biology*. 2012;13:607.
54. Marí M, Morales A, Colell A, García-Ruiz C, Fernández-Checa JC. Mitochondrial cholesterol accumulation in alcoholic liver disease: Role of ASMase and endoplasmic reticulum stress. *Redox Biology*. 2014;3:100-8.
55. Korytowski W, Wawak K, Pabisz P, Schmitt Jared C, Chadwick Alexandra C, Sahoo D, et al. Impairment of Macrophage Cholesterol Efflux by Cholesterol Hydroperoxide Trafficking. *Arteriosclerosis, Thrombosis, and Vascular Biology*. 2015;35(10):2104-13.

Supplementary figures

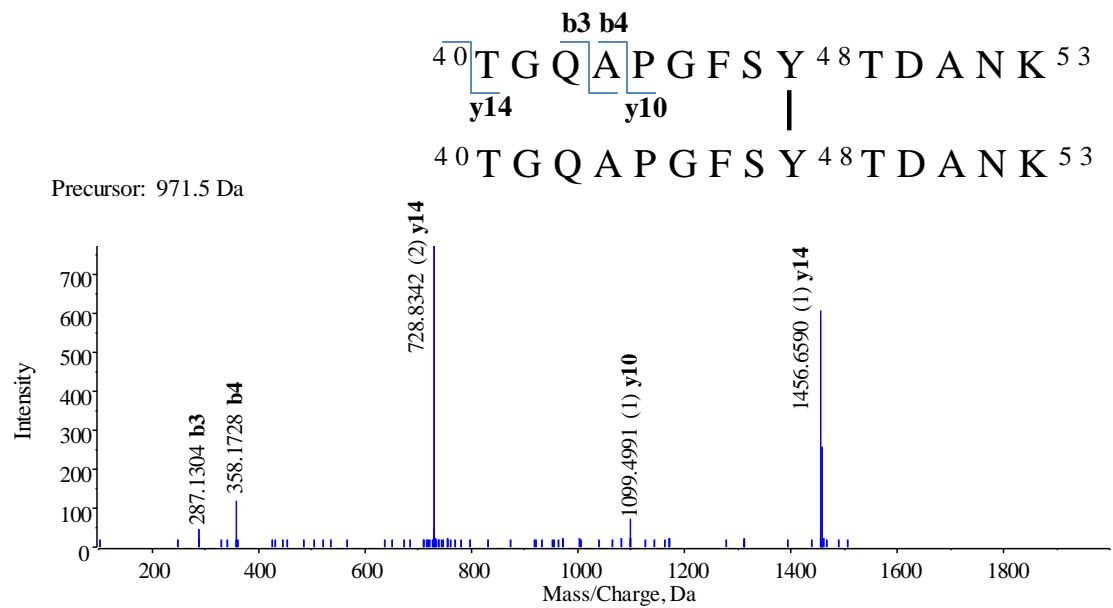
A



B



Supplementary Figure S1. (A) Time course of reaction of cytochrome c oligomerization with 7 α -ChOOH in presence of SDS micelles. (B) Cytochrome c oligomerization depends on concentration of 7 α -ChOOH.



Supplementary Figure S2. nLC-ESI-MS/MS analysis of dityrosine cross-linked peptides from cytochrome c dimers induced by ChOOH mixture. MS/MS spectra of the dityrosine cross-linked ⁴⁰TGQAPGFSTYDANK⁵³ homodimer with [M + 3H]³⁺ at m/z 971.4447, cross-linked between Y48 and Y48.

CHAPTER 3

Lipidomic Analysis Reveals Blood Plasma Signatures in a Rodent Model of Amyotrophic Lateral Sclerosis

Isabella F D Pinto¹, Adriano de B Chaves Filho¹, Lucas S Dantas¹, Marisa H G
Medeiros¹, Isaías Glezer², Marcos Y Yoshinaga¹, Sayuri Miyamoto^{1,*}

¹ Department of Biochemistry, Institute of Chemistry, University of Sao Paulo, Sao Paulo, Brazil

² Department of Biochemistry, Paulista School of Medicine, Federal University of Sao Paulo, Sao Paulo, Brazil.

*Corresponding Author: Sayuri Miyamoto. E-mail address: miyamoto@iq.usp.br
Institutional address: Departamento de Bioquímica, Instituto de Química, Av. Prof. Lineu Prestes 1524, CP 26077, CEP 05313-970, Butantã, São Paulo, SP. Brazil. Phone: + 55 11 30911413

Abstract

Amyotrophic lateral sclerosis (ALS) is a neurodegenerative disease that affects motor neurons in the central nervous system resulting in progressive paralysis and death. There is growing evidence suggesting cross-talk between ALS and lipid metabolism. This study aimed to characterize lipid alterations in blood plasma of asymptomatic and symptomatic SOD1G93A rat model of ALS by untargeted lipidomics approach based on high resolution mass spectrometry. We have identified and quantified fatty acyls, glycerophospholipids, sphingolipids and neutral lipids, covering over 296 lipid species. Univariate analysis revealed a total of 54 lipid species significantly altered in symptomatic relative to asymptomatic rats. Triglycerides esterified to long-chain polyunsaturated fatty acids were considerably decreased in the symptomatic rats, suggesting a possible link to increased hypermetabolism and peripheral clearance induced by the disease. Moreover, significant decreases in phosphatidylcholine species were also noticed. On the other hand, sphingolipids, particularly hexosylceramide and acylceramide were found markedly elevated in the symptomatic rats. Detailed lipidomic analysis of pooled lipoprotein fractions revealed that acylceramide and hexoylceramide were enriched in HDL fractions. Collectively, our results were consistent with recent emerging evidences highlighting the importance of alteration of sphingolipids and triglycerides metabolism in neurodegenerative disease. Of note, we described, for the first time, acylceramide in blood plasma. Although the mechanisms involved in lipid alterations remain still unclear, our study provides interesting insights to potential lipid targets for future studies of ALS.

Keywords: Amyotrophic lateral sclerosis, SOD1G93A rats, blood plasma, lipoproteins, lipidomic analysis, acylceramides, triglyceride, glycerophospholipids, hexosylceramides

Highlights

- We performed a comprehensive lipidomic analysis of blood plasma in SOD1G93A rat model of amyotrophic lateral sclerosis.
- Our results revealed alteration in sphingolipids, glycerophospholipids and triglycerides metabolism which might be related to the lipid dysregulation and disease progression.
- Lipid characterization of pooled lipoprotein fractions, the major source of circulating lipid in blood plasma, suggests alteration in triglycerides and glycerophospholipids were related to very low-density lipoprotein.
- Acylceramides have not been previously described in blood plasma. We demonstrated accumulation of acylceramides and hexosylceramide associated with high-density lipoprotein.

Abbreviation

See Supplementary Information for abbreviation of lipid classes.

ALS: amyotrophic lateral sclerosis

FPLC: fast protein liquid chromatography

HDL: high-density lipoprotein

LC-MS: liquid chromatography coupled to mass spectrometry

LDL: low-density lipoprotein

PUFA: polyunsaturated fatty acid

SOD1: superoxide dismutase 1

VLDL: very low-density lipoprotein

1. Introduction

Amyotrophic lateral sclerosis (ALS) is a progressive neurodegenerative disease that affects motor neurons in the central nervous system. The majority of ALS cases are considered sporadic (90%), but a significant proportion of familial cases (12–20%) results from mutations in the Superoxide Dismutase 1 (SOD1) gene. ALS patients develop muscle weakness and atrophy leading to paralysis and death within 3–5 years after the disease onset. Both sporadic and familial forms are clinically and pathologically undistinguishable linked to a common pathogenic mechanism (1). The pathophysiological mechanisms underlying the development of neurodegeneration in ALS are multifactorial, with emerging evidence pointing to a complex interaction between genetic and molecular pathways. Specifically, glutamate excitotoxicity, generation of free radicals, cytoplasmic protein aggregates combined with mitochondrial dysfunction, and disruption of axonal transport processes through accumulation of neurofilament intracellular aggregates seems to be an important final common pathway in ALS (2). However, the exact pathogenic mechanisms of ALS are still unclear.

The lack of current treatments for ALS or early diagnosis reflects the absence of a comprehensive understanding of biological mechanisms underlying changes that occur during the progression of neurodegeneration. This underscores the urgent need for a blood-based biomarker that could act as a screening tool to identify at-risk individuals but may also support the development of preventative therapies or even therapeutic intervention. There is growing evidence for lipid metabolism alterations playing a crucial role in ALS pathogenesis (3-6). Higher levels of cholesterol, LDL, as well as an elevated LDL/HDL ratio in ALS patient blood have been correlated with increased survival (7, 8). Conversely, similar increases in total cholesterol, LDL and HDL

cholesterol in ALS patient blood (9, 10) and cerebrospinal fluid (CSF) (11) have not been found to be correlated with disease progression. Furthermore, a small number of studies contradict these findings (12-14).

Recently, an increased number of lipidomic analysis has been performed by mass spectrometry in ALS patients and SOD1 mice highlighting the role of lipid compounds in ALS progression (5, 6, 15). Phospholipids, particularly phosphatidylcholine, are significantly increased in the CSF of ALS patients (6). Interestingly, significant predictions of clinical evolution were found to be correlated to CSF sphingomyelins and triglycerides with long-chain fatty acids (6). Such findings are favorable for the development of biomarker assay, but further tests are required to confirm the reliability of predictive models, before use as a prognostic biomarker.

Although lipidomics is becoming increasingly popular, a comprehensive lipidomics analysis of blood plasma from ALS patients or animal model needs to be performed. In this study, we performed a comprehensive and comparative mass spectrometry-based lipidomic analysis of blood plasma and pooled lipoprotein fractions in SOD1G93A rats and wild type littermates. Our results revealed major alterations in bulk plasma of symptomatic SOD1G93A rats linked to triglycerides, glycerophospholipids, acylceramides and hexosylceramides that were reproduced in lipoprotein fractions. Our findings provide further knowledge on lipid metabolism related to ALS.

2. Materials and Methods

2.1 Materials

The lipids used as internal standards, described in supplementary information, were purchased from Avanti Polar Lipids (Alabaster, AL, USA). Methyl tert-butyl ether (MTBE), ammonium formate and ammonium acetate were purchased from Sigma-

Aldrich (St Louis, MO, USA). All HPLC grade organic solvents were obtained from Sigma-Aldrich (St Louis, MO, USA). Ultra-pure water was supplied by a Millipore system (Millipore, Billerica, MA, USA).

2.2 Animals

Male Sprague Dawley rats overexpressing mutant human SOD1G93A (hSODG93A) obtained from Taconics were maintained in our animal facility at room temperature with a 12 h light/dark cycle. They were feed a chow diet and had free access to water. Genotyping was performed for detecting exogenous hSOD1G93A transgene by amplification of ear DNA at 20 days of age (16). At 73 ± 4 days of age (referred as to asymptomatic group, $n=7$), rats were without signs of motor impairment. At 122 ± 6 days of age (referred as to symptomatic group, $n=13$), rats showed partial paralysis, in at least one limb, importantly, with loss of body weight. Age and litter matched wild type (WT) male served as controls (referred as WT 70 days of age, $n = 7$ and WT 120 days of age, $n=15$). The criteria for sacrifice of symptomatic group were loss of 15% of maximum body weight. Rats were fasted for 4h and anesthetized by isoflurane inhalation at dose of 4% for induction and 2% for maintenance. Blood was collected by cardiac puncture into a tube containing heparin (BD, Franklin Lakes, NJ, USA). Plasma was obtained after centrifugation at $2,000 \times g$ for 10 min at 4°C and stored at -80°C until further processing. All procedures were performed in accordance with the National Institute of Health Guidelines for the Humane Treatment of Animal and approved by the local Animal Care and Use Committee of Sao Paulo University (CEUA number 41/2016).

2.3 Blood plasma lipoprotein isolation by FPLC

Lipoproteins were isolated from blood plasma as described previously (17). In brief, an Akta FPLC equipped with a Superose 6 PC 3.2/300 column (GE Healthcare Europe

GmbH, Munich, Germany) was used with Dulbecco's phosphate-buffered saline (PBS) containing 1 mM EDTA as a running buffer. After loading of 50 μ l plasma into the system, a constant flow of 40 μ l/min was applied, and fractionation was started after 18 min with 80 μ l per fraction. Fractions 1–36 containing the plasma lipoproteins were used for further analysis.

2.4 Lipid extraction

Lipids were extracted from plasma and pooled lipoprotein fractions by MTBE method with modification (18, 19). Briefly, 80 μ l of plasma were mixed with 80 μ l of a mixture of internal standards (Supplementary Table S1) and 220 μ l of ice-cold methanol. After thoroughly vortexing for 10 s, 1 ml of MTBE was added to the mixture, which was stirred for 1 h at 20°C. Next, 300 μ l of water was added to the mixture, followed by vortexing 10 s and resting in an ice bath for 10 min. After centrifugation at 10,000 $\times g$ for 10 min at 4°C, the supernatant containing the lipid extract was transferred to a vial and dried under N₂ gas. The extracted lipids were re-dissolved in 80 μ l of isopropanol for the LC-MS/MS analysis. For each lipoprotein fractions or pooled lipoprotein fractions, 60 μ l of the corresponding fraction were extracted as described above using a mixture of internal standard (Supplementary Table S2).

2.5 Lipidomic analysis

Lipids were analyzed by untargeted analysis using liquid chromatography (Nexera UHPLC, Shimadzu, Kyoto, JAP) coupled to a TripleTOF6600 mass spectrometer (Sciex, Concord, ON, CAN) with electrospray ionization (ESI) in both negative and positive modes. Samples were injected into a CORTECS[®] column (UPLC C18 column, 1.6 μ m, 2.1 mm i.d. 100 mm, Waters, Milford, MA, USA). The mobile phases comprised (A) water/acetonitrile (60:40) and (B) isopropanol/acetonitrile/water

(88/10/2) both with 10 mM ammonium acetate or ammonium formate for analysis in negative or positive mode, respectively. The gradient was started from 40 to 100% over the first 10 min, holds at 100%B from 10 to 12 min, and then decreased from 100 to 40%B during 12-13 min, and holds at 40%B from 13 to 20 min. The flow rate was 0.2 ml/min, and column temperature was maintained at 35°C. The MS was operated in Information Dependent Acquisition (IDA[®]) acquisition mode with scan range set a mass-to-charge ratio of 100-2000 Da. Data were obtained in a period cycle time of 1.05 s with 100 ms acquisition time for MS1 scan and 25 ms acquisition time to obtain the top 36 precursor ions. Data acquisition was performed using Analyst[®] 1.7.1 with an ion spray voltage of -4.5 kV and 5.5 kV for negative and positive modes, respectively, and the cone voltage at \pm 80 V. The curtain gas was set at 25 psi, nebulizer and heater gases at 45 psi and interface heater of 450°C.

2.6 Data processing

Lipid species detected were manually identified based on MS/MS fragments from PeakView[®] (Sciex, Concord, ON, CAN) and annotated (identity, exact mass and retention time) using an Excel[®] macro. The ESI negative mode was primarily directed to identification of free fatty acids, glycerophospholipids and sphingolipids, while the ESI positive was directed to identification of neutral lipids (e.g. triglycerides). The area of each lipid species and internal standard were obtained by integration of MS peak using MultiQuant[®] (Sciex, Concord, ON, CAN). The lipid content of sample was determined by dividing the area of lipid to correspondent internal standard, multiplying by concentration of internal standard and then dividing by volume of sample or protein concentration. (Supplementary Table S1–S2). Concentration of lipids without internal standard was calculated using the response factor (Supplementary Table S3). Lipid species were annotated either by sum composition (e.g. isobaric species) or by

molecular species composition. Lipid annotation by sum composition is reported as [lipid class] [total number of carbons atoms in fatty acids moieties]:[total number of double bonds in fatty acids moieties] (e.g. PE 40:3). Lipid species annotated by molecular composition are reported as [lipid class] [total number of carbons atoms in fatty acids 1]:[total number of double bonds in fatty acid 1]/ [total number of carbons atoms in fatty acids 2]:[total number of double bonds in fatty acid 2]/ [total number of carbons atoms in fatty acids 3 (only for TG)]:[total number of double bonds in fatty acid 3 (only for TG)] (e.g. PE 16:0/22:3, TG 16:0/18:1/18:2). The symbol “/” denotes only the fatty acids moieties of the lipid species, and not their sn-1, sn-2 and sn-3 position on the glycerol-backbone.

2.7 Statistical analysis

Univariate and multivariate analysis for lipidomic data were performed using Metaboanalyst 4.0 (20). Zero values in the data were imputed with half of the minimum value of the corresponding lipid across all the samples. The dataset was log-transformed to prior statistical analysis. Statistical significance was evaluated by one-way ANOVA followed by Turkey’s post hoc test for multiple comparison or one-tailed t-test analysis for two comparison ($p < 0.05$). Bar graphs were generated using GraphPad Prism 5 (GraphPad Software Inc., San Diego, CA, USA) and represented as the mean \pm standard deviation (SD).

3. Results

3.1 Global lipidomic analysis of blood plasma in SOD1G93A rats

We studied differences in the plasma lipidome of SOD1G93A rats at asymptomatic (70 ± 3 days of age) and symptomatic stages (120 ± 6 days of age), as well as age-related WT littermates. We identified and quantified 296 molecular lipid species (not including

isomers) encompassing a total of 24 different lipid classes. The largest number of individual lipid species were found in glycerophospholipids ($n = 133$) followed by neutral lipids ($n = 89$), sphingolipids ($n = 55$), acylcarnitines (12) and fatty acyls (7) (Supplementary Figure S1A). Using sparse partial least squares regression discriminant analysis (sPLS-DA), we investigated the clustering pattern of all samples based on the lipid profiles. The sPLS-DA explaining 36.7% of data variation for the first PCs, revealing major differences in lipid composition between symptomatic and asymptomatic rats (Figure 1A).

In terms of relative abundance, neutral lipids such as cholesteryl ester (CE) and triglycerides (TG) are the most abundant lipid classes in blood plasma, comprising 66-73% and 7-10% of the total lipids (Supplementary Figure S1B), followed by glycerophospholipids which were comprised mostly by phosphatidylcholine (PC; 2%), lysophosphatidylcholine (LPC; 2-3%) and phosphatidylinositol (PI; 2-3%). Finally, sphingolipids such as ceramides (Cer), sphingomyelins (SM), hexosylceramides (HexCer) and acylceramides (AcylCer) appeared among lower abundant lipid classes.

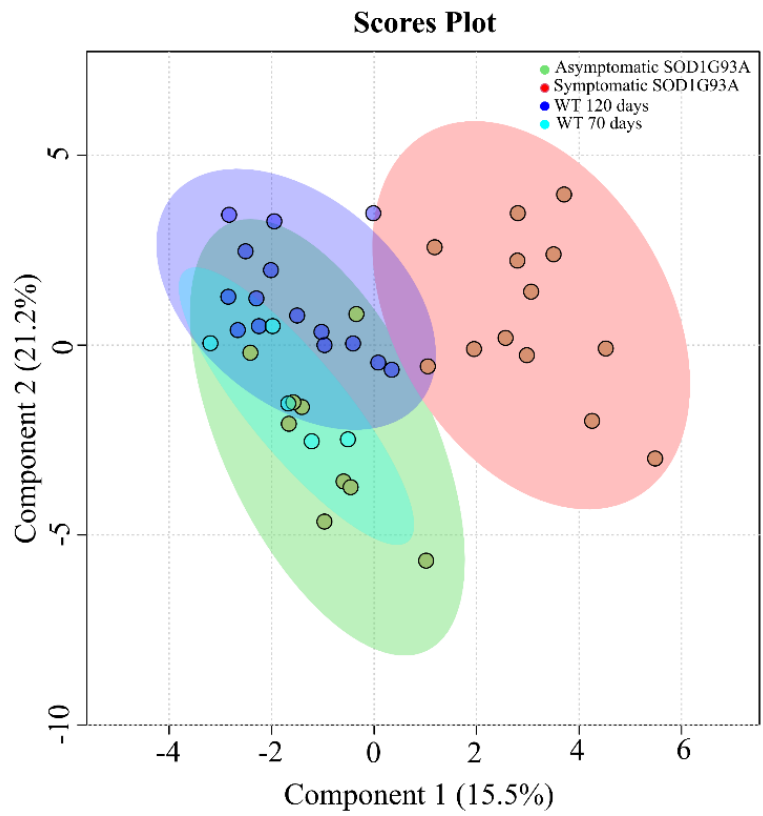
Further, we performed pairwise comparisons to investigate specific lipid changes relative to disease (WT *versus* SOD1G93A), disease progression (asymptomatic SOD1G93A *versus* symptomatic SOD1G93A) and age (WT 70 days *versus* WT 120 days). Venn diagram, constructed for the lipids highlighted by four pairwise comparisons, showed the distribution of 61 significantly altered lipid species (Fold change = 2; FDR adjusted p-value < 0.05) (Figure 1B). The major alterations were found in the pairwise comparison between symptomatic and asymptomatic ALS rats (e.g., 54 lipid species), according to the separation observed in sPLS-DA.

The lipid changes were represented as heat map (Figure 1C). Several TG species linked to polyunsaturated fatty acids (PUFA) were decreased in symptomatic animals, which is

in accordance with increased peripheral clearance of TG-rich lipoproteins in SOD1G93A mice (4) and a switch towards preferential use of lipids as a fuel source as an early event in the disease (21). Among altered phospholipids species, PC linked to PUFA, including linoleic (18:2), arachidonic (20:4) and docosahexaenoic acid (22:6), were decreased in symptomatic animals. Collectively, our results suggest that reduced levels of phospholipids and TG species can potentially result from increased use of lipoprotein-associated TG molecules for energy production (e.g. skeletal muscle) (4, 21).

In contrast, HexCer and AcylCer species (e.g., HexCer d18:2/25:0, HexCer d18:1/23:0 and AcylCer d18:1/24:1+20:4) were found significantly increased in symptomatic relative to asymptomatic rats. Interestingly, AcylCer have not been previously described in the blood plasma. Overall, our results are consistent with previous study that reported high levels of Cer and glucosylceramides (GlcCer) in spinal cord of ALS patients (22), stressing the crucial role of the complex sphingolipids pathway in the pathogenesis of the disease.

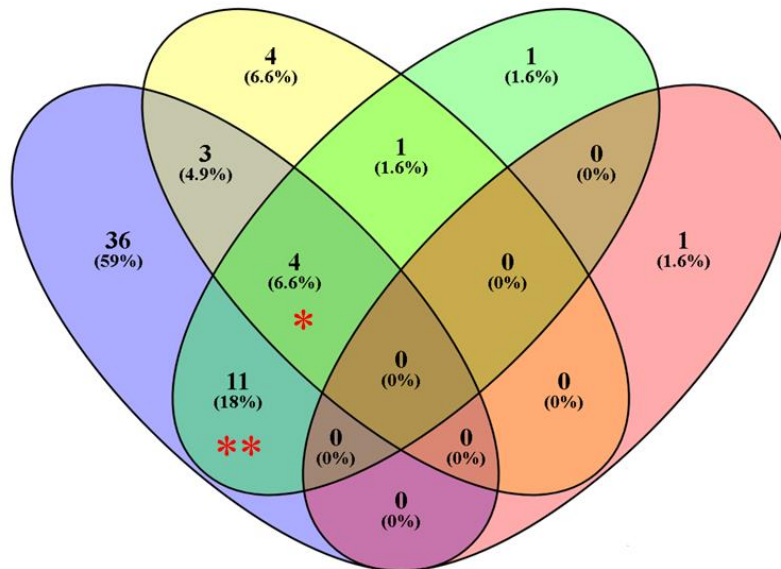
A



B

Symptomatic SOD1G93A vs WT 70 days

Symptomatic SOD1G93A vs WT 120 days



Symptomatic SOD1G93A vs Asymptomatic SOD1G93A

WT 120 days vs WT 70 days

C

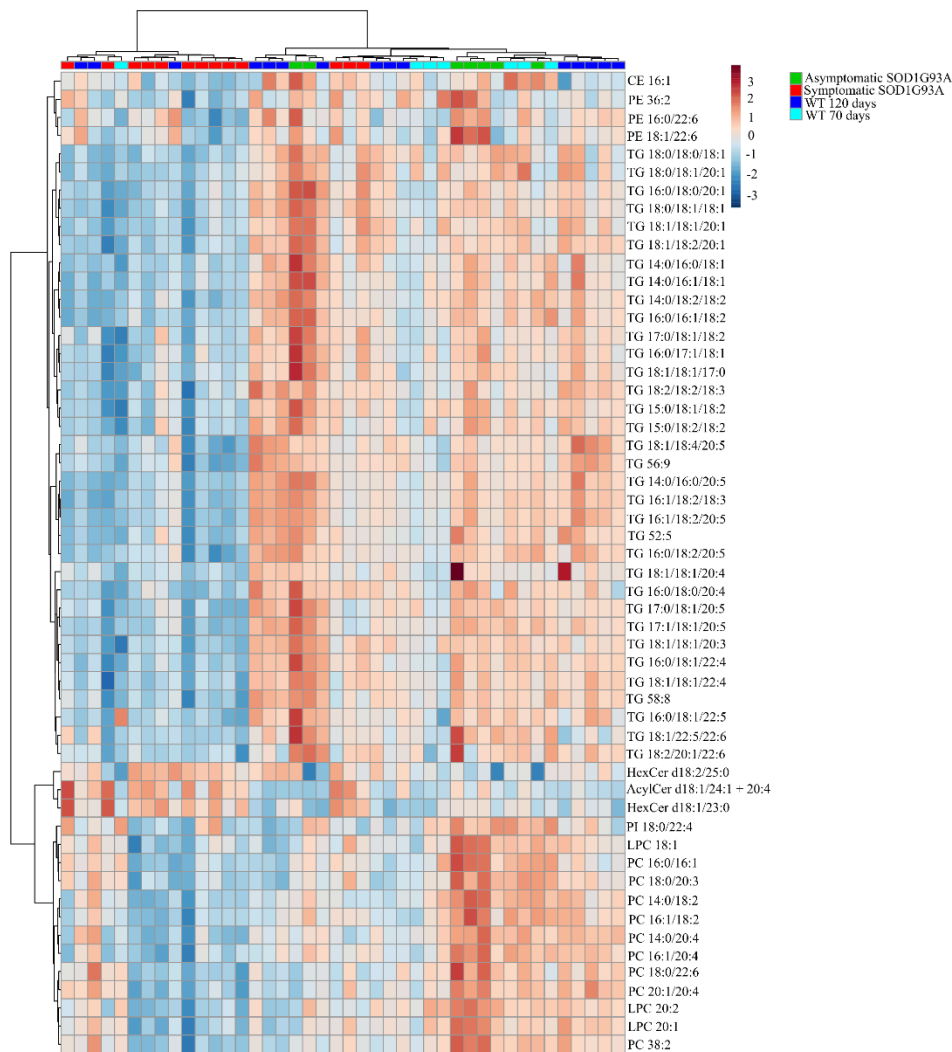


Figure 1. Global lipidomic analysis of blood plasma in SOD1G93A rats and WT littermates. (A) Score plot of the multivariate sPLS-DA model of plasma samples from SOD1G93A rats and WT littermates. Asymptomatic SOD1G93A (n = 7); WT 70 days (n = 7); symptomatic SOD1G93A (n = 12); WT 120 days (n = 15). (B) Venn diagram of significantly altered lipid species from four pairwise comparisons. (C) Heat map of 54 altered lipid species based on volcano plot. Each horizontal row represents lipid specie and each vertical column represents a sample. Euclidean distance and ward cluster algorithm were applied to build the heat map. The color code bar indicates the log of the concentration for a given lipid. TG 58:8 = TG 18:1/18:2/22:5 and 18:2/18:2/22:4; TG 56:9 = TG 18:2/18:3/20:4; TG 52:5 = TG 16:0/18:2/18:3 and 16:1/18:2/18:2; PC 38:2 = PC 18:0/20:2 and 18:1/20:1; PE 36:2 = PE 18:0/18:2 and 18:1/18:1. Asymptomatic SOD1G93A (n = 7); WT 70 days (n = 7); symptomatic SOD1G93A (n = 12); WT 120 days (n = 15). HexCer: hexosylceramide; AcylCer: acylceramide; TG: triglyceride; PC: phosphatidylcholine; LPC: lysophosphatidylcholine; PI: phosphatidylinositol; PE: phosphatidylethanolamine; CE: cholesteryl ester.

3.2 Panel of potential lipids markers in the plasma of SOD1G93A rats

In order to discriminate relevant lipid biomarkers from all altered lipid species described above, we used a filtration strategy based on Venn diagram (Figure 1B). As highlighted by asterisks in Figure 1B, 15 lipid species including TG-linked to polyunsaturated fatty acids, PC 14:0/20:4, LPC 20:2, HexCer d18:1/23:0 and AcylCer d18:1/24:1+20:4, were selectively altered by the disease thus being potential candidate biomarkers for monitoring ALS disease progression. TG-linked to long-chain polyunsaturated fatty acids, PC 14:0/20:4 and LPC 20:2 were significantly decreased in symptomatic rats compared to asymptomatic and control rats (Figure 2). In contrast, HexCer d18:1/23:0 and AcylCer d18:1/24:1+20:4 were significantly increased (~2 fold) in symptomatic rats.

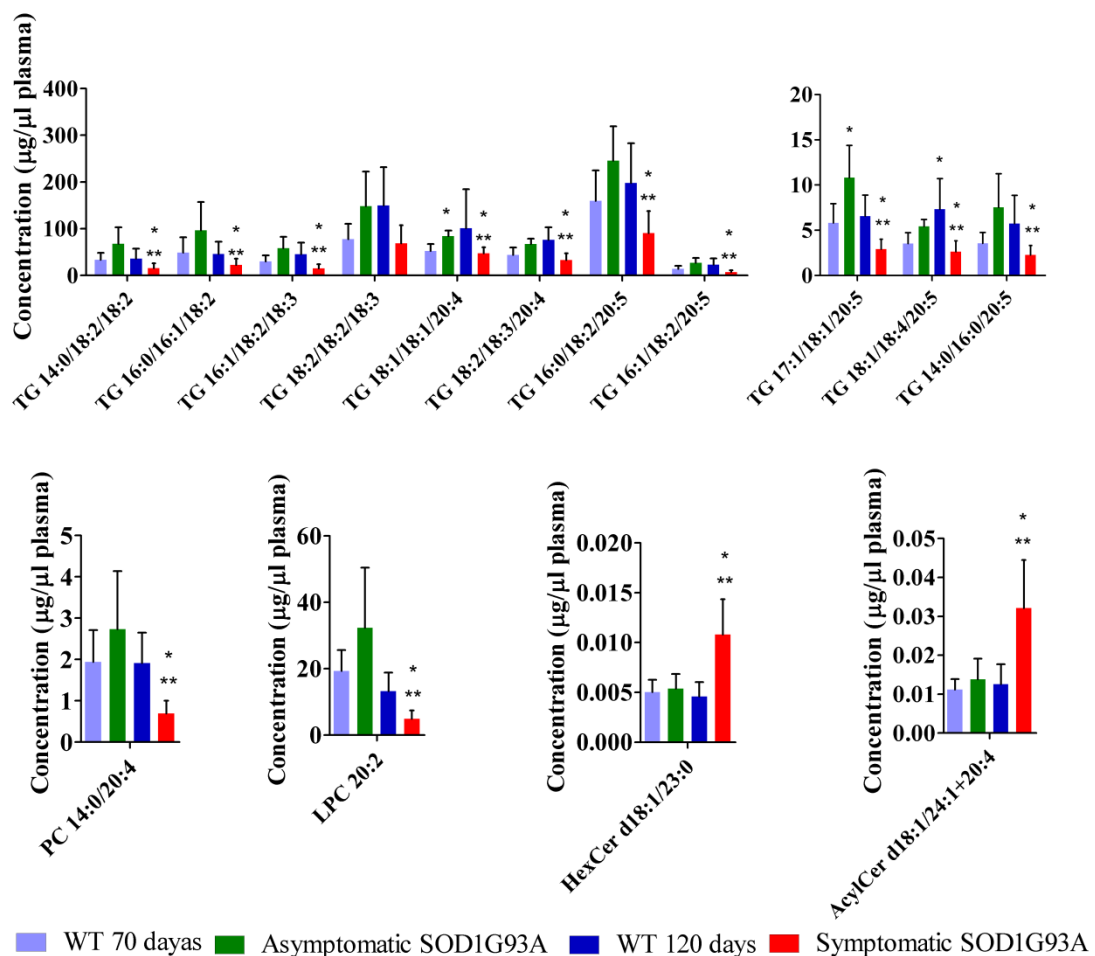


Figure 2. Lipid panels for disease prediction in ALS. Plasma concentration of TG, PC, LPC, HexCer and AcylCer in SOD1G93A and WT rats. Concentration values are given in $\mu\text{g lipid}/\mu\text{l plasma}$. Data are represented as mean \pm SD. Prior to statistical analysis the dataset was log transformed and analyzed by one-way ANOVA followed by Turkey's test. * FDR p-value <0.05 versus WT; ** FDR p-value <0.05 versus SOD1G93A. Asymptomatic SOD1G93A (n = 7); WT 70 days (n = 7); symptomatic SOD1G93A (n = 12); WT 120 days (n = 15).

3.3 Lipid profile of lipoproteins fractions

To investigate the plasma lipidome alterations in more detail, we inspected the lipid composition of lipoproteins. We isolated 36 fractions from 50 μl blood plasma of symptomatic SOD1G93A rats and age-related WT rats by FPLC - size exclusion chromatography. In order to check whether the major lipoprotein classes were properly separated, total cholesterol (Ch) and TG in each fraction were analyzed by mass spectrometry. Based on TG and Ch profile, three major peaks were pooled to perform a detailed lipidomic analysis (I - fraction 9 to 13, II - fraction 14 to 20 and III - fraction 22 to 27) (Figure 3).

We identified 202 lipid species comprising 16 different lipid classes (Supplementary Figure S2A). PCA of pooled lipoprotein fractions revealed a clear separation of the fractions 9-13 from 14-20 and 22-27 (Supplementary Figure S2B). In addition, to confirm the lipoprotein identity, we checked apolipoprotein content in each pooled lipoprotein fractions by proteomic analysis (Supplementary Table S4). Collectively, our results revealed that fraction 9-13 corresponds to VLDL, given the presence of apoB-100 and high content of TG followed by CE. Fraction 14-20 corresponds to HDL, with some LDL contamination. This fraction contained apoA-IV, apoE, apoA-I and apoB-100 with CE as the most abundant lipid. Finally, we attributed the fraction 22-27 to HDL with albumin contamination, since albumin partially co-eluted with HDL fractions. This fraction lacks apoB and is characterized by the presence of apoH and apoA-I. The lipid composition showed high percentage of CE and LPC.

After characterization of pooled lipoprotein fractions, we evaluated the presence significantly altered lipid species among the lipids detected in the isolated fractions (Figure 3). As expected, altered TG species were present in VLDL, while PC and CE were present in HDL/LDL. Additionally, LPC was found in HDL-albumin fraction. Importantly, AcylCer and HexCer was largely found in HDL/LDL fractions consistent.

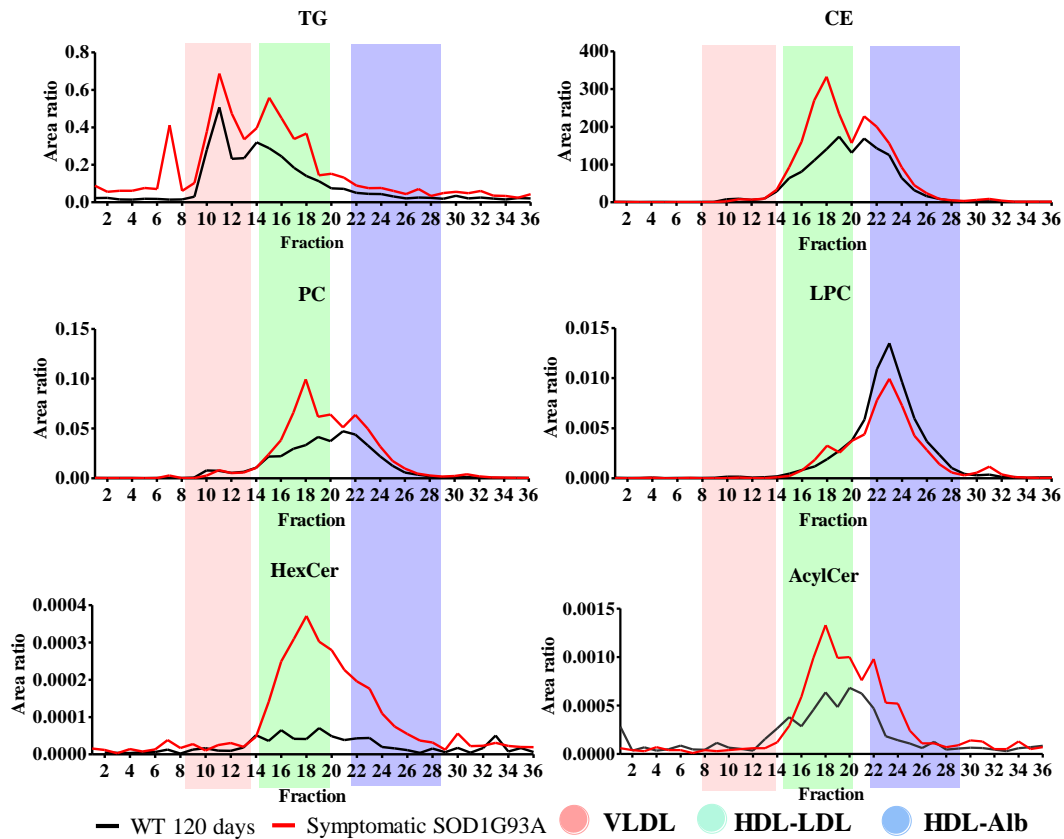


Figure 3. Distribution of altered lipid species from blood plasma in lipoprotein fractions.

FPLC profile showed the sum of altered lipid in symptomatic SOD1G93A and WT rat. AcylCer: acylceramide; TG: triglyceride; PC: phosphatidylcholine; LPC: lysophosphatidylcholine; CE: cholesteryl ester. Monitored species: TG - TG 14:0/16:0/18:1; TG 14:0/16:1/18:1; TG 16:0/16:1/18:2; TG 18:0/18:1/18:1; TG 15:0/18:1/18:2; TG 18:2/18:2/20:5; TG 16:0/18:2/20:5; TG 18:1/18:1/20:4; TG 16:0/18:1/22:4; TG 18:1/18:2/20:1; TG 17:0/18:1/18:2; TG 18:2/18:2/22:4; TG 18:2/18:3/20:4. LPC – LPC 18:1; LPC 20:1; LPC 20:2. CE – CE 18:1. AcylCer - AcylCer d18:1/24:1. PC – PC 16:1/18:2; PC 18:0/22:6; PC 18:0/20:3; PC 16:0/18:1; PC 18:0/20:2; PC 20:1/20:4. HexCer – HexCer d18:1/23:0; HexCer d18:2/25:0.

4. Discussion

In the present study, we investigated alterations in the blood plasma lipidome of SOD1G93A rat model for ALS and WT littermates by an untargeted lipidomic approach based on high resolution mass spectrometry. We found reliable evidence of significant decrease of TG and glycerophospholipids species in symptomatic compared with asymptomatic rats. Those lipids were associated with VLDL fractions. In contrast, sphingolipids such as HexCer and AcylCer were found elevated in plasma and enriched in HDL fractions.

Glycerophospholipids and triglycerides are abundant in blood plasma as major component of lipoproteins (23). PC is the most abundant phospholipids in all lipoproteins, specially HDL, while TG is majorily present in VLDL. In fact, PC carries out a crucial and unique function, in that it is the only phospholipid currently known to be required for lipoprotein assembly and secretion (24). In our study, decreased phospholipids such as PC species were mostly linked to omega-6 fatty acids, such as linoleic acid (18:2) and arachidonic acid (20:4) and omega-3 fatty acid 22:6 (DHA). Previous lipidomics analysis in CSF from ALS patients showed an elevated concentration of PC linked to 20:4 (6). This data may reflect the metabolic activity of phospholipase A2 (PLA2), resulting in an increased production of lipid mediators, such as eicosanoids that promote inflammation and are generally considered to play a role in the pathophysiology of ALS (25). Whereas some authors have reported an association between loss of motor neuron in spinal cord of ALS model mice and reduction of PC linked to DHA (26), others have highlighted the significant increase of DHA in frontal cortex of ALS patients relative to controls (26, 27).

Emerging evidence indicates high energy expenditure in SOD1G86R and G93A mice as well as in sporadic ALS patients (3, 28, 29). As far as the energy deficit is observed in

ALS, previous study reported increased peripheral clearance of TG-rich lipoprotein (4). It is known that VLDL delivered TG to peripheral tissues (primarily muscle and adipose tissue) for storage and energy production (30). In line with previous finds, our study shows that circulating TG species linked to PUFA is drastically reduced in the symptomatic ALS animals (4). The reduced TG levels were also found in post-mortem human spinal cord (31) and CSF from ALS patients (6). This result might be attributed to skeletal muscle hypermetabolism that use fatty acid oxidation for energy production (4).

The levels of specific hexosylceramide and acylceramide species were largely increased in symptomatic relative to asymptomatic animals. Emerging evidence suggests that accumulation of sphingolipids play an important role in the pathogenesis of a number of neurodegenerative (32-37) and metabolic diseases (38-40). Elevated plasma sphingolipids levels were also reported for Alzheimer's and Parkinson's disease patients (37, 41). Additionally, increased amounts of SM, Cer and glucosylceramides (GlcCer) were also previously reported in the muscle, spinal cord and CSF of ALS patients (5, 22, 42). Sphingolipids are complex lipids, and are found associated with cellular membranes and plasma lipoproteins (43). These lipids act as structural lipids, signaling molecules or ligands form cells receptors. The causes behind the modification of sphingolipids metabolism could be multiple. Sphingolipids are involved in key pathways for ALS such as autophagy and protein clearance, cell survival, energy metabolism and neuroinflammation (44, 45). An excess of ceramide thus induces accumulation of lipids, triggers endoplasmic reticulum and lipotoxic stress (46). However, there is growing evidence that cells convert the excess ceramides into hexosylceramide in Golgi apparatus to prevent toxic accumulation of ceramides and apoptosis (47, 48).

Here, we described, for the first time, AcylCer species associated with plasma lipoproteins, specially HDL. In support to these findings, AcylCer generation and sequestration in lipid droplet were demonstrated in hepatocytes and liver of mice subjected to a high-fat diet (49). The generation of AcylCer might possibly be associated to another protective mechanism that removes ceramide from cellular membranes thereby increasing the oxidative capacity of mitochondria (49). Our study suggests that plasma AcylCer could serve as predictive markers for ALS progression.

In conclusion, our study underlines the power of untargeted lipidomic analysis for plasma and pooled lipoprotein fractions lipidome of SOD1G93A rat model of ALS. The major alterations in plasma of symptomatic rats were associated to TG, glycerophospholipids, acylcer and hexosylceramide. The later two species were mostly found in HDL-albumin fractions. Collectively, our results were consistent with recent emerging evidences highlighting the importance of alteration of sphingolipids, triglycerides and phospholipids metabolism in neurodegenerative disease. Of note, we described for the first time AcylCer in plasma lipoprotein likely derived from liver. Although the mechanisms involved in lipid alterations in ALS remain still unclear, our study provides interesting insights to potential lipid targets for future studies of ALS.

5. Acknowledgments

This study was supported by Fundação de Amparo à Pesquisa do Estado de São Paulo [FAPESP, CEPID–Redoxoma grant 13/07937-8], Conselho Nacional de Desenvolvimento Científico e Tecnológico [CNPq, Universal 424094/2016-9], Coordenação de Aperfeiçoamento de Pessoal de Nível Superior [CAPES, Finance Code 001] and Pro-Reitoria de Pesquisa da Universidade de São Paulo [PRPUSP]. The PhD scholarship of Isabella F. D. Pinto was supported by FAPESP [grant 2014/11556-2],

Adriano B Chaves Filho and Lucas S Dantas by CNPq. The post- doctoral scholarship of Marcos Y Yoshinaga was supported by CAPES.

6. References

1. Kiernan MC, Vucic S, Cheah BC, Turner MR, Eisen A, Hardiman O, et al. Amyotrophic lateral sclerosis. *The Lancet*. 2011;377(9769):942-55.
2. Geevasinga N, Menon P, Ozdinler PH, Kiernan MC, Vucic S. Pathophysiological and diagnostic implications of cortical dysfunction in ALS. *Nat Rev Neurol*. [Review]. 2016;12(11):651-61.
3. Dupuis L, Oudart H, René F, de Aguilar J-LG, Loeffler J-P. Evidence for defective energy homeostasis in amyotrophic lateral sclerosis: Benefit of a high-energy diet in a transgenic mouse model. *Proceedings of the National Academy of Sciences of the United States of America*. 2004;101(30):11159.
4. Fergani A, Oudart H, Gonzalez De Aguilar J-L, Fricker B, René F, Hocquette J-F, et al. Increased peripheral lipid clearance in an animal model of amyotrophic lateral sclerosis. *Journal of lipid research*. 2007;48(7):1571-80.
5. Henriques A, Croixmarie V, Priestman DA, Rosenbohm A, Dirrig-Grosch S, D'Ambra E, et al. Amyotrophic lateral sclerosis and denervation alter sphingolipids and up-regulate glucosylceramide synthase. *Human Molecular Genetics*. 2015;24(25):7390-405.
6. Blasco H, Veyrat-Durebex C, Bocca C, Patin F, Vourc'h P, Kouassi Nzoughet J, et al. Lipidomics Reveals Cerebrospinal-Fluid Signatures of ALS. *Scientific Reports*. 2017;7(1):17652.
7. Dorst J, Kühnlein P, Hendrich C, Kassubek J, Sperfeld AD, Ludolph AC. Patients with elevated triglyceride and cholesterol serum levels have a prolonged survival in amyotrophic lateral sclerosis. *Journal of Neurology*. 2011;258(4):613-7.
8. Dupuis L, Corcia P, Fergani A, Gonzalez De Aguilar JL, Bonnefont-Rousselot D, Bittar R, et al. Dyslipidemia is a protective factor in amyotrophic lateral sclerosis. *Neurology*. 2008;70(13):1004.
9. Rafiq MK, Lee E, Bradburn M, McDermott CJ, Shaw PJ. Effect of lipid profile on prognosis in the patients with amyotrophic lateral sclerosis: Insights from the olesoxime clinical trial. *Amyotrophic Lateral Sclerosis and Frontotemporal Degeneration*. 2015;16(7-8):478-84.
10. Delaye JB, Patin F, Piver E, Bruno C, Vasse M, Vourc'h P, et al. Low IDL-B and high LDL-1 subfraction levels in serum of ALS patients. *Journal of the Neurological Sciences*. 2017;380:124-7.
11. Abdel-Khalik J, Yutuc E, Crick PJ, Gustafsson J-Å, Warner M, Roman G, et al. Defective cholesterol metabolism in amyotrophic lateral sclerosis. *Journal of Lipid Research*. 2017;58(1):267-78.
12. Pradat P-F, Bruneteau G, Gordon PH, Dupuis L, Bonnefont-Rousselot D, Simon D, et al. Impaired glucose tolerance in patients with amyotrophic lateral sclerosis. *Amyotrophic Lateral Sclerosis*. 2010;11(1-2):166-71.

13. Chiò A, Calvo A, Ilardi A, Cavallo E, Moglia C, Mutani R, et al. Lower serum lipid levels are related to respiratory impairment in patients with ALS. *Neurology*. 2009;73(20):1681.
14. Huang R, Guo X, Chen X, Zheng Z, Wei Q, Cao B, et al. The serum lipid profiles of amyotrophic lateral sclerosis patients: A study from south-west China and a meta-analysis. *Amyotrophic Lateral Sclerosis and Frontotemporal Degeneration*. 2015;16(5-6):359-65.
15. Henriques A, Blasco H, Fleury M-C, Corcia P, Echaniz-Laguna A, Robelin L, et al. Blood Cell Palmitoleate-Palmitate Ratio Is an Independent Prognostic Factor for Amyotrophic Lateral Sclerosis. *PLOS ONE*. 2015;10(7):e0131512.
16. Linares E, Seixas LV, dos Prazeres JN, Ladd FVL, Ladd AABL, Coppi AA, et al. Tempol Moderately Extends Survival in a hSOD1(G93A) ALS Rat Model by Inhibiting Neuronal Cell Loss, Oxidative Damage and Levels of Non-Native hSOD1(G93A) Forms. *PLoS ONE*. 2013;8(2):e55868.
17. Wiesner P, Leidl K, Boettcher A, Schmitz G, Liebisch G. Lipid profiling of FPLC-separated lipoprotein fractions by electrospray ionization tandem mass spectrometry. *J Lipid Res*. 2009;50.
18. Matyash V, Liebisch G, Kurzchalia TV, Shevchenko A, Schwudke D. Lipid extraction by methyl-tert-butyl ether for high-throughput lipidomics. *Journal Lipid Research*. 2008;49(0022-2275 (Print)):1137-46.
19. Wang HY, Quan C, Hu C, Xie B, Du Y, Chen L, et al. A lipidomics study reveals hepatic lipid signatures associating with deficiency of the LDL receptor in a rat model. *Biology Open*. 2016;5(7):979-86.
20. Chong J, Soufan O, Li C, Caraus I, Li S, Bourque G, et al. MetaboAnalyst 4.0: towards more transparent and integrative metabolomics analysis. *Nucleic Acids Research*. 2018:gky310-gky.
21. Palamiuc L, Schlagowski A, Ngo ST, Vernay A, Dirrig-Grosch S, Henriques A, et al. A metabolic switch toward lipid use in glycolytic muscle is an early pathologic event in a mouse model of amyotrophic lateral sclerosis. *EMBO Molecular Medicine*. 2015;7(5):526.
22. Dodge JC, Treleaven CM, Pacheco J, Cooper S, Bao C, Abraham M, et al. Glycosphingolipids are modulators of disease pathogenesis in amyotrophic lateral sclerosis. *Proceedings of the National Academy of Sciences*. 2015;112(26):8100.
23. Giammanco A, Cefalù AB, Noto D, Averna MR. The pathophysiology of intestinal lipoprotein production. *Front Physiol*. 2015;6:61.
24. Cole LK, Vance JE, Vance DE. Phosphatidylcholine biosynthesis and lipoprotein metabolism. *Biochimica et Biophysica Acta (BBA) - Molecular and Cell Biology of Lipids*. 2012;1821(5):754-61.
25. Peters OM, Ghasemi M, Brown RH, Jr. Emerging mechanisms of molecular pathology in ALS. *The Journal of Clinical Investigation*. 2015;125(6):2548-.
26. Arima H, Omura T, Hayasaka T, Masaki N, Hanada M, Xu D, et al. Reductions of docosahexaenoic acid-containing phosphatidylcholine levels in the anterior horn of an ALS mouse model. *Neuroscience*. 2015;297:127-36.

27. Ilieva EV, Ayala V, Jové M, Dalfó E, Cacabelos D, Povedano M, et al. Oxidative and endoplasmic reticulum stress interplay in sporadic amyotrophic lateral sclerosis. *Brain*. 2007;130(12):3111-23.
28. Kim S-M, Kim H, Kim J-E, Park KS, Sung J-J, Kim SH, et al. Amyotrophic Lateral Sclerosis Is Associated with Hypolipidemia at the Presymptomatic Stage in Mice. *PLOS ONE*. 2011;6(3):e17985.
29. Dupuis L, Pradat P-F, Ludolph AC, Loeffler J-P. Energy metabolism in amyotrophic lateral sclerosis. *The Lancet Neurology*. 2011;10(1):75-82.
30. Bradbury MW. Lipid Metabolism and Liver Inflammation. I. Hepatic fatty acid uptake: possible role in steatosis. *American Journal of Physiology-Gastrointestinal and Liver Physiology*. 2006;290(2):G194-G8.
31. Hanrieder J, Ewing AG. Spatial Elucidation of Spinal Cord Lipid- and Metabolite-Regulations in Amyotrophic Lateral Sclerosis. *Scientific Reports*. 2014;4:5266.
32. Mielke MM, Maetzler W, Haughey NJ, Bandaru VVR, Savica R, Deuschle C, et al. Plasma Ceramide and Glucosylceramide Metabolism Is Altered in Sporadic Parkinson's Disease and Associated with Cognitive Impairment: A Pilot Study. *PLoS ONE*. 2013;8(9):e73094.
33. Rodriguez-Cuenca S, Pellegrinelli V, Campbell M, Oresic M, Vidal-Puig A. Sphingolipids and glycerophospholipids – The “ying and yang” of lipotoxicity in metabolic diseases. *Progress in Lipid Research*. 2017;66:14-29.
34. Giles C, Takechi R, Mellett NA, Meikle PJ, Dhaliwal S, Mamo JC. Differential regulation of sphingolipid metabolism in plasma, hippocampus, and cerebral cortex of mice administered sphingolipid modulating agents. *Journal of Neurochemistry*. 2017;141(3):413-22.
35. Han X, Rozen S, Boyle SH, Hellegers C, Cheng H, Burke JR, et al. Metabolomics in Early Alzheimer's Disease: Identification of Altered Plasma Sphingolipidome Using Shotgun Lipidomics. *PLoS ONE*. 2011;6(7):e21643.
36. Mielke MM, Lyketsos CG. Alterations of the Sphingolipid Pathway in Alzheimer's Disease: New Biomarkers and Treatment Targets? *Neuromolecular medicine*. 2010;12(4):331-40.
37. Chan RB, Perotte AJ, Zhou B, Liang C, Shorr EJ, Marder KS, et al. Elevated GM3 plasma concentration in idiopathic Parkinson's disease: A lipidomic analysis. *PLOS ONE*. 2017;12(2):e0172348.
38. Drobnik W, Liebisch G, Audebert F-X, Fröhlich D, Glück T, Vogel P, et al. Plasma ceramide and lysophosphatidylcholine inversely correlate with mortality in sepsis patients. *Journal of Lipid Research*. 2003;44(4):754-61.
39. Haus JM, Kashyap SR, Kasumov T, Zhang R, Kelly KR, DeFronzo RA, et al. Plasma Ceramides Are Elevated in Obese Subjects With Type 2 Diabetes and Correlate With the Severity of Insulin Resistance. *Diabetes*. 2009;58(2):337.
40. Hiukka A, Ståhlman M, Pettersson C, Levin M, Adiels M, Teneberg S, et al. ApoCIII-Enriched LDL in Type 2 Diabetes Displays Altered Lipid Composition, Increased Susceptibility for Sphingomyelinase, and Increased Binding to Biglycan. *Diabetes*. 2009;58(9):2018.

41. Wong MW, Braidy N, Poljak A, Pickford R, Thambisetty M, Sachdev PS. Dysregulation of lipids in Alzheimer's disease and their role as potential biomarkers. *Alzheimer's & Dementia: The Journal of the Alzheimer's Association*. 2017;13(7):810-27.
42. Cutler RG, Pedersen WA, Camandola S, Rothstein JD, Mattson MP. Evidence that accumulation of ceramides and cholesterol esters mediates oxidative stress-induced death of motor neurons in amyotrophic lateral sclerosis. *Annals of Neurology*. 2002;52(4):448-57.
43. Iqbal J, Walsh MT, Hammad SM, Hussain MM. Sphingolipids and Lipoproteins in Health and Metabolic Disorders. *Trends in Endocrinology & Metabolism*. 2017;28(7):506-18.
44. Henriques A, Huebecker M, Blasco H, Keime C, Andres CR, Corcia P, et al. Inhibition of β -Glucocerebrosidase Activity Preserves Motor Unit Integrity in a Mouse Model of Amyotrophic Lateral Sclerosis. *Scientific Reports*. 2017;7(1):5235.
45. Bartke N, Hannun YA. Bioactive sphingolipids: metabolism and function. *Journal of Lipid Research*. 2009;50 Suppl(Suppl):S91-S6.
46. Martínez-Sánchez N, Seoane-Collazo P, Contreras C, Varela L, Villarroja J, Rial-Pensado E, et al. Hypothalamic AMPK-ER Stress-JNK1 Axis Mediates the Central Actions of Thyroid Hormones on Energy Balance. *Cell Metab*. 2017;26(1):212-29.e12.
47. Liu Z, Navathe SB, Stasko JT. Ploceus: Modeling, visualizing, and analyzing tabular data as networks. *Information Visualization*. 2013 2014/01/01;13(1):59-89.
48. Liu L-K, Choudhary V, Toulmay A, Prinz WA. An inducible ER-Golgi tether facilitates ceramide transport to alleviate lipotoxicity. *The Journal of Cell Biology*. 2017;216(1):131.
49. Senkal CE, Salama MF, Snider AJ, Allopenna JJ, Rana NA, Koller A, et al. Ceramide Is Metabolized to Acylceramide and Stored in Lipid Droplets. *Cell Metab*. 2017;25(3):686-97.

Supplementary information**Lipid nomenclature**

AC, Acylcarnitine

AcylCer, Acylceramide

ADG, Alkyl-diacylglycerol

Cer, Ceramide

CE, Cholesteryl ester

FA, Free fatty acid

HexCer, Hexosylceramide,

LPC, Lysophosphatidylcholine

LPE, Lysophosphatidylethanolamine

PC, Phosphatidylcholine

PE, Phosphatidylethanolamine

PI, Phosphatidylinositol

PA, Phosphatidic acid

PG, Phosphatidylglycerol

Sitosteryl, Sitosteryl ester

SM, Sphingomyelin

TG, Triglyceride

The 'o-' prefix is used to indicate the presence of an alkyl ether substituent (e.g. oPC), whereas the 'p-' prefix is used for the alkenyl ether (plasmalogen) substituent (e.g. pPC).

Internal standard

1-heptadecanoyl-2-(9Z-tetradecenoyl)-sn-glycero-3-phospho-(1'-myo-inositol), PI
14:1/17:0

Cholest-(25R)-5-ene-3 β ,27-diol, 27-hydroxy-Cholesterol

1,2,3-Triheptadecanoylglycerol, TG 17:0/17:0/17:0

N-heptadecanoyl-D-erythro-sphingosylphosphorylcholine, SM d18:1/17:0

1,2-diheptadecanoyl-sn-glycero-3-phospho-(1'-rac-glycerol), PG 17:0/17:0

1,3 diheptadecanoyl-glycerol (d5)

N-decanoyl-D-erythro-sphingosine, Cer d18:1/10:0

N-heptadecanoyl-D-erythro-sphingosine, Cer d18:1/17:0

1,2-dimyristoyl-sn-glycero-3-phosphocholine, PC 14:0/14:0

Cholesteryl-d7 pentadecanoate, CE 15:0

1-heptadecanoyl-2-hydroxy-sn-glycero-3-phosphocoline, LPC 17:0

1,2-diheptadecanoyl-sn-glycero-3-phosphate, PA 17:0/17:0

1,2-diheptadecanoyl-sn-glycero-3-phosphocholine, PC 17:0/17:0

1,2-diheptadecanoyl-sn-glycero-3-phosphoethanolamine, PE 17:0/17:0

1-(10Z-heptadecenoyl)-sn-glycero-3-phosphoethanolamine, LPE 17:1

These lipids were purchased from Avanti Polar Lipids (Alabaster, AL, USA)

1,2,3-trimyristoylglycerol, TG 14:/14:0/14:0

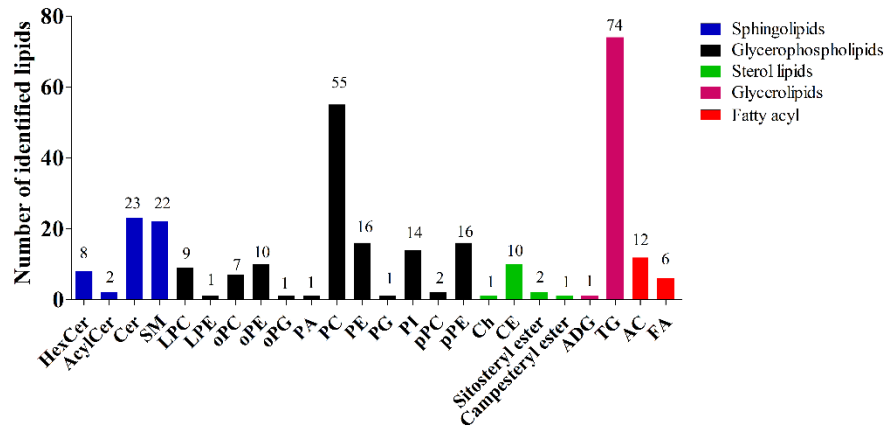
Cholesterol Decanoate, CE 10:0

Methyl heptadecanoate, FA 17:0

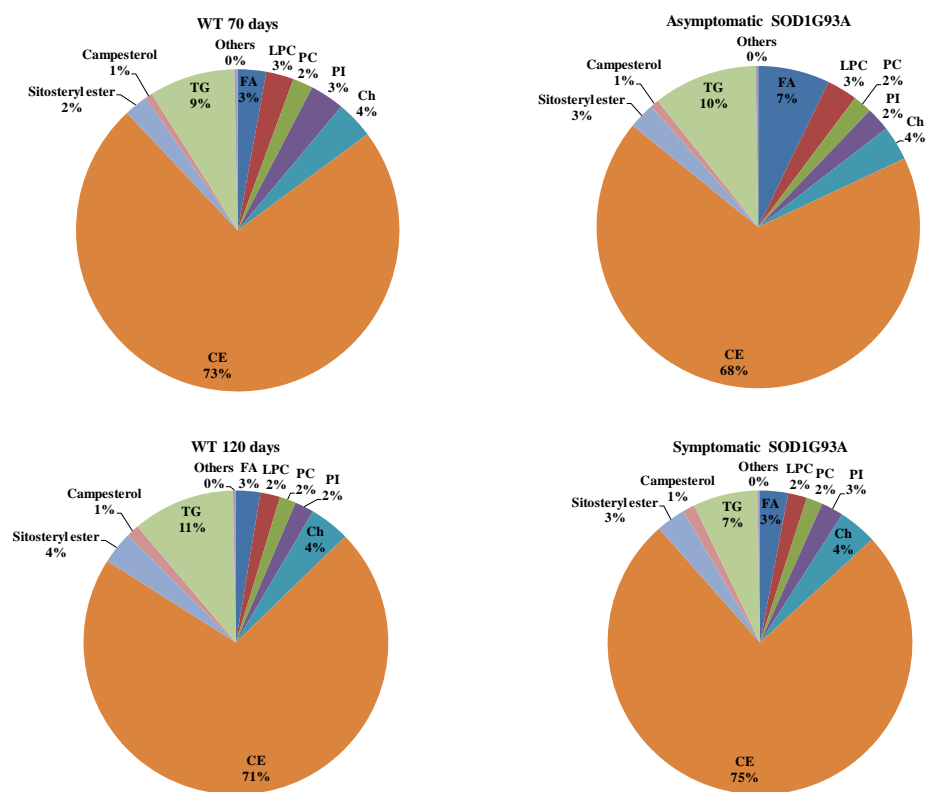
These lipids were purchased from Sigma-Aldrich (St Louis, MO, USA)

Supplementary figures

A

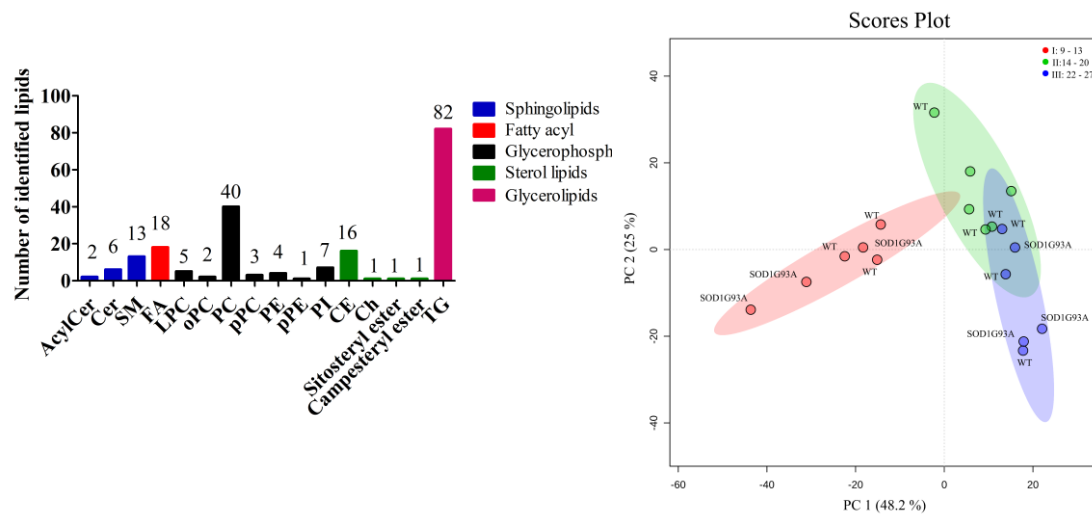


B

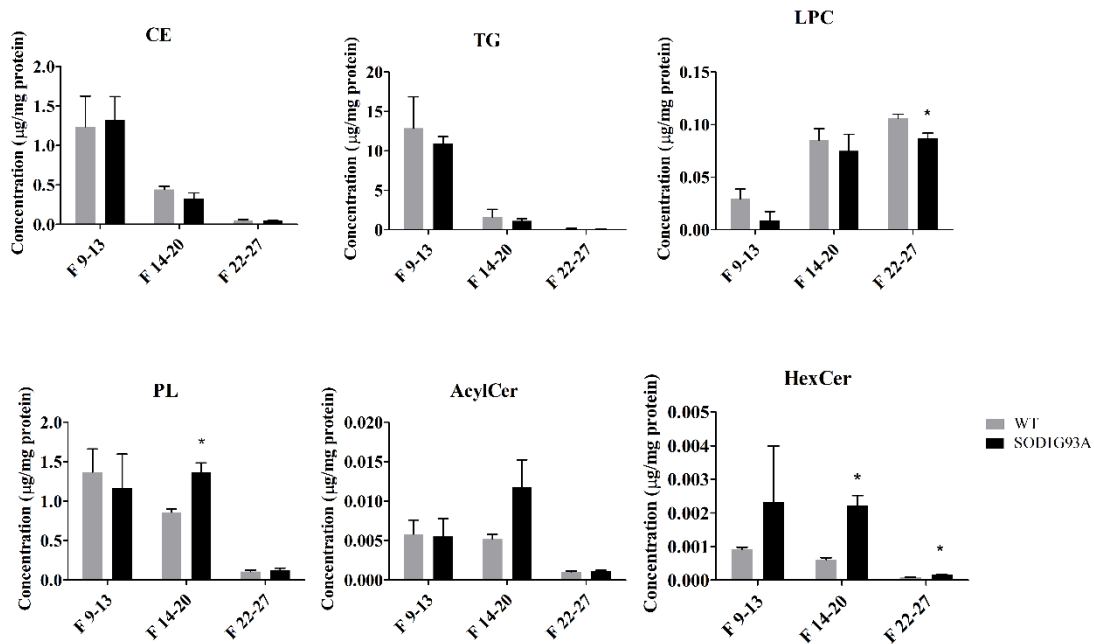


Supplementary Figure S1. Global lipidomic analysis of blood plasma. (A) Bar plot of number of identified lipids in blood plasma of SOD1G93A rats and WT littermates. (B) Pie diagrams for relative distribution of most abundant lipid classes in blood plasma of SOD1G93A rats and WT littermates. Data are represented as % concentration (mean) of the lipid classes related to the content of the respective group. Others: AcylCer, Cer, SM, LPE, oPE, pPE, oPC, oPG, PG, campesterol, ADG and AC. Asymptomatic SOD1G93A (n = 7); WT 70 days (n = 7), symptomatic SOD1G93A (n = 12); WT 120 days (n = 15). Lipid nomenclature in supplementary information.

A



B



Supplementary Figure S2. Global lipidomic analysis of pooled lipoprotein fractions. (A) Bar plot for number of identified lipids in pooled lipoprotein fractions from blood plasma of symptomatic SOD1G93A rats and age-related WT littermates. **(B)** Principal Component Analysis (PCA) score plot showing the spatial distribution of 202 lipid species identified in pooled lipoproteins fractions. **(C)** Distribution of lipid classes of pooled lipoprotein fractions. Symptomatic SOD1G93A (n = 3) and WT 120 days (n = 3).

Supplementary methods

Response curve for factor response calculation

For quantification of lipids without matched-internal standard, we used a response curve to correct the ionization differences between different lipid classes. To obtain the response curve we constructed a calibration curve containing a mixture of internal standard lipids as described below. Calibration curve was plotted at concentrations of 1.0, 0.5, 0.25, 0.125 and 0.0625 $\mu\text{g/mL}$ in isopropanol. The response factors were calculated as the ratio of the slope of calibration curve of individual lipid species to slopes obtained for internal standard. Three replicate injections of each sample were performed. Therefore, concentration of individual lipid classes was calculated from the ratio of the peak area of lipid class to the peak area of internal standard multiplied by the response factor. Parameters of response curve are described in Supplementary Table S3.

Lipid composition of calibration curve

27-hydroxy-cholesterol

TG 17:0/17:0/17:0

LPC 17:0

CE 15:0

FA 17:0

PI 14:0/17:0

PC 17:0/17:0

PG 17:0/17:0

LPE 17:1

D5 DG 17:0

All lipids were purchased from Avanti Polar Lipids

Proteomic analysis of pooled lipoprotein fractions

Pooled lipoprotein fractions was assayed with a BCA-assay (1). According to the manufacturer's protocol (Thermo Scientific, Rockford, IL, USA). Samples were diluted in 0.2% Rapigest SF (Waters Corporation, Milford, MA, USA), 50 mM ammonium bicarbonate and reduced with DTT 5 mM (50°C for 30 min). Subsequently, samples were alkylated with 15 mM iodoacetamide (ambient temperature, dark, 30 min). Proteolytic digestion was performed with modified trypsin (gold grade, Promega, Madison WI) at concentration 0.1 µg/µl (1:40) (37°C, 18 hours). Following digestion, Rapigest SF was broken down by adding 0.5% formic acid (pH<2, 37°C, 45 min). Peptide solutions were centrifuged (12,000 x g, 20min) and supernatant was collected. LC-MS analyses were performed using ~ 0.2 µg of protein digest mixtures.

Nanoscale LC separations of tryptic peptides were performed with a NanoAcquity system (Waters, Milfold, MA USA). Samples were loaded onto a Symmetry® C18 5 µm, 2 cm x 180 µm trap column (Waters, Milfold, MA USA). at a flow rate of 10 µl/min with 1%B prior to separation on Symmetry® C18 3.5 µm, 150 mm x 75 µm column (Waters, Milfold, MA USA). The mobile phases comprised (A) 0.1% formic acid and (B) acetonitrile with gradient elution of 1-35%B from 0 to 60 min; 35-90%B from 60 to 61 min, holds at 90%B from 61 to 73 min and then 90-1%B from 73 to 74 min. The flow rate was 0.40 µl/min. Nano-electrospray ion source was operated at 2.4 kV (ion spray voltage floating, ISVF), curtain gas 20, interface heater (IHT) 120, ion source gas 1 (GS1) 3, ion source gas 2 (GS2) zero, declustering potential (DP) 80 V. TOFMS and MS/MS data were acquired using information-dependent acquisition (IDA) mode. For IDA parameters, a 100 ms survey scan in the m/z range of 300–2000 was followed by 25 MS/MS ions in the m/z range of 100–2000 acquired with an accumulation time of 50 ms (total cycle time 1.4 s). Switch criteria included, intensity

greater than 150 counts and charge state 2–5. Former target ions were excluded for 20 s. Software used for acquisition and data processing were Analyst[®] and PeakView[®] (Sciex, Concord, ON, CAN), respectively. For the protein coverage and modifications, MASCOT software (Matrix Science, London, UK) was used against Rat Uniprot revised and unrevised database. Parameters were set as follow: Carbamidomethyl (C) as fixed modification, methionine oxidation as variable modification, MS error set as 20 ppm and MS/MS set as 0.05 Da. Trypsin was used to proteins cleavage with 3 missed cleavages.

Reference

1. Smith PK, Krohn RI, Hermanson GT, Mallia AK, Gartner FH, Provenzano MD, et al. Measurement of protein using bicinchoninic acid. *Analytical Biochemistry*. 1985;150(1):76-85.

Supplementary tables

Supplementary Table S1. Internal Standard (IS) used for the quantification in blood plasma.

IS	Work concentration (ng/ μ L)	Normalized lipid classes	Response factor*
Cer d18:1/10:0	10	HexCer	
		Cer	
		AcylCer	
LPC 17:0	20	LPC	
		LPE	1.89
		FA	4.17
		PC	0.42
		pPC	
		oPC	
		PI	0.76
		TG	0.78
		ADG	
		CE	0.01
		Sitosteryl ester	0.01
		Campesterol	0.01
		AC	
Ch	0.78		
PA 17:0/17:0	20	PA	
PE 17:0/17:0	20	PE	
		pPE	
		oPE	
PG 17:0/17:0	20	PG	
		oPG	
SM d18:1/17:0	16	SM	

*Response factors were determined as ratio of the slope (a) of lipid class to slope of internal standard according to the procedures described in supplementary method. Parameters of response curve are described in Supplementary Table S3.

Supplementary Table S2. Internal Standard (IS) used for the quantification in pooled lipoprotein fraction

IS	Work concentration (ng/ μ L)	Normalized lipid classes	Response factor*
Cer d18:1/17:0	10	AcylCer	
		Cer	
SM d18:1/17:0	10	SM	
PC 14:0/14:0	10	PC	
		oPC	
		pPC	
PE 17:0/17:0	10	PE	
		pPE	
PG 17:0/17:0	10	PI	0.12
LPC 17:0	10	FA	4.17
		LPC	
		PI	
TG 14:0/14:0/14:0	10	TG	
CE 10:0	10	CE	
		Ch	
		Sitosteryl ester	
		Campesterol	

*Response factors were determined as ratio of the slope (a) of lipid class to slope of internal standard according to the procedures described in supplementary method. Parameters of response curve are described in Supplementary Table S3.

Supplementary Table S3. Parameter of response curve for individual lipid species in negative and positive modes.

Lipid species	a (Slopes)	b (intercepts)	r²
Negative mode			
PI 14:1/17:0	48870	-1952	0.9917
PC 17:0/17:0	27380	26540	0.6031
PG 17:0/17:0	376500	-8653	0.9951
LPC 17:0	63930	-2138	0.9938
LPE 17:1	120900	-5356	0.9930
FFA 17:0	267100	-8769	0.9957
Positive mode			
27-hydroxy-cholesterol	40760	-2876	0.9835
TAG 17:0/17:0/17:0	147000	1018	0.9591
CE 15:0	1951	-7.199	0.9520
D5 DAG 17:0	24140	505.9	0.9738
PC 17:0/17:0	244600	-7445	0.9876
LPC 17:0	188500	-8384	0.9931

Each lipid species is described by parameters of the linear dependence, $y = ax + b$, where y is the peak area, x is the concentration, and r^2 is the regression coefficients. The values were obtained from GraphPad Prism 5.0.

Supplementary Table S4. Proteomic analysis of pooled lipoprotein fractions by FPLC.

	Protein	Accession	Mr (Da)	Peptides Matched	Sequences	Score	Coverage (%)	ID
Fraction 9-13	Apo B-100	F1M6Z1	510801	132	61	943	16	VLDL
	Apo E	A0A0G2K151	41573	74	15	1077	45	
	Apo A-I	P04639	30100	36	11	296	52	
	ApoA-IV	A0A0G2JVX7	44335	36	12	204	43	
	Apo H	Q5I0M1	39743	29	10	315	34	
	Apo C-III	A0A0G2K8Q1	11022	18	2	247	39	
	Apo C-II (Predicted)	G3V8D4	10688	14	3	377	32	
	Apo C-I	P19939	9854	7	3	77	22	
	Apo C-IV	P55797	14807	7	4	56	24	
Fraction 14-20	Apo A-IV	P02651	44429	112	24	1354	61	HDL (LDL contamination)
	Rat apo E	Q65ZS7	38359	92	17	1766	55	
	Apo A-I	P04639	30100	87	18	1027	61	
	Apo B-100	F1M6Z1	510801	37	28	68	8	
	Clusterin (ApoJ)	G3V836	52015	34	13	467	33	
	Apo H	Q5I0M1	39743	24	10	159	37	
	Apo A-II	P04638	11489	16	4	130	49	
	ApoI C-II (Predicted)	G3V8D4	10688	14	3	306	32	
	Apo C-III	A0A0G2K8Q1	11022	8	1	200	19	
Apo C-I	P19939	9854	5	2	73	22		

Supplementary Table S4. (Continued)

	Protein	Accession	Mr (Da)	Peptides Matched	Sequences	Score	Coverage (%)	ID
Fraction 21-27	ApoH	P04639	30100	62	18	511	65	HDL (Albumin contamination)
	Apo A-I	Q5I0M1	39743	49	13	609	40	
	Rat apo E	Q65ZS7	38359	42	11	352	31	
	Apo A-IV	A0A0G2JVX7	44335	20	10	132	32	
	Apo C-II (Predicted)	Q6P7S6	52002	13	8	44	26	
	Apo C-III	P04638	11489	7	2	63	15	
	Apo A-II	G3V8D4	10688	4	1	71	9	
	Clusterin (ApoJ)	A0A0G2K8Q1	11022	3	1	65	19	

Parameters: Mascot search performed using Rat Uniprot revised and unrevised database. Trypsin was used to proteins cleavage (3 missed cleavages). Carbamidomethyl (C) was used as fixed modification and methionine oxidation as variable modification. MS error set as 20 ppm and MS/MS set as 0.05 Da.

CHAPTER 4

Effect of High-Fat Diet in Plasma Lipidome of Amyotrophic Lateral Sclerosis

Rodent Model

Isabella F D Pinto, Adriano B Chaves Filho, Lucas SDantas, Marisa H G Medeiros,

Marcos Y Yoshinaga, Sayuri Miyamoto*

Department of Biochemistry, Institute of Chemistry, University of Sao Paulo, Sao Paulo, Brazil

*Corresponding Author: Sayuri Miyamoto. E-mail address: miyamoto@iq.usp.br

Institutional address: Departamento de Bioquímica, Instituto de Química, Av. Prof.

Lineu Prestes 1524, CP 26077, CEP 05313-970, Butantã, São Paulo, SP. Brazil. Phone:

+ 55 11 30911413

Abstract

Amyotrophic lateral sclerosis (ALS) is an adult-onset neurodegenerative disease of motor neurons in the central nervous system resulting in progressive muscle weakness, paralysis, and finally death. Moreover, a population of patients with sporadic ALS exhibits a generalized hypermetabolic state of as yet unknown origin. To address the significant gap in knowledge regarding the effect of high-fat diet on the blood plasma lipidome, we used untargeted lipidomics by mass spectrometry-based approach. We analyzed blood plasma lipid profiles of SOD1G93A transgenic ALS fed a high-lard diet, high-fish diet and control diet. We examined body weight gain, food intake and survival in treated and disease controls. Multivariate analysis indicated differences in dietary blood plasma profiles. High-lard diet and control diet altered phospholipids, glycerolipids, acylcarnitines, hexosylceramides and acylceramides, while high-fish oil diet altered only acylcarnitines and acylceramides in SOD1G93A rats in comparison to WT controls. This is the first study showing that high-fat diet alters the plasma lipidome of the SOD1G93A rat model of ALS. These findings indicate an interaction between dietary fat consumption and ALS with widespread effects on the lipidome, which may provide a basis for identification of ALS-specific related lipid biomarkers.

Keywords: high-fat diet, ALS, triglyceride, acylcarnitine, acylceramide, hexosylceramide

Highlights

- Both high-lard and high-fish oil diets had the greatest effect on blood plasma lipidome than disease.
- High-lard diet altered phospholipids, glycerolipids, acylcarnitines, hexosylceramides and acylceramides, while high-fish oil diet altered only acylcarnitines and acylceramides in SOD1G93A rats in comparison to WT controls.
- Blood plasma lipidome analysis highlighted acylceramides as potential markers of ALS.

Abbreviation

See Supplementary Information for abbreviation of lipid classes.

ALS: amyotrophic lateral sclerosis

SOD1: Cu,Zn superoxide dismutase 1

LC-MS: liquid chromatography coupled to mass spectrometry

PUFA: polyunsaturated fatty acid

1. Introduction

Amyotrophic lateral sclerosis (ALS) is a progressive neurodegenerative disease characterized by selective degeneration of upper and lower motor neurons causing relentlessly progressive weakness and wasting of skeletal muscle throughout the body (1). Death usually occurs 3 to 5 years from symptom onset, usually from respiratory paralysis (2). The cause of neuronal cell death is uncertain. Glutamate excitotoxicity, generation of free radicals, cytoplasmic protein aggregates combined with mitochondrial dysfunction, and disruption of axonal transport processes through accumulation of neurofilament intracellular aggregates are implicated in the pathogenesis of ALS (3). A large portion of familial forms of ALS have been linked to a mutation in the gene encoding the enzyme Cu/Zn Superoxide Dismutase 1 (SOD1), and several rodent models that expressed disease related mutant SOD1 develop motor neuron degeneration similar to that in humans (4).

Due the current lack of casual therapeutic options, increasing attention is being directed towards prognostic factors in order to identify possible additional therapeutic targets. Systemic metabolism is emerging as an important modifying factor in ALS. Of clinical significance identification of a high body mass index acts as an independent positive prognostic factor of ALS (5). Therefore, metabolic abnormalities such as increased energy expenditure have been reported in some ALS patients and are being investigated more intensively (6, 7). Higher levels of cholesterol, LDL, as well as an elevated LDL/HDL ratio in ALS patient blood have been correlated with increased survival (8, 9). Conversely, similar increases in total cholesterol, LDL and HDL cholesterol in ALS patient blood (10, 11) and cerebrospinal fluid (12) have not been found be correlated with disease progression. Furthermore, a small number of studies contradict these findings (13-15).

Dietary interventions to treat ALS are attractive for several reasons. First, there is evidence that malnutrition contributes to the weight loss that occurs as the disease progresses (16). Malnutrition can be due to dysphagia from bulbar weakness, or it can be due to a high energy expenditure reported in some studies (6, 7, 17). Second, several studies have reported an association between body mass index and survival (6, 7, 16-18). Body weight and therefore the prognosis of ALS patients can be improved by high-caloric food supplements. In a retrospective cohort study of ALS patient using a high-caloric food supplement resulted in improved survival (19). Similarly, in a prospective study of ALS patients using a food supplement with high fat content might be more effective than a supplement with high carbohydrate content (20).

Several studies have shown that high-fat diet can slow disease progression in the mutant SOD1G93A mouse model. In these animals, a diet consisting of 38% carbohydrates, 47% fats, and 15% protein (by calorie content) increased the median survival time of SOD1G93A by approximately 90% (21). In other study, a high fat diet consisting of 21% of butter fat and 0.15% cholesterol (by weight) increased the mean survival of SOD1G86R mice by 20 days (22). Conversely, caloric restriction in the mutant SOD1 mouse model significantly reduced survival (23, 24). A ketogenic diet (consisting of 60% fat, 20% carbohydrate, and 20% protein) did not show a significant increase in survival but an improvement in the rotarod performance was observed in SOD1G93A mouse model (25). Additionally, treatment with caprylic acid (medium chain triglycerides) appeared to improve mitochondrial function and motor neuron numbers in the ALS mouse model, although it did not lead to overall increased survival (26).

Although the origin of this ALS hypermetabolism still remains unsolved, these combined data point to metabolic perturbations as playing an important role in the disease. To gain insight into this question, we evaluated the effects of high-lard and

high-fish oil diets in plasma lipidome of SOD1G93A transgenic ALS lines. In summary, this study provides a basis for identification of ALS-specific related lipid biomarkers.

2. Materials and Methods

2.1. Materials

The lipids used as internal standards (described in supplementary information) were purchased from Avanti Polar Lipids (Alabaster, AL, USA). Methyl tert-butyl ether (MTBE), ammonium formate and ammonium acetate were purchased from Sigma-Aldrich (St Louis, MO, USA). All HPLC grade organic solvents were obtained from Sigma-Aldrich (St Louis, MO, USA). Ultra-pure water was supplied by a Millipore system (Millipore, Billerica, MA, USA).

2.2. Animals and Diets

All animal experiments and procedures were conducted in conformity with local Animal Care and Use Committee of University of Sao Paulo (CEUA number 41/2016). Male SOD1G93A mutant transgenic rats were obtained from the Jackson Laboratory and bred in our transgenic rat facility to generate SOD1G93A rats and wild type (WT) control littermates. At 52 days of age animals placed on either a lard or fish oil diets (caloric composition, fat 60%, carbohydrate 20%, protein 20%) or a standard rodent laboratory diet (fat 10%, carbohydrate 70%, protein 20%) (27). Rats were kept under a 12-hr light/dark regimen and allowed ad libitum access to food and water. Rats were weighed at the start of treatment, during treatment and at study end point. The study endpoint was defined as meeting of the following conditions: loss of 15% of maximum body weight and/or apparent muscle paralysis. Rats were fasted for 4h and anesthetized by isoflurane inhalation at dose of 4% for induction and 2% for maintenance. Blood was

collected by cardiac puncture into a tube containing heparin (BD, Franklin Lakes, NJ, USA). Plasma was obtained after centrifugation at 2,000 x g for 10 min at 4°C and stored at -80°C until further processing.

2.3. Lipidomic Analysis

A mixture of internal standards was added prior to lipid extraction for quantification of all reported lipid species (Supplementary Information). Briefly, 80 µl of plasma were mixed with 80 µl of a mixture of internal standards (Supplementary Table S1) and 240 µl of ice-cold methanol. After thoroughly vortexing for 10 s, 1 ml of MTBE was added to the mixture, which was stirred for 1 h at 20°C. Next, 300 µl of water was added to the mixture, followed by vortexing 10 s and resting in an ice bath for 10 min. After centrifugation at 10,000 x g for 10 min at 4°C, the supernatant containing the lipid extract was transferred to a vial and dried under N₂ gas. The extracted lipids were re-dissolved in 80 µl of isopropanol for LC-MS/MS analysis.

Lipids were analyzed by untargeted analysis using liquid chromatography (Nexera UHPLC, Shimadzu, Kyoto, JAP) coupled to a TripleTOF6600 mass spectrometer (Sciex, Concord, ON, CAN) with electrospray ionization (ESI) in both negative and positive modes. Samples were injected into a CORTECS[®] column (UPLC C18 column, 1.6 µm, 2.1 mm i.d. 100 mm, Waters, Milford, MA, USA). The mobile phases were (A) water/acetonitrile (60:40) and (B) isopropanol/acetonitrile/water (88/10/2) both with 10 mM ammonium acetate or ammonium formate for analysis in negative or positive mode, respectively. The gradient was started from 40 to 100% B over the first 10 min, held at 100% B from 10 to 12 min, and then decreased from 100 to 40% B during 12-13 min, and held at 40%B from 13 to 20 min. The flow rate was 0.2 ml/min and column was maintained at 35°C. The MS was operated in Information Dependent Acquisition (IDA[®]) mode with scan range set a mass-to-charge ratio of 100-2000 Da. Data were

obtained in a period cycle time of 1.05 s with 100 ms acquisition time for MS1 scan and 25 ms acquisition time to obtain the top 36 precursor ions. Data acquisition was performed using Analyst[®] 1.7.1 with an ion spray voltage of -4.5 kV and 5.5 kV for negative and positive modes, respectively, and the cone voltage at \pm 80 V. The curtain gas was set at 25 psi, nebulizer and heater gases at 45 psi and interface heater of 450°C.

2.4. Data analysis

Lipid species detected were manually identified based on MS/MS fragments using PeakView[®] (Sciex, Concord, ON, CAN) and annotated (identity, exact mass and retention time) using an “in house” developed Excel[®] macro. The ESI negative mode was primarily directed to identification of free fatty acids, glycerophospholipids and sphingolipids, while the ESI positive was directed to identification of neutral lipids (e.g. triglycerides). The area of each lipid species and internal standards were obtained by integration of MS peak using MultiQuant[®] (Sciex, Concord, ON, CAN). The lipid content of sample was determined by dividing the area of the lipid to the correspondent internal standard, multiplying by concentration of internal standard and then dividing by volume of sample. Concentration of lipids without internal standard was calculated using the response factor relative to the standard PC (17:0/17:0) (Supplementary Information). Lipid species were either annotated by sum composition (e.g. isobaric species) or by molecular species composition. Lipid species annotated by molecular composition are reported as [lipid class] [total number of carbons atoms in fatty acids 1]:[total number of double bonds in fatty acid 1]/ [total number of carbons atoms in fatty acids 2]:[total number of double bonds in fatty acid 2]/ [total number of carbons atoms in fatty acids 3 (only for TG)]:[total number of double bonds in fatty acid 3 (only for TG)] (e.g. PE 16:0/22:3, TG 16:0/18:1/18:2). The symbol “/” denotes only the fatty

acids moieties of the lipid species, and not their sn-1, sn-2 and sn-3 positions on the glycerol-backbone.

2.5. Statistical analysis

Univariate and multivariate analysis of the lipidomic data were performed using Metaboanalyst 4.0 (28). Zero values in the data were imputed with half of the minimum value of the corresponding lipid across all the samples. The dataset was log-transformed to prior statistical analysis. Statistical comparisons of total triglyceride, acylcarnitine, acylceramide and hexosylceramide levels were evaluated by unpaired t-test. Effect of high fat diet on longevity was assessed by the Kaplan-Meier survival with “failure” defined as death of an animal. Animals’ body weight data were analysed by a two-way repeated measure ANOVA followed by Bonferroni’s post hoc test. Differences with p values less than 0.05 were considered statistically significant. Graphs were generated using GraphPad Prism 5 (GraphPad Software Inc., San Diego, CA, USA) and represented as the mean \pm standard deviation (SD).

3. Results

3.1. Effect of high-fat diet on body weight, food intake and survival

We first analyzed whether the different source of fat (lard or fish oil) in high-fat diets differentially affect body weight gain, food intake and survival related to ALS SOD1G93A rat model. The weight analysis revealed a significant weight gain in ALS rats on high-lard diet compared to control diet only after 100 days of age (Figure 1A). No change in weight seems to occur between ALS rats on high-fish oil diet and control diet (Figure 1A). On the other hand, rats fed a high-lard and high-fish oil diets displayed similar food intake but significantly lower compared to the rats fed control diet (Figure

1B). Additionally, no significant effect on survival extension was observed in ALS rats fed high-lard or high-fish oil diets relative to control diet (Figure 1C).

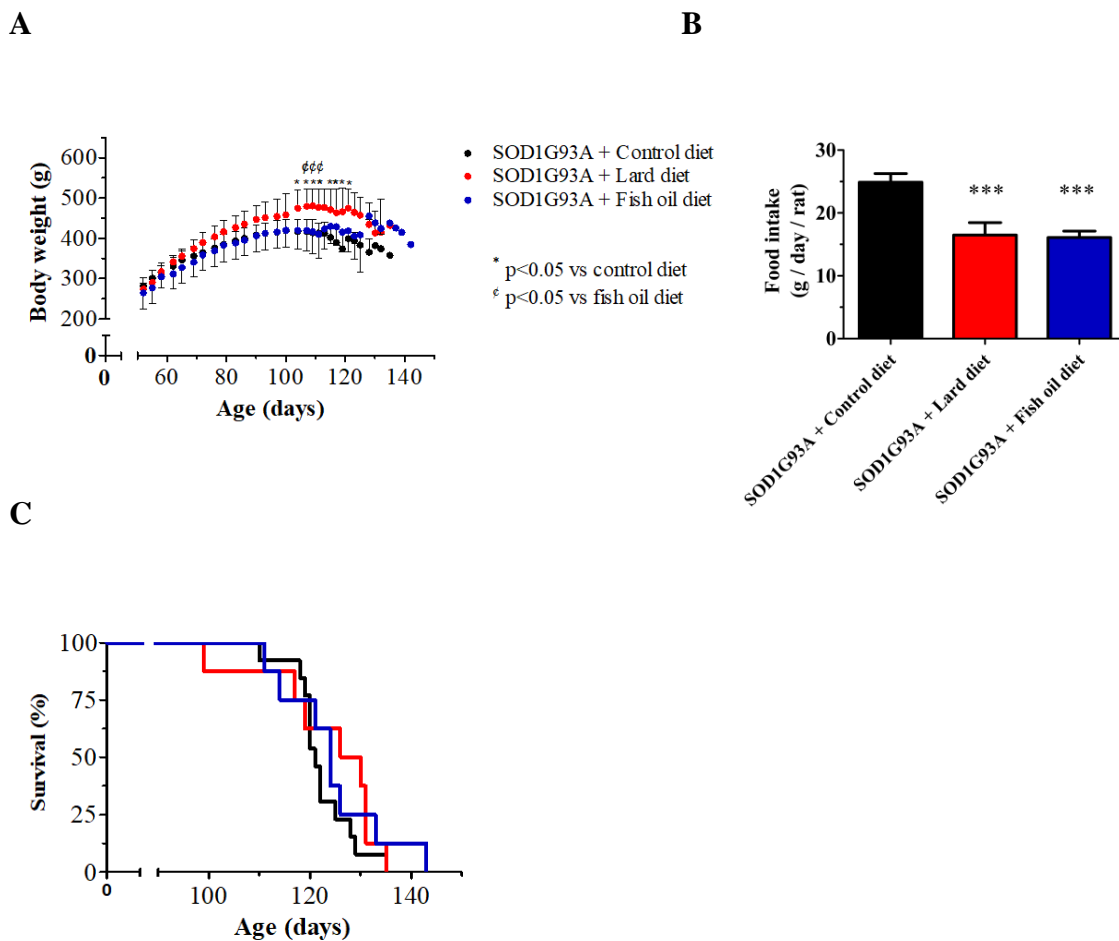


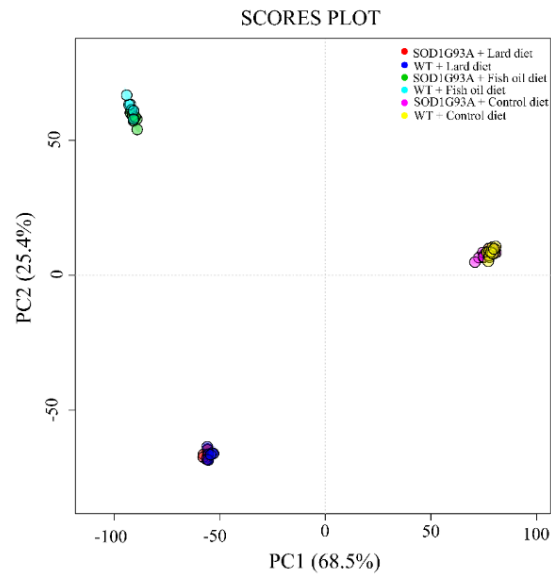
Figure 1. Regulation of body weight gain, food intake and survival in high fat diet-fed ALS SOD1G93A rats. (A) Modulation of body weight by high fat diet. Data are presented as mean \pm SD. Symbols demote statistical significance of $p < 0.05$. Significance by two-way ANOVA followed by Bonferroni's post-hoc test. (B) Effects of high fat diet on food intake. Food intake was measured twice per week during 14 days of cumulative exposition. Food intake was calculated as the difference between feed offered and left over. $***p < 0.0001$ versus control diet. Significance by one-way ANOVA followed by Bonferroni's post-hoc test. (C) Line graph shows Kaplan-Meier analysis of the probability of survival with age for SOD1G93A rats fed a high fat diet. $n=13$ (control diet) and $n=8$ (high-lard and high-fish oil diets).

3.2 Plasma lipidomic signature of ALS SOD1G93A fed a high-fat diet

Principal component analysis (PCA) shows that rats fed a control diet segregates from high-lard and high-fish oil diets along the first principal component (PC1) (Figure 2A). This dimension, which explains about 68% of the variance, reveals that groups of samples differ mainly according to diet type. In contrast, PC2 mainly explains high-fat

diet-related differences, which high lard and high fish oil diets can be clearly distinguished. Interestingly, WT and SOD1G93A samples overlap in the PCA reduced space. Nevertheless, glycerophospholipids and glycerolipids such as triglycerides were the major lipid classes involved in groups segregation (Figure 2B).

A



B

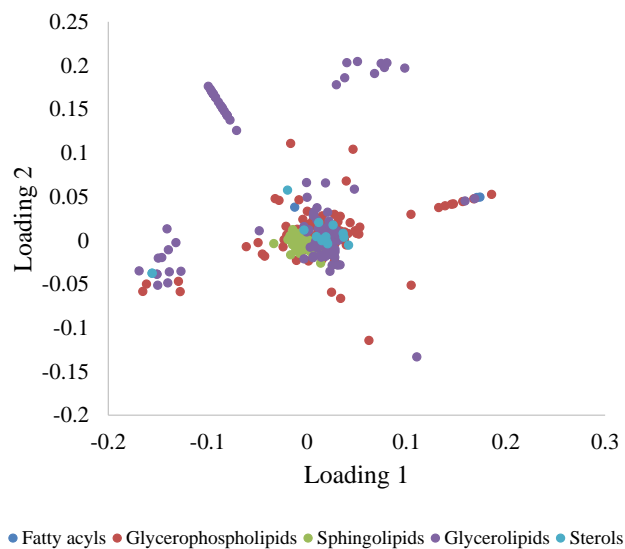
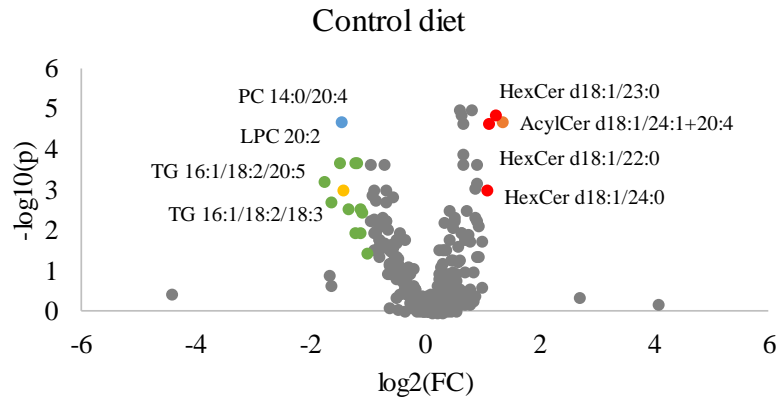


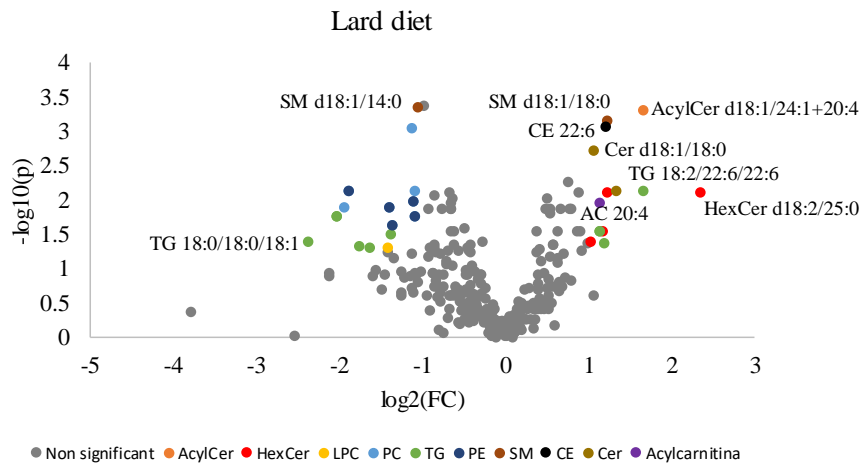
Figure 2. Rats fed on a high fat diet showed distinct plasma lipid profile relative to control diet. (A) Principal Component Analysis (PCA) of plasma lipidome. PC1 and PC2 clearly segregate samples according to diet. (B) Loading plot obtained from PCA analysis.

To further understand the disease-dependent changes affecting the lipidome of the various high-fat diet treatments, we inspected the differences between the WT and ALS rats using volcano plot (Figure 3). A major difference in the comparison between ALS and WT rats on control diet is the decrease of triglycerides, lysophosphatidylcholine and phosphatidylcholine species, and increase of hexosylceramides and acylceramide species (Figure 3A). High-lard diet-fed rats showed largest differences in the number and species of altered lipids in ALS relative to WT rats. The levels of sphingomyelin, cholesteryl ester, acylcarnitine, acylceramide, ceramide, hexosylceramide and polyunsaturated triglycerides were increased, while lysophosphatidylcholine, phosphatidylcholine, phosphatidylethanolamine, sphingomyelin and some monounsaturated triglycerides were decreased in ALS rats on high lard diet (Figure 3B). Additionally, a few lipid species comprising acylcarnitine and acylceramide were markedly increased in ALS relative to WT rats on high fish oil diet (Figure 3C). Interestingly, we found HexCer d18:1/23:0, HexCer d18:1/22:0 and LPC 20:2 altered in control and high-lard diets, whereas AcylCer d18:1/24:1+20:4 was consistently increased in all three diet treatments. This highlighted lipid species, specially AcylCer, could be considered as an important marker of plasma lipid signature in ALS.

A



B



C

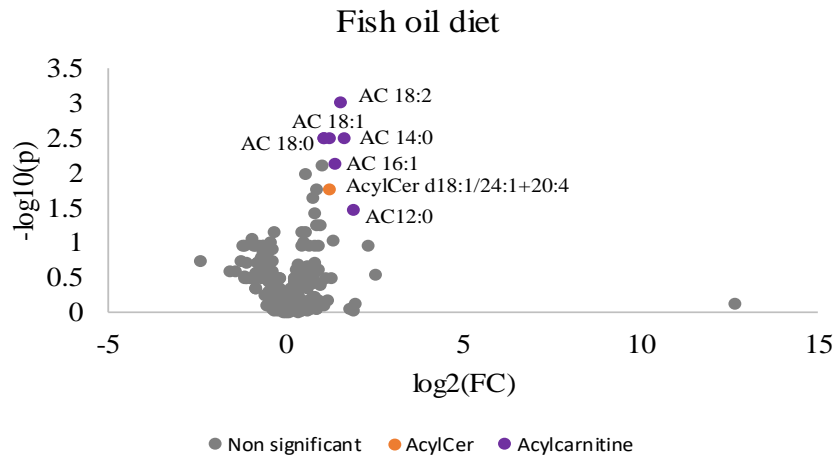


Figure 3. Volcano Plot showing plasma lipidome differences in ALS SOD1G93A rats compared to WT controls on diet treatments. (A) Control diet. (B) High-lard diet. (C) High-fish oil diet. Lipids from the same class are represented with the same color. X-axis corresponds to $\log_2(\text{Fold Change})$ and Y-axis to $-\log_{10}(\text{p-value})$. Lipid detected with a fold change above 2 and FDR adjusted p-value at or less than 0.05.

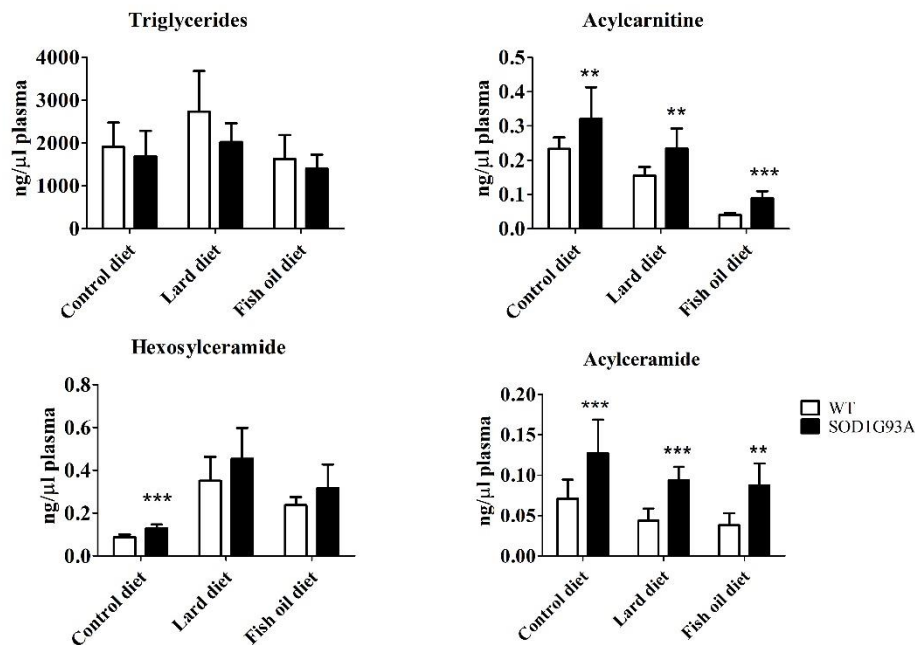
3.3 Effect of high fat diets on plasma triglyceride, acylcarnitine, hexosylceramide and acylceramide in ALS

Because energetic metabolism, mitochondrial dysfunction and sphingolipid metabolism plays a central role in ALS, we also studied the effect of high fat diets on triglyceride, acylcarnitine, hexosylceramide and acylceramide levels in SOD1G93A rat model. Although specific triglycerides species were altered in plasma, as highlighted by volcano plot, we found no statistical difference in total triglycerides content in ALS rats relative to WT controls on whatever diet treatments (Figure 4A). In contrast, the plasma acylcarnitine pool was considerably increased in ALS rats in comparison to WT controls among three diets (Figure 4A and Supplementary Figure S1). This result suggests a reduced capacity for fatty acid oxidation in SOD1G93A rats that may be involved in the etiology of ALS.

Since plasma sphingolipids have been implicated in the pathogenesis of neurodegenerative diseases (29), we determined the effect of a high-lard and high-fish oil diets on blood plasma hexosylceramide and acylceramide levels. In comparison to WT rats, total hexosylceramide levels were significantly increased in ALS rats on control diet (Figure 4A). However, both high-lard and high-fish oil diets were not statistically significant. Lipidomic profiling of individual hexosylceramide indicates the largest increase of HexCer d18:1/22:0 and HexCer d18:1/23:0 species in ALS rats fed a high control and high-lard diets in comparison to respective WT control (Figure 4B). Interestingly, no differences were observed in these hexosylceramide species between ALS rats and WT on high-fish oil diet. Additionally, total acylceramide levels were increased in plasma ALS rats compared to WT placed on a control and both high fat diets (Figure 4A). As showed above, AcylCer d18:1/24:1+20:4 was observed increased in SOD1G93A rats relative to WT in all diet treatments (Figure 4B). In accordance to

previous studies, our results reinforce the importance of sphingolipids in ALS pathogenesis.

A



B

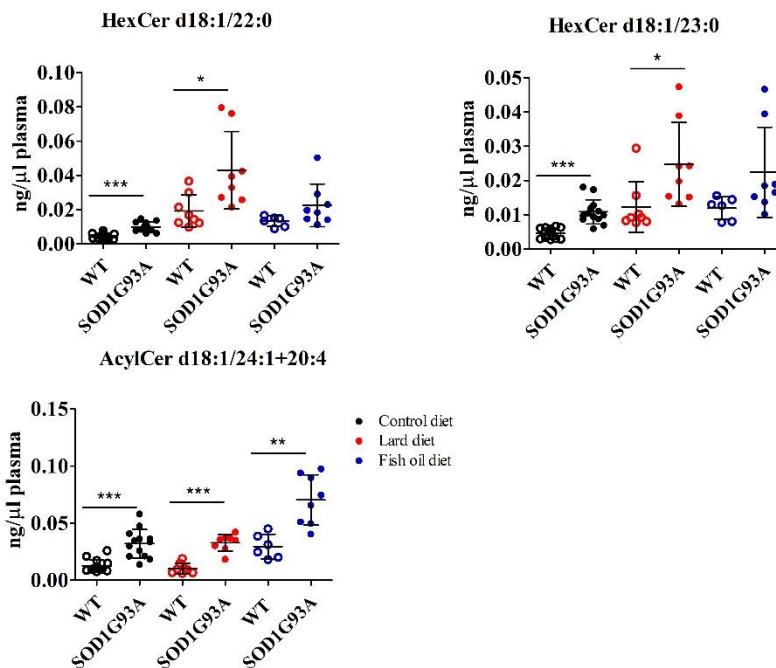


Figure 4. Plasma triglyceride, acylcarnitine, hexosylceramide and acylceramide profiles. (A) Total levels of triglyceride, acylcarnitine, hexosylceramide, acylceramide in blood plasma. (B) Plasma concentration of hexosylceramide and acylceramide species. Values are means \pm SD. *p < 0.05, **p < 0.001 and ***p < 0.0001. Significance by unpaired t-test. n=13 (control diet) and n=8 (lard and fish oil diet).

4. Discussion

Given the ALS is associated with the metabolic syndrome, identifying mechanisms in the pathogenesis of these disorders is crucial for the development of rational therapeutic options. This alteration is accompanied by a decrease in adipose tissue, and consequently a decrease in body mass during disease progression. While several studies have highlighted effect of high fat diet in motor neuron performance, longevity, and motor neuron counts, there have been few studies examining the effects of diet on the plasma lipidome and their interaction between diet and disease. In this study we used untargeted lipidomics to assess the effect of dietary fat consumption in ALS, and their interaction at the level of the blood lipidome. We correlated changes in the blood plasma lipidome to changes in the metabolic regulation of ALS.

A significant gain of weight was found in ALS rats fed a high-lard diet in comparison to control diet, although the feed intake was significantly less than control diet. This result suggests that high-lard diet fed animals gained weight during asymptomatic phase and lost weight slower as the disease progressed without show hyperphagia which that may due the high caloric density. In contrast, ALS rats fed a high-fish oil diet did not gain weight or increase food consumption in comparison to the group fed a control diet which this may be related to high caloric content or less palatability of diet. The highest body weight gain in the lard group could be attributed to lard diet composition mostly in saturated fatty acids and monounsaturated fatty acids, while fish oil diet was more competent to maintain the body because of high levels of omega-3 polyunsaturated fatty acids (30, 31). The proposed mechanism by which omega-3 PUFA may affect body weight includes modulation in the expression of genes involved in the fat oxidation and deposition (32). Similar to study performed by Zhao et al., we did not observe a significant survival extension in ALS rats fed high-fat diets (25). In contrast, others

studied reported an increase of the life expectancy of animals fed high-fat diets (22, 33). This could be explained by a distinct composition and caloric content among high-fat diets. From a clinical point of view, nutritional status is a prognosis for ALS survival, and evidence suggests that nutritional management of individual patients may constitute a primary treatment for the disease (22). Although several studies report a significant delay and increased life expectancy in ALS treated with high fat diet it is not known which mechanisms lead to an improvement in the disease.

One of the most interesting findings of this study was that the effect of diet superseded the effect of disease with regard to alterations in the blood plasma lipidome. These data emphasize the need to characterize and stratify lipidomic alterations not only to diet, but also to disease. The accentuated effect of diet on the lipidome between all three diet treatments indicated distinct shifts in lipid composition, an interesting note since glycerolipids composition were important to cluster the groups. With regard to disease, ALS rats presented striking lipidomic responses to control diet-consumption while high-lard diet had a more tapered shift, possibly a result of lard diet composition. In this regard it is interesting to note that high-fish oil diet appears to be a major driver of decreased differences between ALS rats relative to WT controls. Given the limitations of the untargeted approach along with the number of lipids identified and use of relative quantification in this study, we reported general lipidomic changes in blood plasma of SOD1G93A rats and WT controls. In terms of lipid species, these alterations falling into three classes: triglyceride (TG), acylcarnitine (AC), hexosylceramide (HexCer) and acylceramide (AcylCer). Lipids changing showed a class-specific trend in terms of differential lipid expression; however, most changes indicated species-specific alterations.

Lipidomic analysis demonstrated alterations in lipid classes within spinal cord, cerebrospinal fluid and muscle of ALS patients and animal model where the majority of reported changes encompass cholesteryl ester, glucosylceramides, phospholipids and triglycerides (34-36). Moreover, previous work by our group has reported that cholesteryl ester and cardiolipin were altered in spinal cord of ALS SOD1G93A rats (Chaves-Filho, et al., manuscript submitted). On other hand, a fewer number of studies have demonstrated a detailed alteration in blood plasma lipidome of ALS patients or animal model (37, 38). Altered levels of saturated fatty acid were described in the cell fraction of blood of ALS patients and higher content of monounsaturated fatty acids was associated with higher survival (38). Additionally, Fergani et al. demonstrated a markedly increased peripheral clearance of triglycerides-rich lipoproteins in SOD1G93A mice model (37). In this study, we showed a trend toward decreased total triglycerides levels in ALS rats. Likewise, specific triglyceride species were significantly decreased in ALS rats fed a control and high-lard diets. However, rats fed a high-fish oil diet did not show differences in triglycerides in blood plasma. Collectively, animals fed high-fat diets did not have a prolonged life span as compared to the control diet, possibly due to the fact that dietary treatments did not result in increased plasma triglycerides levels. It should be pointed out that ALS patients with elevated triglyceride and cholesterol serum levels have a prolonged survival (8) and a better functional status (39). Others reports, however, failed to reproduce these finding (9, 15, 40).

Plasma acylcarnitine levels were most affected by high-fish oil diet; however, it was increased in ALS rats compared to WT controls irrespective of diet treatments. Thus, plasma acylcarnitine profile can characterize the pattern of metabolism and may indicate the presence of fatty acid oxidation and metabolism disruption (41). Acylcarnitine is formed from carnitine and acyl-CoA by carnitine acyltransferase in

mitochondria or peroxisomes (42). Acylcarnitine is generally considered a fatty acid transport (C2-C26) and can be used to produce energy in the mitochondria or for the synthesis of endogenous molecules (43). An increased concentration of acylcarnitine has been linked to insulin resistance (44) and cardiovascular disease (45). Plasma acylcarnitine concentration is determined by the nutritional status and contribution of some specific tissues. Unlike short chain acylcarnitine, which are from glucose, amino acids and fatty acid degradation produce medium chain acylcarnitine, and long chain acylcarnitine are exclusively derived from fatty acids metabolism. Long chain fatty acids are more commonly used by cardiac and skeletal muscle for energy production (46). While some studies suggest that liver accumulates long chain acylcarnitine instead of releasing into the plasma (47, 48), Villanueva group's reported an elegant mechanism whereby they have identified liver-derived long-chain acylcarnitines in plasma as a fuel source for brown fat thermogenesis (49). In line with this finding, we hypothesized that increase in plasma acylcarnitines is required as an adaptive mechanism to compensate the hypermetabolism in ALS. Thus, monitoring acylcarnitines species should lead to a better understanding of the mechanism of disease and allow for a better design of treatment regimens.

Our analysis revealed that sphingolipids, including HexCer and AcylCer, were discriminant between ALS and WT rats fed a control and high-lard diets. Overall, our results revealing higher levels of HexCer in plasma blood of symptomatic ALS rats are consistent with those of other studies that reported high levels of sphingomyelin and glucosylceramide (GlcCer) in the CSF of ALS patients (34, 50). Furthermore, ceramides and glucosylceramides in the spinal cord of ALS patients (35) have been associated to increased gluco-cerebrosidase activity (51). Importantly, the authors suggested that the higher level of glucosylceramide was not related to its synthesis but

to the decreased expression of the palmitoyltransferase long-chain subunit 2 in ALS motor neurons (52). It should be noted that ceramides have been associated not only with apoptosis in response to cytotoxic humoral factors (53), but also with a self-reparative process after injury (54), and with the synthesis of neurotropic gangliosides (55). It has been also suggested that the accumulation of ceramide-derived agents may be protective by reducing ceramide synthesis and increasing the entry of ceramides into the glucosylceramide pathway, thus limiting the direct toxic effect on motor neurons (51). Higher GlcCer and downstream glycosphingolipids levels have been also reported in the muscle of ALS model mice as well as in other mice after muscle injury, and GlcCer, Cer and gangliosides were also increased in spinal cord of ALS model mice (36). These authors also observed the associated upregulation of glucosylceramide synthase in the muscle of ALS model mice and in the CSF of ALS patients. Importantly, for the first time, we reported acylceramides in plasma of rats (Pinto et al., manuscript in preparation). Here, we showed ALS rats even fed a high-lard or high-fish oil diets have higher acylceramide levels compared to WT rats. Enhanced accumulation of ceramide and acylceramide was described for the first time preferentially in the LDs from steatotic liver of oleate high-fat diet-fed mice (56). We hypothesized that the increased of ceramides into the acylceramide pathway may be a protective mechanism that removes ceramide from cellular membranes and increase the oxidative capacity of mitochondria. Hence, acylceramide generation might be a therapeutic link for treatment of metabolic syndrome (56).

In conclusion, we demonstrated an interaction between dietary fat consumption and ALS with widespread effects on the blood lipidome. The evidence supporting a disease-modifying effect of dietary regimens on ALS is, however, less conclusive and warrants further investigations. Collectively, these finding highlighted the need for additional

studies to obtain comprehensive understanding of the lipidome with regard to dietary changes.

5. Acknowledgments

This study was supported by Fundação de Amparo à Pesquisa do Estado de São Paulo [FAPESP, CEPID–Redoxoma grant 13/07937-8], Conselho Nacional de Desenvolvimento Científico e Tecnológico [CNPq, Universal 424094/2016-9], Coordenação de Aperfeiçoamento de Pessoal de Nível Superior [CAPES, Finance Code 001] and Pro-Reitoria de Pesquisa da Universidade de São Paulo [PRPUSP]. The PhD scholarship of Isabella F. D. Pinto was supported by FAPESP [grant 2014/11556-2], Adriano B Chaves Filho and Lucas S Dantas by CNPq. The post-doctoral scholarship of Marcos Y Yoshinaga was supported by CAPES.

6. References

1. Rowland LP, Shneider NA. Amyotrophic Lateral Sclerosis. *New England Journal of Medicine*. 2001;344(22):1688-700.
2. Strong M, Rosenfeld J. Amyotrophic lateral sclerosis: A review of current concepts. *Amyotrophic Lateral Sclerosis and Other Motor Neuron Disorders*. 2003;4(3):136-43.
3. Wiedemann FR, Manfredi G, Mawrin C, Beal MF, Schon EA. Mitochondrial DNA and respiratory chain function in spinal cords of ALS patients. *Journal of Neurochemistry*. 2002;80(4):616-25.
4. Rosen DR, Siddique T, Patterson D, Figlewicz DA, Sapp P, Hentati A, et al. Mutations in Cu/Zn superoxide dismutase gene are associated with familial amyotrophic lateral sclerosis. *Nature*. 1993;362(6415):59-62.
5. Desport JC, Preux PM, Truong TC, Vallat JM, Sautereau D, Couratier P. Nutritional status is a prognostic factor for survival in ALS patients. *Neurology*. 1999;53(5):1059.
6. Genton L, Viatte V, Janssens JP, Héritier AC, Pichard C. Nutritional state, energy intakes and energy expenditure of amyotrophic lateral sclerosis (ALS) patients. *Clinical Nutrition*. 2011;30(5):553-9.
7. Desport JC, Preux PM, Magy L, Boirie Y, Vallat JM, Beaufrère B, et al. Factors correlated with hypermetabolism in patients with amyotrophic lateral sclerosis. *The American Journal of Clinical Nutrition*. 2001;74(3):328-34.

8. Dorst J, Kühnlein P, Hendrich C, Kassubek J, Sperfeld AD, Ludolph AC. Patients with elevated triglyceride and cholesterol serum levels have a prolonged survival in amyotrophic lateral sclerosis. *Journal of Neurology*. 2011;258(4):613-7.
9. Dupuis L, Corcia P, Fergani A, Gonzalez De Aguilar JL, Bonnefont-Rousselot D, Bittar R, et al. Dyslipidemia is a protective factor in amyotrophic lateral sclerosis. *Neurology*. 2008;70(13):1004.
10. Rafiq MK, Lee E, Bradburn M, McDermott CJ, Shaw PJ. Effect of lipid profile on prognosis in the patients with amyotrophic lateral sclerosis: Insights from the olesoxime clinical trial. *Amyotrophic Lateral Sclerosis and Frontotemporal Degeneration*. 2015;16(7-8):478-84.
11. Delaye JB, Patin F, Piver E, Bruno C, Vasse M, Vourc'h P, et al. Low IDL-B and high LDL-1 subfraction levels in serum of ALS patients. *Journal of the Neurological Sciences*. 2017;380:124-7.
12. Abdel-Khalik J, Yutuc E, Crick PJ, Gustafsson J-Å, Warner M, Roman G, et al. Defective cholesterol metabolism in amyotrophic lateral sclerosis. *Journal of Lipid Research*. 2017;58(1):267-78.
13. Pradat P-F, Bruneteau G, Gordon PH, Dupuis L, Bonnefont-Rousselot D, Simon D, et al. Impaired glucose tolerance in patients with amyotrophic lateral sclerosis. *Amyotrophic Lateral Sclerosis*. 2010;11(1-2):166-71.
14. Chiò A, Calvo A, Ilardi A, Cavallo E, Moglia C, Mutani R, et al. Lower serum lipid levels are related to respiratory impairment in patients with ALS. *Neurology*. 2009;73(20):1681.
15. Huang R, Guo X, Chen X, Zheng Z, Wei Q, Cao B, et al. The serum lipid profiles of amyotrophic lateral sclerosis patients: A study from south-west China and a meta-analysis. *Amyotrophic Lateral Sclerosis and Frontotemporal Degeneration*. 2015;16(5-6):359-65.
16. Kasarskis EJ, Berryman S, Vanderleest JG, Schneider AR, McClain CJ. Nutritional status of patients with amyotrophic lateral sclerosis: relation to the proximity of death. *The American Journal of Clinical Nutrition*. 1996;63(1):130-7.
17. Desport JC, Torny F, Lacoste M, Preux PM, Couratier P. Hypermetabolism in ALS: Correlations with Clinical and Paraclinical Parameters. *Neurodegenerative Diseases*. 2005;2(3-4):202-7.
18. Paganoni S, Deng J, Jaffa M, Cudkowicz ME, Wills A-M. Body mass index, not dyslipidemia, is an independent predictor of survival in amyotrophic lateral sclerosis. *Muscle & Nerve*. 2011;44(1):20-4.
19. Desport C, Preux PM, Truong CT, Courat L, Vallat JM, Jean PC. Nutritional assessment and survival in ALS patients. *Amyotrophic Lateral Sclerosis and Other Motor Neuron Disorders*. 2000;1(2):91-6.
20. Dorst J, Cypionka J, Ludolph AC. High-caloric food supplements in the treatment of amyotrophic lateral sclerosis: A prospective interventional study. *Amyotrophic Lateral Sclerosis and Frontotemporal Degeneration*. 2013;14(7-8):533-6.
21. Mattson MP, Cutler RG, Camandola S. Energy intake and amyotrophic lateral sclerosis. *NeuroMolecular Medicine*. 2007;9(1):17-20.
22. Dupuis L, Oudart H, René F, de Aguilar J-LG, Loeffler J-P. Evidence for defective energy homeostasis in amyotrophic lateral sclerosis: Benefit of a high-energy diet in a

transgenic mouse model. *Proceedings of the National Academy of Sciences of the United States of America*. 2004;101(30):11159.

23. Pedersen WA, Mattson MP. No benefit of dietary restriction on disease onset or progression in amyotrophic lateral sclerosis Cu/Zn-superoxide dismutase mutant mice. *Brain Research*. 1999;833(1):117-20.

24. Hamadeh MJ, Rodriguez MC, Kaczor JJ, Tarnopolsky MA. Caloric restriction transiently improves motor performance but hastens clinical onset of disease in the Cu/Zn-superoxide dismutase mutant G93A mouse. *Muscle & Nerve*. 2005;31(2):214-20.

25. Zhao Z, Lange DJ, Voustantiouk A, MacGrogan D, Ho L, Suh J, et al. A ketogenic diet as a potential novel therapeutic intervention in amyotrophic lateral sclerosis. *BMC Neuroscience*. 2006 2006/04/03;7(1):29.

26. Zhao W, Varghese M, Vempati P, Dzhun A, Cheng A, Wang J, et al. Caprylic triglyceride as a novel therapeutic approach to effectively improve the performance and attenuate the symptoms due to the motor neuron loss in ALS disease. *PLOS ONE*. 2012;7(11):e49191.

27. Oliveira TE, Castro É, Belchior T, Andrade ML, Chaves-Filho AB, Peixoto AS, et al. Fish Oil Protects Wild Type and Uncoupling Protein 1-Deficient Mice from Obesity and Glucose Intolerance by Increasing Energy Expenditure. *Molecular Nutrition & Food Research*. 2019;63(7):1800813.

28. Xia J, Wishart DS. Using MetaboAnalyst 3.0 for Comprehensive Metabolomics Data Analysis. *Current Protocols in Bioinformatics*. 2016;55(1):14.0.1-.091.

29. Mielke MM, Haughey NJ. Could plasma sphingolipids be diagnostic or prognostic biomarkers for Alzheimer's disease? *Clin Lipidol*. 2012;7(5):525-36.

30. Li Y, Zhao F, Wu Q, Li M, Zhu Y, Song S, et al. Fish oil diet may reduce inflammatory levels in the liver of middle-aged rats. *Scientific Reports*. 2017;7(1):6241.

31. Hassanali Z, Ametaj BN, Field CJ, Proctor SD, Vine DF. Dietary supplementation of n-3 PUFA reduces weight gain and improves postprandial lipaemia and the associated inflammatory response in the obese JCR:LA-cp rat. *Diabetes, Obesity and Metabolism*. 2010;12(2):139-47.

32. Albracht-Schulte K, Kalupahana NS, Ramalingam L, Wang S, Rahman SM, Robert-McComb J, et al. Omega-3 fatty acids in obesity and metabolic syndrome: a mechanistic update. *The Journal of Nutritional Biochemistry*. 2018 2018/08/01;58:1-16.

33. Coughlan KS, Halang L, Woods I, Prehn JHM. A high-fat jelly diet restores bioenergetic balance and extends lifespan in the presence of motor dysfunction and lumbar spinal cord motor neuron loss in TDP-43A315T mutant C57BL6/J mice. *Disease Models & Mechanisms*. 2016;9(9):1029.

34. Blasco H, Veyrat-Durebex C, Bocca C, Patin F, Vourc'h P, Kouassi Nzoughet J, et al. Lipidomics Reveals Cerebrospinal-Fluid Signatures of ALS. *Scientific Reports*. 2017;7(1):17652.

35. Cutler RG, Pedersen WA, Camandola S, Rothstein JD, Mattson MP. Evidence that accumulation of ceramides and cholesterol esters mediates oxidative stress-induced death of motor neurons in amyotrophic lateral sclerosis. *Annals of Neurology*. 2002;52(4):448-57.

36. Henriques A, Croixmarie V, Priestman DA, Rosenbohm A, Dirrig-Grosch S, D'Ambra E, et al. Amyotrophic lateral sclerosis and denervation alter sphingolipids and up-regulate glucosylceramide synthase. *Human Molecular Genetics*. 2015;24(25):7390-405.
37. Fergani A, Oudart H, Gonzalez De Aguilar J-L, Fricker B, René F, Hocquette J-F, et al. Increased peripheral lipid clearance in an animal model of amyotrophic lateral sclerosis. *Journal of lipid research*. 2007;48(7):1571-80.
38. Henriques A, Blasco H, Fleury M-C, Corcia P, Echaniz-Laguna A, Robelin L, et al. Blood Cell Palmitoleate-Palmitate Ratio Is an Independent Prognostic Factor for Amyotrophic Lateral Sclerosis. *PLOS ONE*. 2015;10(7):e0131512.
39. Ikeda K, Hirayama T, Takazawa T, Kawabe K, Iwasaki Y. Relationships between Disease Progression and Serum Levels of Lipid, Urate, Creatinine and Ferritin in Japanese Patients with Amyotrophic Lateral Sclerosis: A Cross-Sectional Study. *Internal Medicine*. 2012;51(12):1501-8.
40. Barros ANAB, Dourado MET, Jr., Pedrosa LdFC, Leite-Lais L. Association of Copper Status with Lipid Profile and Functional Status in Patients with Amyotrophic Lateral Sclerosis. *J Nutr Metab*. 2018;2018:7.
41. Rinaldo P, Cowan TM, Matern D. Acylcarnitine profile analysis. *Genetics In Medicine*. 2008;10:151.
42. Violante S, Ijlst L, te Brinke H, Koster J, Tavares de Almeida I, Wanders RJA, et al. Peroxisomes contribute to the acylcarnitine production when the carnitine shuttle is deficient. *Biochimica et Biophysica Acta (BBA) - Molecular and Cell Biology of Lipids*. 2013;1831(9):1467-74.
43. Makrecka-Kuka M, Sevostjanovs E, Vilks K, Volska K, Antone U, Kuka J, et al. Plasma acylcarnitine concentrations reflect the acylcarnitine profile in cardiac tissues. *Scientific Reports*. 2017;7(1):17528.
44. Mihalik SJ, Goodpaster BH, Kelley DE, Chace DH, Vockley J, Toledo FGS, et al. Increased Levels of Plasma Acylcarnitines in Obesity and Type 2 Diabetes and Identification of a Marker of Glucolipotoxicity. *Obesity*. 2010;18(9):1695-700.
45. Hunter WG, Kelly JP, McGarrah RW, 3rd, Kraus WE, Shah SH. Metabolic Dysfunction in Heart Failure: Diagnostic, Prognostic, and Pathophysiologic Insights From Metabolomic Profiling. *Curr Heart Fail Rep*. 2016;13(3):119-31.
46. Nigel T, Gregory JC, Edward WK, Clinton RB. Fatty acid metabolism, energy expenditure and insulin resistance in muscle. *Journal of Endocrinology*. 2014;220(2):T61-T79.
47. Lee J, Choi J, Scafidi S, Wolfgang MJ. Hepatic Fatty Acid Oxidation Restrains Systemic Catabolism during Starvation. *Cell Reports*. 2016;16(1):201-12.
48. Schooneman MG, Ten Have GAM, van Vlies N, Houten SM, Deutz NEP, Soeters MR. Transorgan fluxes in a porcine model reveal a central role for liver in acylcarnitine metabolism. *American Journal of Physiology-Endocrinology and Metabolism*. 2015;309(3):E256-E64.
49. Simcox J, Geoghegan G, Maschek JA, Bensard CL, Pasquali M, Miao R, et al. Global Analysis of Plasma Lipids Identifies Liver-Derived Acylcarnitines as a Fuel Source for Brown Fat Thermogenesis. *Cell Metab*. 2017;26(3):509-22.e6.

50. Henriques A, Huebecker M, Blasco H, Keime C, Andres CR, Corcia P, et al. Inhibition of β -Glucocerebrosidase Activity Preserves Motor Unit Integrity in a Mouse Model of Amyotrophic Lateral Sclerosis. *Scientific Reports*. 2017;7(1):5235.
51. Dodge JC, Treleaven CM, Pacheco J, Cooper S, Bao C, Abraham M, et al. Glycosphingolipids are modulators of disease pathogenesis in amyotrophic lateral sclerosis. *Proceedings of the National Academy of Sciences*. 2015;112(26):8100.
52. Kirby J, Ning K, Ferraiuolo L, Heath PR, Ismail A, Kuo S-W, et al. Phosphatase and tensin homologue/protein kinase B pathway linked to motor neuron survival in human superoxide dismutase 1-related amyotrophic lateral sclerosis. *Brain*. 2011;134(2):506-17.
53. Ariga T, Jarvis WD, Yu RK. Role of sphingolipid-mediated cell death in neurodegenerative diseases. *Journal of Lipid Research*. 1998;39(1):1-16.
54. Abdullah L, Evans JE, Ferguson S, Mouzon B, Montague H, Reed J, et al. Lipidomic analyses identify injury-specific phospholipid changes 3 mo after traumatic brain injury. *The FASEB Journal*. 2014;28(12):5311-21.
55. Inokuchi Ji. Chapter 22 Neurotrophic and Neuroprotective Actions of an Enhancer of Ganglioside Biosynthesis. *International Review of Neurobiology*: Academic Press; 2009. p. 319-36.
56. Senkal CE, Salama MF, Snider AJ, Allopenna JJ, Rana NA, Koller A, et al. Ceramide Is Metabolized to Acylceramide and Stored in Lipid Droplets. *Cell Metab*. 2017;25(3):686-97.

Supplementary information

Lipid nomenclature

AC, Acylcarnitine

AcylCer, Acylceramide

ADG, Alkyl-diacylglycerol

Cer, Ceramide

CE, Cholesteryl ester

FA, Free fatty acid

HexCer, Hexosylceramide,

LPC, Lysophosphatidylcholine

LPE, Lysophosphatidylethanolamine

PC, Phosphatidylcholine

PE, Phosphatidylethanolamine

PI, Phosphatidylinositol

PA, Phosphatidic acid

PG, Phosphatidylglycerol

Sitosteryl, Sitosteryl ester

SM, Sphingomyelin

TG, Triglyceride

The 'o-' prefix is used to indicate the presence of an alkyl ether substituent (e.g. oPC), whereas the 'p-' prefix is used for the alkenyl ether (plasmalogen) substituent (e.g. pPC).

Internal standard

1-heptadecanoyl-2-(9Z-tetradecenoyl)-sn-glycero-3-phospho-(1'-myo-inositol), PI
14:1/17:0

Cholest-(25R)-5-ene-3 β ,27-diol, 27-hydroxy-Cholesterol

1,2,3-Triheptadecanoylglycerol, TG 17:0/17:0/17:0

N-heptadecanoyl-D-erythro-sphingosylphosphorylcholine, SM d18:1/17:0

1,2-diheptadecanoyl-sn-glycero-3-phospho-(1'-rac-glycerol), PG 17:0/17:0

1,3 diheptadecanoyl-glycerol (d5)

N-decanoyl-D-erythro-sphingosine, Cer d18:1/10:0

N-heptadecanoyl-D-erythro-sphingosine, Cer d18:1/17:0

1,2-dimyristoyl-sn-glycero-3-phosphocholine, PC 14:0/14:0

Cholesteryl-d7 pentadecanoate, CE 15:0

1-heptadecanoyl-2-hydroxy-sn-glycero-3-phosphocoline, LPC 17:0

1,2-diheptadecanoyl-sn-glycero-3-phosphate, PA 17:0/17:0

1,2-diheptadecanoyl-sn-glycero-3-phosphocholine, PC 17:0/17:0

1,2-diheptadecanoyl-sn-glycero-3-phosphoethanolamine, PE 17:0/17:0

1-(10Z-heptadecenoyl)-sn-glycero-3-phosphoethanolamine, LPE 17:1

These lipids were purchased from Avanti Polar Lipids (Alabaster, AL, USA)

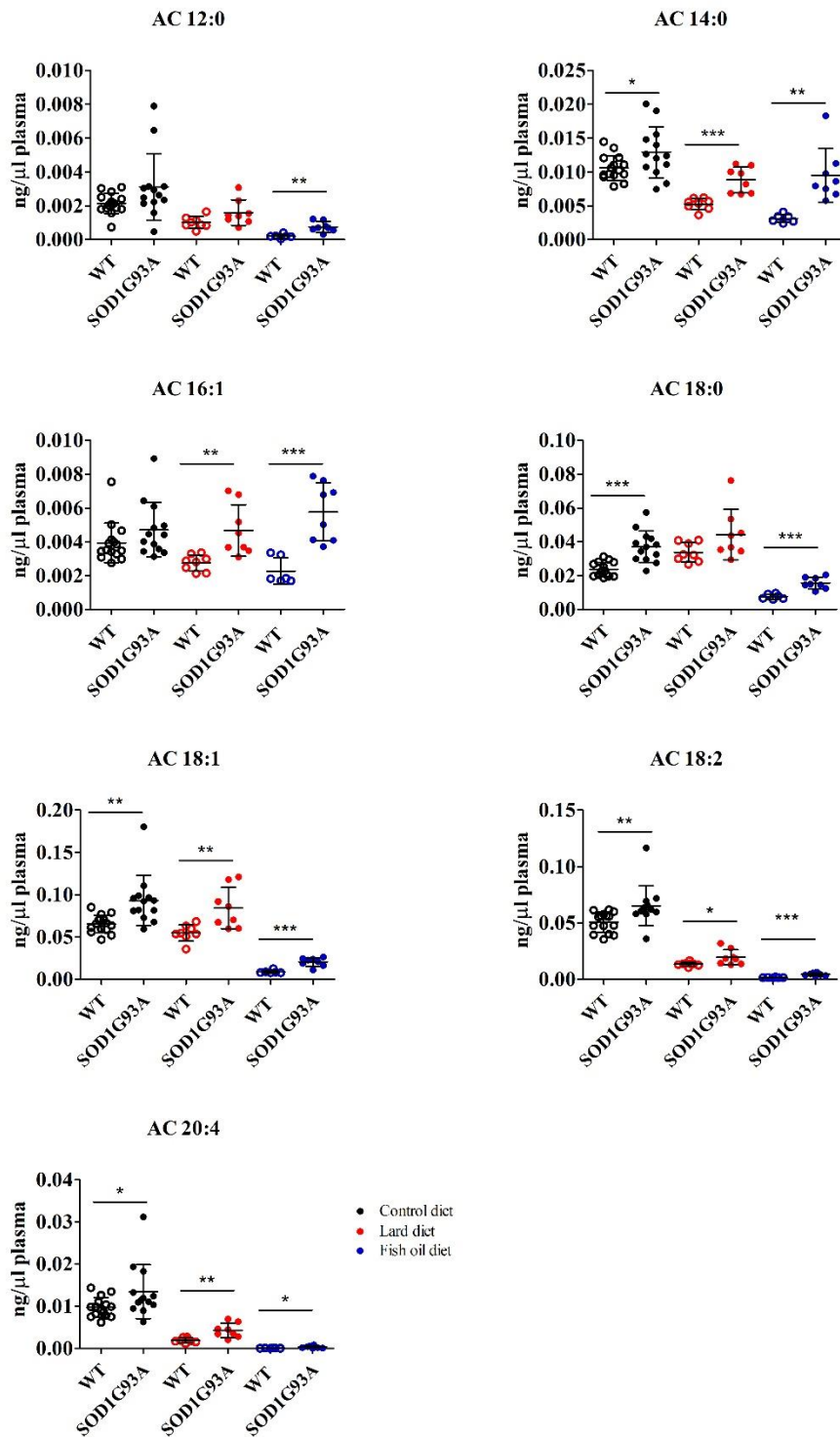
1,2,3-trimyristoylglycerol, TG 14:/14:0/14:0

Cholesterol Decanoate, CE 10:0

Methyl heptadecanoate, FA 17:0

These lipids were purchased from Sigma-Aldrich (St Louis, MO, USA)

Supplementary figure



Supplementary Figure S1. Acylcarnitine concentration in blood plasma of ALS and WT rats. Data are means \pm SD. * p <0.05, ** p <0.001 and *** p <0.0001. Significance by unpaired t-test. n =13 (control diet) and n =8 (lard and fish oil diet).

Supplementary tables

Supplementary Table S1. Internal Standard (IS) used for the quantification in blood plasma.

IS	Work concentration (ng/ μ L)	Normalized lipid classes	Response factor*
Cer d18:1/10:0	10	HexCer	
		Cer	
		AcylCer	
LPC 17:0	20	LPC	
		LPE	1.89
		FA	4.17
		PC	0.42
		pPC	
		oPC	
		PI	0.76
		TG	0.78
		ADG	
		CE	0.01
		Sitosteryl ester	0.01
		Campesterol	0.01
		AC	
Ch	0.78		
PA 17:0/17:0	20	PA	
PE 17:0/17:0	20	PE	
		pPE	
		oPE	
PG 17:0/17:0	20	PG	
		oPG	
SM d18:1/17:0	16	SM	

*Response factors were determined as ratio of the slope (a) of lipid class to slope of internal standard according to the procedures described in supplementary method. Parameters of response curve are described in Supplementary Table S3.

Supplementary Table S2. Internal Standard (IS) used for the quantification in pooled lipoprotein fraction

IS	Work concentration (ng/ μ L)	Normalized lipid classes	Response factor*
Cer d18:1/17:0	10	AcylCer	
		Cer	
SM d18:1/17:0	10	SM	
PC 14:0/14:0	10	PC	
		oPC	
		pPC	
PE 17:0/17:0	10	PE	
		pPE	
PG 17:0/17:0	10	PI	0.12
LPC 17:0	10	FA	4.17
		LPC	
		PI	
TG 14:0/14:0/14:0	10	TG	
CE 10:0	10	CE	
		Ch	
		Sitosteryl ester	
		Campesterol	

*Response factors were determined as ratio of the slope (a) of lipid class to slope of internal standard according to the procedures described in supplementary method. Parameters of response curve are described in Supplementary Table S3.

Supplementary Table S3. Parameter of response curve for individual lipid species in negative and positive modes.

Lipid species	a (Slopes)	b (intercepts)	r²
Negative mode			
PI 14:1/17:0	48870	-1952	0.9917
PC 17:0/17:0	27380	26540	0.6031
PG 17:0/17:0	376500	-8653	0.9951
LPC 17:0	63930	-2138	0.9938
LPE 17:1	120900	-5356	0.9930
FFA 17:0	267100	-8769	0.9957
Positive mode			
27-hydroxy-cholesterol	40760	-2876	0.9835
TAG 17:0/17:0/17:0	147000	1018	0.9591
CE 15:0	1951	-7.199	0.9520
D5 DAG 17:0	24140	505.9	0.9738
PC 17:0/17:0	244600	-7445	0.9876
LPC 17:0	188500	-8384	0.9931

Each lipid species is described by parameters of the linear dependence, $y = ax + b$, where y is the peak area, x is the concentration, and r^2 is the regression coefficients. The values were obtained from GraphPad Prism 5.0.

3. Final remarks

Lipids are a diverse and ubiquitous group of compounds which have several biological functions such as acting as structural components of cell membranes, serving as energy storage source, participating in signaling pathways. Nonetheless, there is a staggering number of studies evidencing that disruption of lipid homeostasis may affect several pathological processes. For instance, lipid damage, especially polyunsaturated fatty acids, by free radicals and reactive oxygen species plays an important role in cell biology and human health. Indeed, lipid peroxidation involving production of cardiolipin hydroperoxide is a hallmark of early apoptosis stage. Furthermore, lipid peroxidation triggers neurodegeneration process. In this context, we propose to study the role of lipid in protein aggregation involving cardiolipin and cholesterol hydroperoxides (Chapter 1 and Chapter 2), and to study the lipid metabolism alterations in blood plasma of a rodent model of ALS (Chapter 3 and Chapter 4).

In chapter 1, we estimated cytc reacts with CLOOH two orders faster than with H₂O₂ ($9.58 \pm 0.16 \times 10^2 \text{ M}^{-1}\text{s}^{-1}$ versus $5.91 \pm 0.18 \times 10^1 \text{ M}^{-1}\text{s}^{-1}$, respectively). Binding analysis revealed that most of cytc (ca. 96%) remains strongly attached to membranes containing CLOOH even by increasing the ionic strength of the medium. Moreover, this binding was further demonstrated to be time-dependent SDS-PAGE analysis, with dimeric and trimeric species observed in the first 15 min and increased high molecular weight aggregates formation afterwards. Using nLC-MS/MS, we have identified H26 and K72 consistently modified by 4-HNE, and K27, K73 and K88 modified by 4-OHE. For the first time we identify dityrosine cross-linking between peptides at Y48-Y74, Y48-Y97 and Y74-Y97. Collectively, our findings suggest that CLOOH induce covalent modifications of cytc, being an important mechanism of protein aggregation.

In chapter 2, we showed that cholesterol hydroperoxide reacts with cytc promoting changes in the structure of protein by increase of exposure of their hydrophobic sites. In addition, mass spectrometry analysis of tryptic peptide digested from dimeric cytc revealed dityrosine cross-linked peptides involving Y48, Y74 and Y97. In accordance to previous study published by our research group, the mechanism by which protein oligomerization occurs may be mediated by the formation of tyrosine radical that subsequently recombines giving dimers and trimers. For instance, identification of these modifications *in vivo* remains unknown. New approaches, such as cell culture could be used to assess the role of cytc aggregates induced by lipid hydroperoxides, it would be interesting uncover the role of these protein modification in biological perspective.

In Chapter 3, untargeted analysis performed by LC-MS/MS allowed us to characterize the lipidome of plasma SOD1G93A rats, a model for ALS. Analysis of the plasma showed that triglycerides esterified to long-chain polyunsaturated fatty acid were profoundly decreased in the symptomatic rats, suggesting an increased hypermetabolism and peripheral clearance. Moreover, glycerophospholipids species were also significantly decreased. Interestingly, sphingolipids, particularly hexosylceramide and acylceramide were found markedly elevated in the symptomatic rats. Detailed lipidomic analysis of pooled lipoprotein revealed altered triglycerides and glycerophospholipids species associated with VLDL, whereas acylceramide and hexosylceramide were related to HDL. Collectively, our results were consistent with recent emerging evidences highlighting the importance of alteration of sphingolipids and triglycerides metabolism in ALS (Figure 1). Importantly, we described, for the first time, acylceramide in blood plasma. Although the mechanism involving lipid alterations still remains unclear, our study provides interesting insights to potential lipid targets for further studies in ALS.

In Chapter 4, based on the current evidence supporting the potential role of high-fat diet intervention as therapeutic tool for ALS we evaluated the effect of high-lard and high-fish oil diets in blood plasma lipidome of ALS rat model. Although the high-lard and high-fish oil diets did not show significant survival extension in the ALS rats, a marked change in the lipid profile was observed in plasma of rats fed a high-fat diet. Since high plasma levels of triglycerides had a significantly positive effect on prognosis in ALS, our data showed significant decrease in plasma triglycerides species in ALS rats fed a high-fish oil diet. Acylcarnitine, acylceramide and hexosylceramide levels were significantly altered in ALS rats compared to WT controls even on high-fat diet. Importantly, our results suggest that acylceramide and acylcarnitine could play an important role in ALS pathophysiology. Furthermore, lipidomics will not only provide insights into the specific functions of lipid in health and disease, but also identify potential biomarkers for establishing preventive or therapeutic programs for several diseases. In this thesis, emphasis is given to the discovery of potential lipid markers in ALS studies that may provide insights into lipid profiling and pathophysiological mechanism.

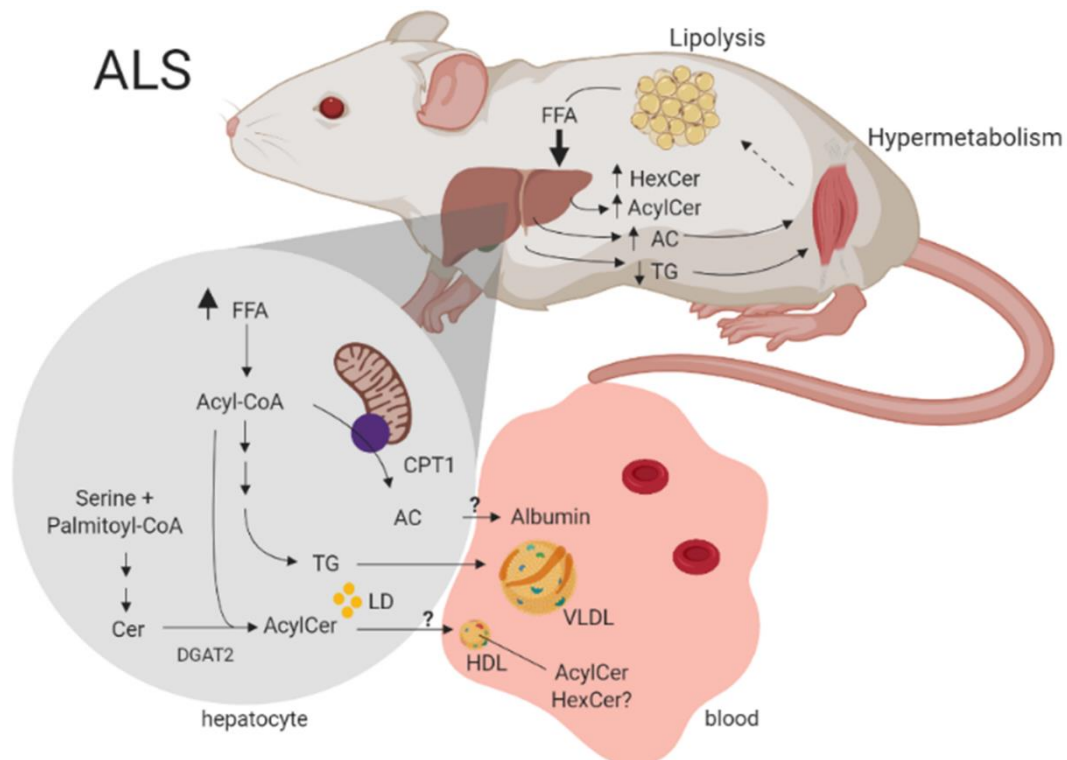
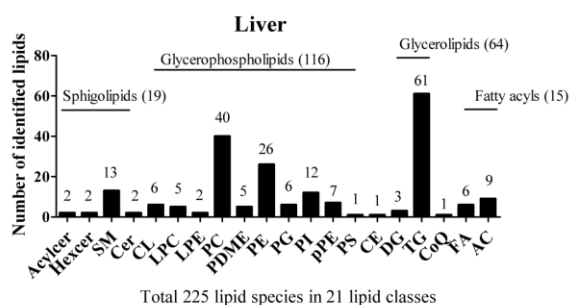


Figure 1. Summary of alterations in lipid plasma metabolism of symptomatic SOD1G93A rats, and how we hypothesize they may be related. We hypothesize that muscle-induced hypermetabolism in ALS stimulates lipolysis in adipocyte tissue. Increased fatty acid uptake in liver is required for acylcarnitine, acylceramide and triglycerides production in the liver. Once in plasma, triglycerides are transported to tissues by VLDL, while acylcarnitines are transported to tissues by plasma albumin as a fuel source for peripheral tissue in rats. In addition, fatty acyl-CoA was utilized with ceramide for the generation of acylceramides, poorly studied ceramide metabolite. Acylceramides could be effluxed to circulation by HDL.

APPENDIX

**Supplementary results: lipid signature in peripheral tissues of rat model of
amyotrophic lateral sclerosis**

A



B

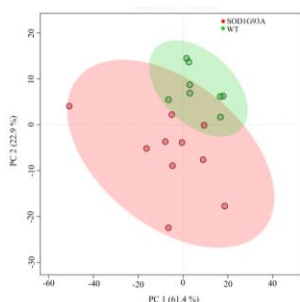
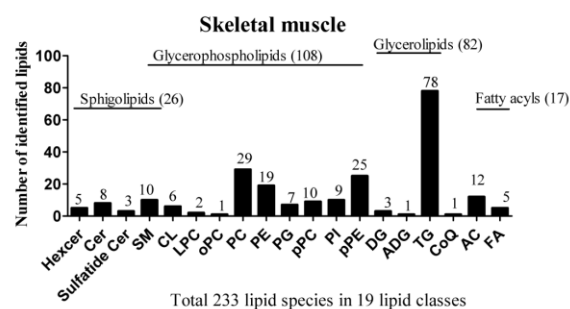
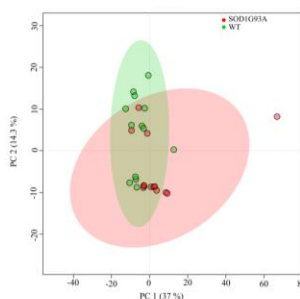
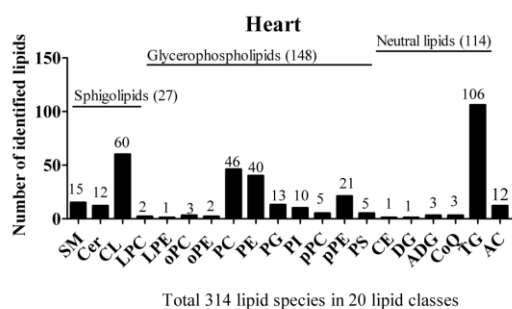
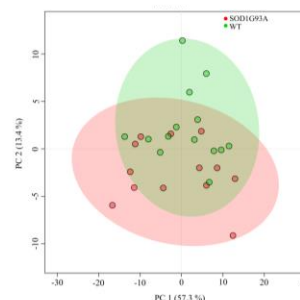


Figure 1. Global lipidomic analysis of peripheral tissue from SOD1G93A rats model of ALS. (A) Lipid classes diversity in liver, plasma, heart and skeletal muscle from SOD1G93A and WT rats. The bar graphs show the number of molecular species in each lipid classes identified by untargeted analysis. (B) Score plot of PC1 and PC2 from PCA analysis demonstrated of lipid profile of each tissue of SOD1G93A and WT rats. Abbreviation: AcylCer: acylceramide, HexCer: hexosylceramide, SM: sphingomyelin, Cer: ceramide, CL: cardiolipin, LPC: lysophosphatidylcholine, LPE: lysophosphatidylethanolamine, PC: phosphatidylcholine, PDME: phosphatidyl-dimethylethanolamine, PE: phosphatidylethanolamine, PG: phosphatidylglycerol, PI: phosphatidylinositol, PS: phosphatidylserine, PA: phosphatidic acid, Ch: cholesterol, CE: cholesteryl ester, DG: diacylglycerol, TG: triglyceride, SE: sitosteryl ester, ADG: alkyldiacylglycerol, CoQ: coenzyme Q, FA: free fatty acid, AC: acylcarnitine. The “o” and “p” prefixes indicate the presence of alkyl or alkenyl ether substituent, respectively.

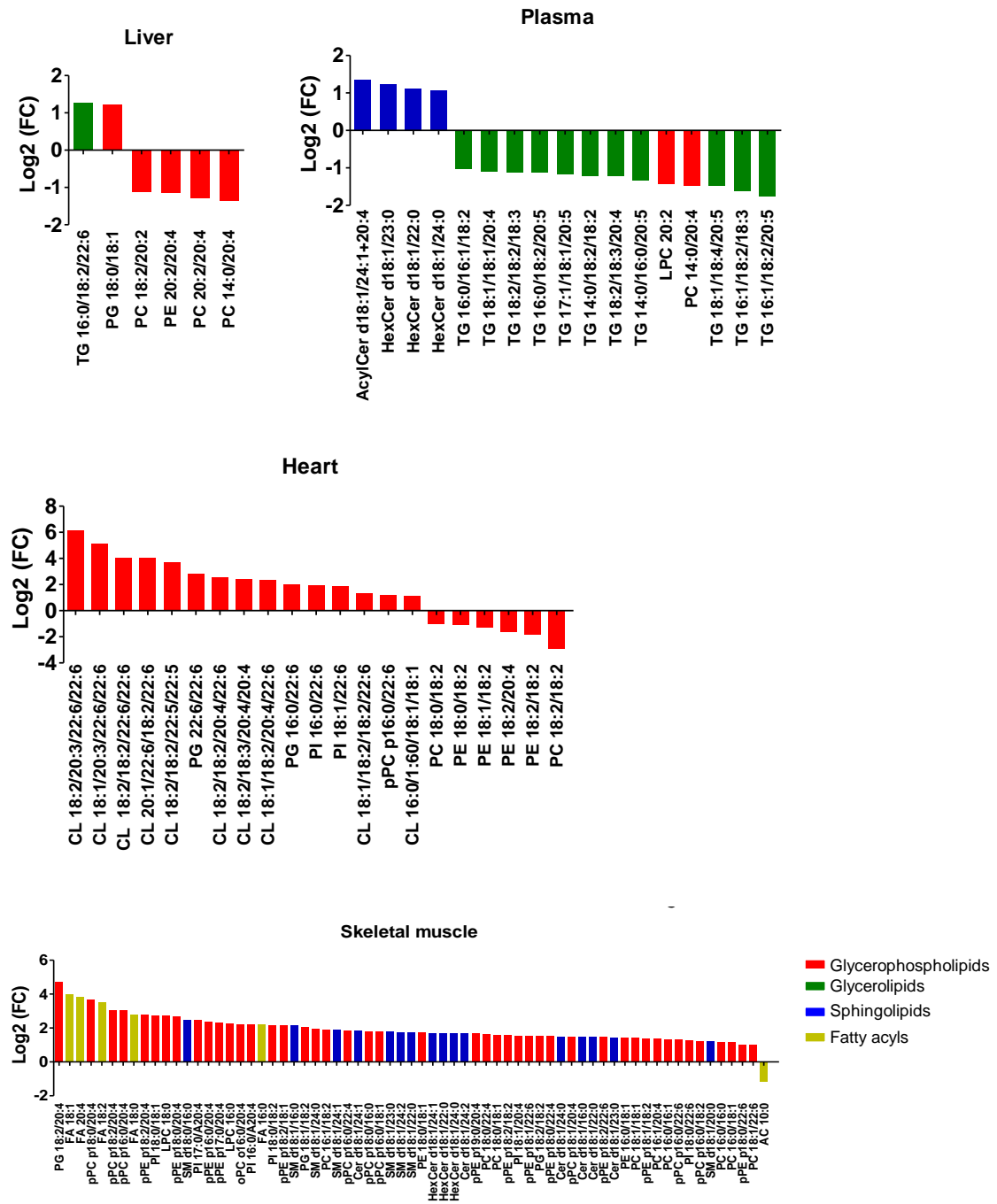


Figure 2. Lipidomic analysis revealed a broad response in liver, plasma, heart and skeletal muscle from SOD1G93A rats. The bar graphs provide a global view of lipid alteration in each tissue. The y-axis represents the cut-off values for significant levels (log2FC), while the x-axis represents lipid species comparing SOD1G93A *versus* WT rats (FC>2 and p-value FDR-adjusted<0.05). AcylCer: acylceramide, HexCer: hexosylceramide, SM: sphingomyelin, Cer: ceramide, CL: cardiolipin, LPC: lysophosphatidylcholine, LPE: lysophosphatidylethanolamine, PC: phosphatidylcholine, PDME: phosphatidyl-dimethylethanolamine, PE: phosphatidylethanolamine, PG: phosphatidylglycerol, PI: phosphatidylinositol, PS: phosphatidylserine, PA: phosphatidic acid, Ch: cholesterol, CE: cholesteryl ester, DG: diacylglycerol, TG: triglyceride, SE: sitosteryl ester, ADG: alkyl-diacylglycerol, CoQ: coenzyme Q, FA: free fatty acid, AC: acylcarnitine. The “o” and “p” prefixes indicate the presence of alkyl or alkenyl ether substituent, respectively.

CURRICULUM VITAE

PERSONAL DATA

Name: Isabella Fernanda Dantas Pinto

Place and date of birth: March 14, 1990, Sergipe, Brazil

OCUPATION

Scholarship Doutorado Direto, FAPESP, 08/01/2014 to 04/30/2019.

EDUCATION

2008 - 2014 Bachelor's degree at Pharmacy, Universidade Federal de Sergipe, São Cristóvão, Sergipe, Brazil with sandwich degree at Universitat de Barcelona, Spain.

2001 – 2008 High School degree at Colégio de Aplicação, Universidade Federal de Sergipe, São Cristóvão, Sergipe, Brazil.

COMPLEMENTARY EDUCATION

2019 Application training: pre-treatment function of SIL-30AC Shimadzu, São Paulo, SP, Brazil (6h).

2017 Structural Biology in Redox Process Course, Center for Free Radical and Biomedical Research (CEINBIO), Department of Biochemistry, Faculty of Medicine, Montevideo, Uruguay.

2015 Application training LC-MS/MS SCIEX TripleTOF 6600 System, SCIEX, São Paulo, Brazil (40h).

2014 1st Mass spectrometry Brazilian School – BrMASS, Natal, RN, Brazil.

RESEARCH EXPERIENCE

2014 – 2019 PhD student in Sayuri Miyamoto's laboratory. University of Sao Paulo, São Paulo, Brazil. "Cardiolipin in Neurodegenerative Diseases: Characterization of Oxidized Products and Modified Proteins in a Model of Amyotrophic Lateral Sclerosis".

2013 Undergraduate student in Dra. Laura Baldomà's laboratory. Universitat de Barcelona, Spain. "Analysis of the expression of the serin protease-sat through promoter fusion on the probiotic strain of *E. coli* Nissle 1917".

2009 – 2012 Undergraduate student in Dr. Humberto Reis Mato's laboratory. Universidade Federal de Sergipe, São Cristóvão, Sergipe, Brazil. "Study of Antiglycation, Hypoglycemic, and Nephroprotective Activities of the Green Dwarf Variety Coconut Water (*Cocos nucifera* L.) in Alloxan-Induced Diabetic Rats"

TEACHING AND MENTORING EXPERIENCE

2018 Lecture on lipid characterization using MS-based technologies and laboratory practice to postgraduate course Omics Sciences in Infectious Disease – ICB5747.

2017 Lecture on lipid characterization using MS-based technologies and laboratory practice to postgraduate course Omics Sciences in Infectious Disease – ICB5747.

2016 PAE to graduate course Experimental Biochemistry - QBQ0316 (120h)

FELLOWSHIPS AND AWARDS

2019 Keystone Symposia Future of Science Fund Scholarship.

2017 Center for Free Radical and Biomedical Research Scholarship

LIST OF PUBLICATIONS

Journals

Chaves-Filho, AB; Yoshinaga, MY, Dantas, LS; Diniz, LR; **Pinto, IFD**; Miyamoto, S. Mass spectrometry characterization of thiol conjugates linked to polyoxygenated polyunsaturated fatty acid species. *Chem. Res. Toxicol.* 2019. <https://doi.org/10.1021/acs.chemrestox.9b00199>

Chaves-Filho, AB; **Pinto, IFD**; Dantas, LS; Xavier, AM; Inague, A; Faria, RL; Medeiros, MHG; Glezer, I; Yoshinaga, MY; Miyamoto, S. Alteration in lipid metabolism of spinal cord linked to amyotrophic lateral sclerosis. *Scientific Reports*, 12;9(1):11642, 2019.

Queiroz, A; **Pinto, IFD**; Lima, M; Giovanetti, M; Jesus, JG; Xavier, J; Barreto, FK; C, GAB; Amaral, HR; Filippis, AMB; Mascarenhas, DL; Falcão, MB; Santos, NP; Azevedo, VAC; Yoshinaga, MY; Miyamoto, S; Alcântara, LCJ. Lipidomic Analysis Reveals Serum Alteration of Plasmalogens in Patients Infected with ZIKA Virus. *Frontiers in Microbiology*, 2019, 10, 753. doi:10.3389/fmicb.2019.00753

Bispo, VS; Dantas, LS; Chaves Filho, AB; **Pinto, IFD**; Silva, RP; Otsuka, FAM; Santos, RB; Santos, AC; Trindade, DJ; HR. Reduction of the DNA damages, Hepatoprotective Effect and Antioxidant Potential of the Coconut Water, ascorbic and Caffeic Acids in Oxidative Stress Mediated by Ethanol. *Anais da Academia Brasileira de Ciências*, v. 89, p. 1095-1109, 2017.

Menezes-Filho, SL; Amigo, I; Prado, FM; Ferreira, NC; Koike, MK; **Pinto, IFD**; Miyamoto, S; Montero, EFS; Medeiros, MHG; Kowaltowski, AJ. Caloric Restriction Protects Livers from Ischemia/Reperfusion Damage by Preventing Ca²⁺-Induced Mitochondrial Permeability Transition. *Free Radical Biology and Medicine*, v. 19, p. 219-227, 2017.

Pinto, IFD; Silva, RP; Chaves Filho, AB; Dantas, LS; Bispo, VS; Matos, IA; Otsuka, FAM; Santos, Aline C; Matos, H. R. Study of Antiglycation, Hypoglycemic, and Nephroprotective Activities of the Green Dwarf Variety Coconut Water (*Cocos nucifera* L.) in Alloxan-Induced Diabetic Rats. *Journal of Medicinal Food*, v. 18 (7), p. 802-809, 2015.

Santos, JLA; Bispo, VS; Chaves Filho, AB; **Pinto, IFD**; Dantas, LS; Vasconcelos, DF; Abreu, FF; Melo, DA; Matos, IA; Freitas, FP; Gomes, OF; Medeiros, MHG; Matos, HR. Evaluation of Chemical Constituents and Antioxidant Activity of Coconut Water (*Cocus nucifera* L.) and Caffeic Acid in Cell Culture. *Anais da Academia Brasileira de Ciências (Impresso)*, v. 85, p. 1235-1246, 2013.

Pinto, IFD; Biagi, D.G; et al. A comparative lipid profile of human induced pluripotent stem cell-derived cardiomyocytes with primary human heart tissue (*In preparation*).

Conferences

Lipidomics and Functional Metabolic Pathways in Disease (C6). Steamboat Springs, CO, EUA, 2019. Poster presentation: Metabolism dysregulation induces a specific lipid signature in peripheral tissues of rat model of amyotrophic lateral sclerosis.

47th Annual Meeting of the Brazilian Society for Biochemistry and molecular Biology. Joinville, SC, Brazil, 2019. Poster presentation: Lipidomics analysis of blood plasma reveals alterations in sphingolipid, glycerophospholipid and glycerolipid metabolism in a rodent model of amyotrophic lateral sclerosis.

7th European Lipidomics Meeting. Leipzig, Germany, 2018. Poster presentation: Lipidomic analysis of human induced pluripotent stem cell-derived cardiomyocytes.

15th Euro Fed Lipid Congress: Oil, fats and lipids: New Technologies and applications for a healthier. Uppsala, Sweden, 2017. Poster presentation: Lipidomic analysis of blood plasma: lessons from a rodent model of Amyotrophic lateral sclerosis

23rd Annual Meeting Society for redox biology and Medicine. San Francisco, EUA. 2016. Poster presentation: Covalent modification and aggregation of cytochrome c induced by cardiolipin hydroperoxide.

45th Annual Meeting of the Brazilian Society for Biochemistry and molecular Biology, Natal, RN, Brazil, 2016. Poster presentation: Characterization of dityrosine crosslinking of cytochrome c induced by cholesterol 7 α -hydroperoxide.